USING ISOTOPES TO ANALYZE SOIL EROSION AND DEPOSITION FOR THE BULL CREEK WATERSHED IN OKLAHOMA

By

BING LIU

Bachelor of Science in School of Geography and Remote Sensing Beijing Normal University
Beijing, China
2007

Master of Science in School of Geography and Remote Sensing Beijing Normal University
Beijing, China
2010

Submitted to the Faculty of the
Graduate College of the
Oklahoma State University
in partial fulfillment of
the requirements for
the Degree of
DOCTOR OF PHILOSOPHY
December, 2013

USING ISOTOPES TO ANALYZE SOIL EROSION AND DEPOSITION FOR THE BULL CREEK WATERSHED IN OKLAHOMA

Dissertation Approved:

Dr. Daniel E. Storm

Dissertation Adviser

Dr. Glenn O. Brown

Dr. Chris B. Zou

Dr. Jason G. Warren

ACKNOWLEDGEMENTS

I would like to express my gratitude to all those who have helped me during my studies at Oklahoma State University. First, I would like to express my heartfelt gratitude to my advisor Dr. Storm who gave me his best support on both my course study and research. I gratefully acknowledge his encouragement and instruction in completion of this dissertation. Second, I would like to thank all my committee members, Dr. Brown, Dr. Zou, Dr. Warren and Dr. Turton, who gave me valuable advice and shared their knowledge, which inspired me during the dissertation writing. I also want to give special thanks to Dr. John Zhang and Mark Smith from the Rangeland Research Lab, US Department of Agriculture Agricultural Research Service in El Reno, OK. They provided me great help on my research design, field sampling and laboratory tests. Thanks to Dr. Guanghui Zhang and his students from the School of Geography, Beijing Normal University, for testing the Cs-137 samples. Last but not least, my thanks go to my beloved family and friends who have always helped me out of difficulties and supported me over the years.

Name: BING LIU

Date of Degree: December, 2013

Title of Study: USING ISOTOPES TO ANALYZE SOIL EROSION AND DEPOSITION FOR THE BULL CREEK WATERSHED IN OKLAHOMA

Major Field: ENVIRONMENTAL SCIENCE

Abstract: Soil erosion is a serious environmental problem worldwide. Extensive research has been conducted identifying and quantifying erosion processes, measuring soil erosion, and evaluating the effectiveness of soil conservation practices. Accurately predicting soil erosion in space and time continues to be a challenge, and detailed spatial erosion data at field and watershed scales are needed to validate, calibrate, and improve erosion models. The Cs-137 and fingerprinting methods have been used to estimate soil erosion and sediment sources in many studies, but uncertainties exist in both methods. The purpose of this study was to evaluate these two methods and compare predictions with the Water Erosion Prediction Project (WEPP) model. The study area for this research was the Bull Creek watershed, located in west central Oklahoma. The Cs-137 method predicted reasonable long-term average soil erosion and deposition rates and integrated spatial and temporal changes in erosion/deposition. Compared to WEPP, the Cs-137 method needed less information and only required a one-time sampling. The fingerprinting method provided useful information about the sediment source contributions and performed best with two sources. For the Bull Creek study area, the mixing model predicted the source contribution with the lowest model errors; however, the results were not significantly different. The new Discriminate Function Analysis method may be a better method since it avoids spurious numerical solutions.
When using the Cs-137 and the fingerprinting methods, sample collection and the proper application of particle size correction factors were critical. When there were two source types, the fingerprinting method and WEPP watershed model predicted similar source contributions. However, with three source types their predictions diverged. In addition, WEPP predicted significantly less sediment yield from the rangeland compared to the fingerprinting method. Combining erosion models with the fingerprinting method provides a more detailed evaluation of erosion predictions, which may result in improved land management recommendations and decisions.

TABLE OF CONTENTS

LIST OF TABLES

LIST OF FIGURES

CHAPTER I

INTRODUCTION

As the world population grows, the demand for food also increases. Due to the unsustainable land use, such as deforestation, overgrazing, and poor land management, soil erosion is a serious environmental problem worldwide. In the United States alone, 23 million hectares of fragile highly erodible cropland was determined to have excessive erosion, and about 20 million hectares of non-highly erodible cropland had erosion that exceeded the tolerable soil loss rate (U.S. Department of Agriculture Natural Resources Conservation Service, 1997). Soil erosion causes soil quality degradation and reduces soil productivity. Sediment contaminates surface waters, impairs aquatic habitat and reduces the capacity of our navigable waterways (Toy et al., 2002). Soil erosion is a "think global, act local" issue, is a severe environmental problem throughout the world, and directly or indirectly affects everyone's life.

Sustainable agriculture requires a soil loss rate that does not exceed the soil-formation rates, and thus accurately quantifying soil erosion rates is critical. In the 20th century, extensive research has been conducted on soil erosion theories and processes, measuring and modeling soil erosion, and quantifying the effect of conservation practices on soil loss (Hudson, 1995). Early studies focused on how soil erosion was affected by factors such as rainfall, soil properties, runoff, landforms, and land cover. Zingg (1940) used slope and slope length to calculate the soil loss, and Smith (1941) added crop and conservation practice factors. These equations were the initial basis

for the Universal Soil Loss Equation (USLE) (Wischmeier and Smith, 1978), an empirical model, which was later updated to the Revised Universal Soil Loss Equation (RUSLE) (Renard et al., 1993) and RUSLE 2 (USDA-ARS-NSL, 2003) Process-based erosion models were also developed, such as the Chemicals Runoff Erosion in Agricultural Management Systems (CREAMS) (Toy et al., 2002), the Water Erosion Prediction Project (WEPP) (USDA, 1995), GUEST (Misra and Rose, 1996), and Soil and Water Assessment Tool (SWAT) (Simon et al., 1997). Hydrology and Sedimentology Watershed Model (SEDIMOTII) was also a process-based model (Wilson et al., 1984), which uses SLOSS for erosion and deposition (Wilson et al., 1984). Among the process based models, WEPP was the latest generation process-based continuous simulation model (Robinson et al., 1996), and has been widely used to predict soil loss and deposition at both hillslope and watershed scales (Bhuyan et al., 2002). Flanagan et al. (2007) reviewed the development history of WEPP and concluded that WEPP can predict the long-term average soil loss adequately, and overcomes the inherent issues and limitations with USLE and RUSLE (Laflen et al., 1991).

Although WEPP was created to replace the USLE, with limited input data, USLE and RUSLE have exhibited better model efficiency compared to WEPP (Tiwari et al., 2000). Tiwari et al. (2000) found that soil erosion models tended to overestimate the small rainfall events and underestimate the large rainfall events. Moreover, to precisely predict soil loss, and to identify sediment sources and relative their contributions within a watershed, soil erosion models required detailed and accurate site-specific input data (Zapata, 2002). Lack of available detailed data restricts the soil erosion models' widespread application. If more detailed data on erosion distribution and deposition rates were available, additional model validation and model improvements can be accomplished. Since collecting adequate field data is costly and time consuming, one method to quantify erosion and deposition rates is the use of isotopes, which is

used as tracers to track the movement of soil particles. The isotope method has been used to estimate soil erosion rate since the 1950s (Ritchie and Ritchie, 2008).

The most commonly used isotopes for quantifying soil erosion and deposition are Cs-137 (Cesium-137), Pb-210 (Lead-210) and Be-7 (Beryllium-7). There is no natural Cs-137 in the environment, and thus all Cs-137 in the atmosphere and the soil is a man-made radioisotope produced during nuclear weapon use and testing. The Cs-137 was first introduced into the atmosphere when nuclear tests began in 1945 at Alamogordo, New Mexico, USA. Following the first test, there were more than 2000 nuclear weapon tests worldwide (Bondár et al., 2001). However, the reported Cs-137 fallout began in 1954 and reached its peak in 1963 and 1964 (Cambray et al., 1989). After 1984, there was no detectable fallout of Cs-137. Accidents can also add Cs-137 into the atmosphere; for example the Chernobyl Nuclear Power Plant accident in the Ukraine on April 26, 1986 and the Fukushima Dai-ichi Nuclear Power Plant explosions in Japan on March 11, 2011. However, the Chernobyl accident deposited Cs-137 primarily in Europe (Matisoff et al., 2002). Some measurements indicated that the Fukushima explosion might have increased the total Cs-137 in the soil from 3% to 17%; however, other studies showed no detectable Cs-137 from this explosion due the lack of precipitation during the sampling periods (Wetherbee et al., 2012). In addition, there was no detected Cs-137 from the Fukushima explosion after the sampling periods (Thakur et al., 2012).

Unlike Cs-137, Pb-210 and Be-7 are naturally occurring radioisotopes in the environment. Pb-210 results from the decay series of U-238 (Uranium-238); U-238 decays to Rn-222 (Radon-222), diffuses into the atmosphere and decays to Pb-210. Be-7 is generated when Oxygen and Nitrogen atoms in the troposphere and stratosphere are bombarded by cosmic rays. Among the three isotopes, using Cs-137 to measure soil erosion and deposition were the most studied (Zapata, 2002). The theory of using isotopes to analyze soil erosion is based on the isotopes reaching the soil through precipitation, and strongly binding with the soil particles, especially clay. Although

Cs-137 can be removed by strong acids and certain plants, in most environments the isotopes are not separated from the soil particles by chemical processes and the uptake by plants is small (Fuhrmann et al., 2003). Hence, the isotopes only move with the soil and can be used to tract soil erosion and deposition.

Only a few studies have compared Cs-137 movement to soil erosion model predictions, which include the USLE, RUSLE and WEPP models (Busacca et al., 1993, Turnage et al., 1997, Sparovek et al., 2000, Belyaev et al., 2005, Onori et al., 2006, López-Vicente et al., 2008). These studies have demonstrated that the Cs-137 method can be successfully used to evaluate the performance of the erosion models. In addition, these studies showed that Cs-137 could be used to improve model predictions and validate processes based erosion models at the watershed scale (Sidorchuk and Golosov, 1996, Quine, 1999, Walling et al., 2003, Stefano et al., 2005). However, erosion rates were quite different from the Cs-137 method and the soil erosion models. Therefore, additional research is needed to study the application of the Cs-137 method.

Another method to track sediment is the fingerprinting method (Juracek and Ziegler, 2009). The fingerprinting method has been successfully proved to identify sediment source information, which included the precise types of sediment sources and their spatial distribution (Collins et al. 1997). Collins et al. (1996) used sediment from sub-watersheds as sources to estimate the relative contribution to the entire watershed. Although the fingerprinting method can only provide relative contribution of the sources, this method has been used by the USDA Conservation Effects Assessment Project as well as many countries across the world (de Miguel et al., 2005, Smith and Dragovich, 2008, Wilson et al., 2008, Zhang et al., 2011). Furthermore, sediment eroded from stream banks and gullies can be estimated (Mukundan et al., 2010).

In this study, the Bull Creek watershed, located in Washita, Oklahoma (Figure 1), was selected as the study area to evaluate sediment movement using the Cs-137 and fingerprinting methods. The

Cs-137 method was applied to predict hillslope soil erosion and the fingerprinting method was used to predict sediment sources at a small watershed scale. The limitations and advantages of these two methods were discussed. In addition, WEPP hillslope and watershed model predictions were compared to these methods.

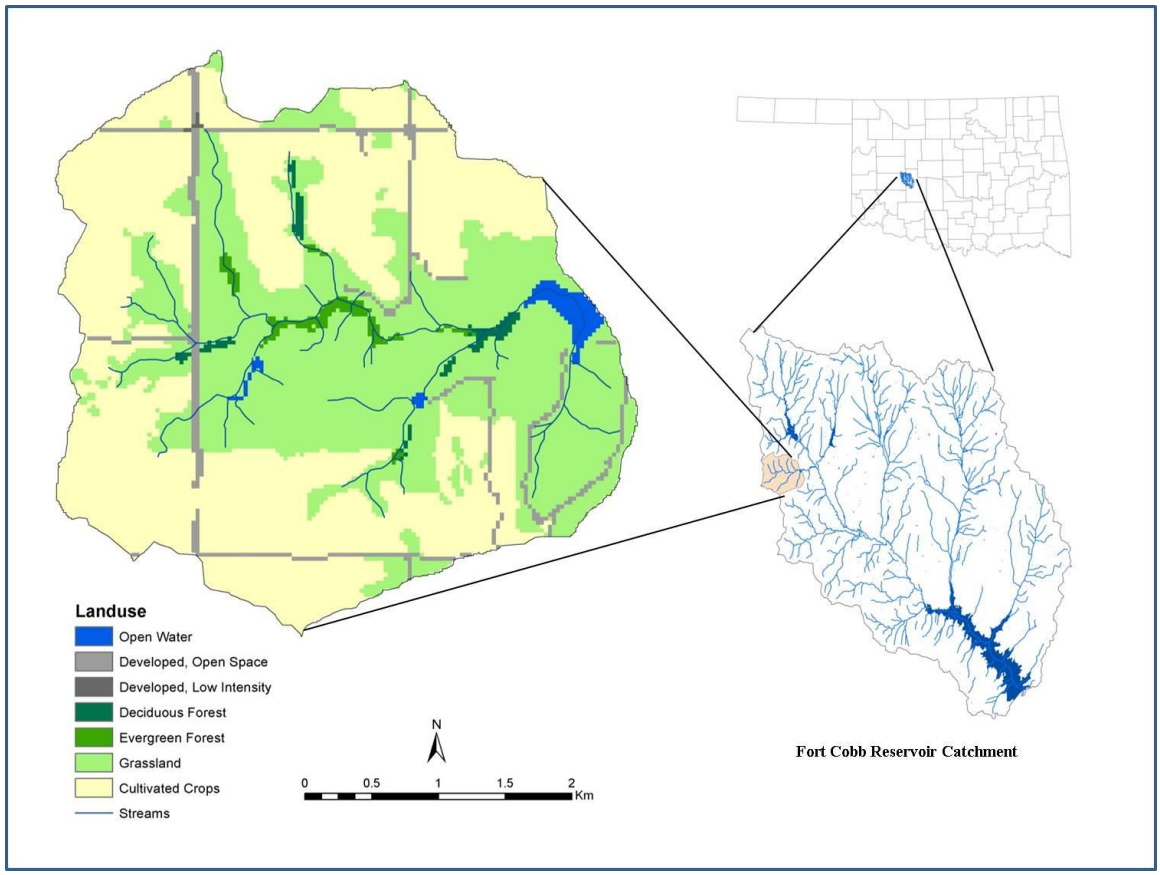

Figure 1 Location of the Bull Creek Watershed.

The hypotheses and research questions addressed are:

Hypothesis 1: Cs-137 soil concentrations in the study area are within a measurable range and can be used to estimate historic soil erosion and deposition rates using conversion models.

Research questions related to hypothesis 1 are:

- How do the measured Cs-137 soil concentrations compare with published data?
- Can statistical relationships between measured Cs-137 soil concentrations, slope, slope length, land use, and other watershed characteristics be used to predict soil erosion and deposition rates at the watershed scale?

Hypothesis 2: Selected soil properties for the "Fingerprinting" or source tracing method are significantly different among the source categories, and can be used in a Mixing model to estimate the sediment contribution by source and spatial distribution at the watershed scale.

Research question related to this Hypothesis 2 is:

- Can the Discriminant Function Analysis (DFA) be used directly to predict source contribution instead of the Mixing model?

CHAPTER II

REVIEW OF LITERATURE

2.1 Using Cecium-137 to Study Soil Erosion

2.1.1 *The beginning of measuring and studying Cs-137 properties*

Radioisotopes resulting from nuclear explosions were discovered in the ecosystem in the middle 1950s. Initially, the research was focused on the isotope movement, and their effect on the ecosystem and human health. Nishita et al. (1956) studied five radioactive products from nuclear explosions and documented the fixation, water-soluble, and exchangeable isotopes varied across different soil types and clay minerals. Radioisotope movements from the atmosphere, soil and plants have been measured in many studies (Davis and Foster, 1958, Nishita et al., 1958, Fredriksson et al., 1959) and have concluded that Cs-137 uptake by plants was small. Rogowski and Tamura (1970a) found that after two years, crabgrass and meadow vegetation only took up 0.4% to 0.5% of the total Cs-137 in the soil. Nishita et al. (1958) measured Cs-137 uptake rate by Ladino clover and found a maximum uptake of 0.13 percent of dose. They also found the Cs-137 uptake was negatively correlated with exchangeable potassium (K) in the soil.

Fredriksson et al. (1959) measured isotope concentrations in different parts of the plants and found a negative correlation with calcium (Ca) concentration in the soil, which may have been due to Cs-137 having similar physiological process as K and Ca (Davis, 1963). Moreover, results

showed that Cs-137 would fix to clay minerals. Anderson (1958) tested the concentration of the radioisotopes Potassium-40 and Cesium-137 in milk, and illustrated the use of Cesium-137 to study environmental problems. This study also identified seasonal variations of the contamination in the troposphere during periods of weapon testing. Radioisotopes, such as Strontium-90 (Sr-90) and Cs-137 have also been used to study soil-plants relationships. Peirson and Salmon (1959) measured deposited fallout in soil samples in the United Kingdom and found that 95% of the fallout was concentrated in the top 7 cm of the soil. Their experiments showed a linear relationship between mean annual rainfall (cm) and the Cs-137 soil concentration. Spitsyn et al. (1958) studied the ability of soils to absorb cesium, and found that a sandy soil absorbed 50% of the available cesium. Evans and Dekker (1966a) found the sand fraction fixed Cs-137 more than the silt and clay fractions.

In the early 1960s, radionuclides were measured in the soil surface and in river and marine sediments. Menzel (1960) reported a positive correlation between soil loss from cultivated land and the Sr-90 concentration in runoff, and introduced the concept of using isotopes to study soil erosion. Yutaka and Masamichi (1967) found that for undisturbed soils, 70% of the Cs-137 was found within the top 2 cm, and the top 2.5 cm river sediment contained 65% to 70% of the Cs-137. They also found that to contain the same amount of Cs-137 as the river sediment, marine sediment required depths of 5 to 11 cm. Using hydrochloric acid extractions, 80% of the radionuclides were found in the fine mud. Squire and Middleton (1966) found similar results indicating that the fixation of Cs-137 increased with clay content. They also found that potassium reduced Cs-137 absorption and organic matter increased the absorption by the soil.

Beck (1966) found and exponential distribution of radioisotopes in the top 3 cm of the soil, and developed equations to calculate the Cs-137 activity distribution with depth using the rainfall deposition data. He studied the relationship between soil organic matter and the uptake of Cs-137 by plants, and found the higher the soil organic matter content the less the plants would uptake

Cs-137. Rogowski and Tamura (1965) used Cs-137 to study the relationship between Cs-137 movement and soil loss. They sprayed Cs-137 on plots and collected data for 81 days under natural rainfall. Though the testing period was short, they reported an exponential relationship between Cs-137 loss and soil loss. The research also indicated that the Cs-137 was distributed in the top 2 cm of the soil, and the vertical movement of Cs-137 depended on infiltration and the translocation by the root system. The experiments were conducted using natural occurring Cs-137 and carrier free Cs-137. More than 80% of the Cs-137 was associated with the clay materials that had to be removed using strong acids. Once combined with clay, very little Cs-137 is released or taken up by plants (Schulz et al., 1960). When 4.00 μc Cs-137 was applied to the soil, plants absorbed 0.09% to 1.29% of the Cs-137 during a one-year experiment (Evans and Dekker, 1966b). Noboru et al. (1969) tested Cs-137 in pine trees, and found the highest fallout rate was in 1963. They reported that about 18% of the Cs-137 was found in the vegetation. However, the pine trees absorbed Cs-137 primarily through aerial deposition.

After the late 1960s, additional research was conducted on Cs-137 properties, using Cs-137 as a tracer to quantify soil erosion in watersheds, and sedimentation rates in lakes and reservoirs. It was widely accepted that the majority of the global input of Cs-137 into the environmental was estimated to be around 1952, with a range of plus or minus two years (Robbins et al., 1978). Research showed that the Cs-137 had already dispersed globally in the late 1952 (Hanson, 1980). However, Cs-137 was first detected in the atmosphere in 1954 with peak levels in 1963 (Pennington et al., 1973, Longmore, 1982), and after 1983 and 1984 Cs-137 was below detectable levels in the northern hemisphere (Cambray et al., 1985). The half-life of Cs-137 was tested through 11-year measurements using four different types of mass spectrometers (Dietz and Pachucki, 1973). They measured the half-life of Cs-137 at 30.174 years with an uncertainty of 0.034 year.

2.1.2 Use Cs-137 as a tracer in soil erosion study

From the 1970s through the 1980s, radionuclides, because of their properties, were used as tracers to estimate soil erosion and deposition rates quantitatively by both water and wind (Alldredge and Whicker, 1972). Prokhorov (1975) studied the vertical migration of Cs-137 in the soil, and developed a regression equation to predict Cs-137 activity with depth based on the thickness of the soil layer, the time of migration, and a dimensionless parameter. However, this equation did not consider the decay of Cs-137. Ritchie and McHenry (1973) studied the vertical distribution of Cs-137 in the cultivated land, and found that Cs-137 was uniformly distributed in the tillage layer, normally 15 to 20 cm. Under the tillage layer, the Cs-137 levels reduced rapidly. McHenry and Ritchie (1977) found that the distribution of Cs-137 in reservoirs was explained by the reservoir surface area, the percentage of total C, watershed area and the soil organic matter. The Cs-137 was found to be concentrated in the top 2.5 cm in the reservoir sediments. Frissel and Pennders (1983) and Livens and Rimmer (1988) found that Cs-137 was more likely to absorbed to clay and silt (the fine) particles, and the vertical distribution of Cs-137 in undisturbed soil showed an exponentially decrease through depth. Most of the Cs-137 was in the top 15 cm and rarely below 30 cm (Hrachowitz et al., 2005). However, peak Cs-137 levels have been found in the top few centimeters below the surface soil (He and Walling, 1997).

Campbell et al. (1982) built a hypothetical model using data collected in the Maluna Creek basin, Australia. In this model:

i. Nuclear weapon tests were the only source for the Cs-137 in the atmosphere;
ii. Once the Cs-137 contacted the soil, it was strongly absorbed to fine soil particles and organic materials, and did not move by natural chemical reactions;
iii. Areas had little or no erosion or deposition; the Cs-137 accumulated in the top soil and reduced through depth exponentially;

iv. Cs-137 in the forest or wooded areas should be used as the total input, since they could trap the most Cs-137 fallout;

v. In cultivated land, the Cs-137 had a uniform distribution in the tillage layer, which was later documented by Walling and Quine (1992) (Figure 2);

vi. Eroded areas had less Cs-137 and had a truncated Cs-137 distribution with depth, while deposition areas had higher Cs-137 levels; these profiles were used to predict the fallout and sedimentation history;

vii. The peak concentration of Cs-137 corresponded to the year 1963 to 1964;

viii. Gullies had lower Cs-137 levels compared to surface erosion areas (Ritchie et al., 1972).

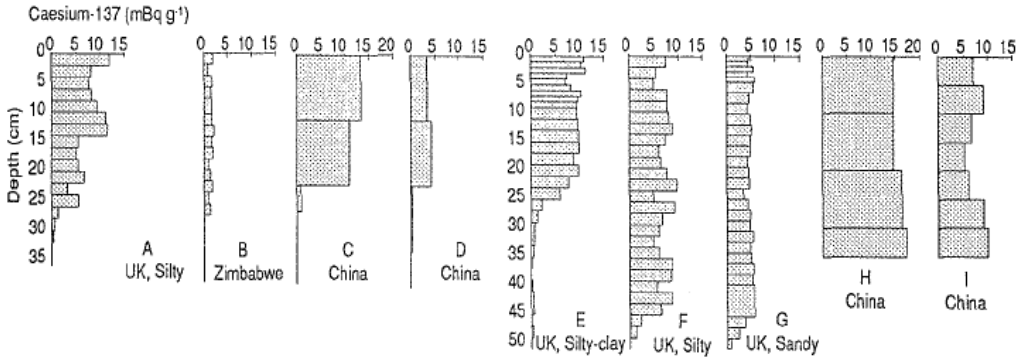

Figure 2 Cs-137 vertical distribution for cultivated soils (Walling and Quine, 1992).

Campbell (1983) summarized the method of using Cs-137 to estimate the sedimentation rates in lakes and reservoirs, and concluded that Cs-137 was an appropriate tracer for erosion and deposition studies. Their study indicated that in the arid region of the southwest United States, USLE rainfall factor, particle size, fallout intensity, average precipitation, the soil nitrogen and phosphorus, and soil cation exchange capacity can explain up to 90% of the variation of Cs-137 content in the soil and sedimentation. Using Cs-137 as a tracer to predict soil erosion in

watersheds has been confirmed by many studies. However, one problem with this method is during low sedimentation rates the results are significantly affected by mixing, disturbance or coring technique of the surface sediment. McHenry and Ritchie (1977) evaluated the variance of Cs-137 in soil and sedimentation in reservoirs.

Ritchie and McHenry (1975) measured soil and Cs-137 losses from plots, and found that Cs-137 loss as a percentage of total Cs-137 input had a logarithmic relationship with soil loss in metric tons per hectare. They also compared deposition rates in reservoirs and valleys using surveying and Cs-137 methods, and concluded that Cs-137 was a useful method to estimate deposition rates. Rogowski and Tamura (1970b) developed a logarithmic relationship to predict Cs-137 from soil loss on bare soil using the form:

$$Y = A\left(\frac{X}{b}\right)^{n} \quad (1)$$

where Y is the cumulative percent of Cs-137 loss, X is the cumulative soil loss (g/m^2), b is the unit constant which is equal to 1.0 g/m^2, n is an exponent between 0 and 1, and A is coefficient. Long-term measured data are needed to estimate these parameters. The problems with this model include: data collected from plot studies may not reflect the natural conditions, the equation does not account for Cs-137 decay, data may not be applicable at other locations, and sampling and measurement methods may significantly affect the results (Ritchie and McHenry, 1975, Elliott et al., 1990, Loughran and Campbell, 1995).

Ritchie et al. (1974) analyzed the relationship between measured Cs-137 in the soil and soil erosion rates predicted from the USLE for different land uses, and found a logarithmic relationship between the Cs-137 loss and soil erosion rates. They combined their data with data from other research in different locations and collection methods, and developed:

$$Y = 1.6X^{0.68} \quad (2)$$

where Y is the radionuclide loss expressed as a percent of radionuclide input, and X is soil erosion in metric ton per hectare. The correlation coefficient for their model was 0.95 and was significant at the 0.01 level, which further confirmed that Cs-137 could be used to predict soil erosion.

Brown et al. (1981a) provided a detailed discussion on Cs-137 transect sampling, and used these data to estimate soil erosion rates for agriculture land. Assumptions used to predict erosion that differed from Campbell et al. (1982) were:

i. Cs-137 fallout in the study area started in 1954;
ii. Incoming Cs-137 for the study area was uniform;
iii. Cs-137 loss related to erosion and deposition was affected by the particle size distribution of the soils;
iv. Uniform absorption of Cs-137 by all plants;
v. Cs-137 loss in surface runoff prior to being absorbed by the soil was neglected.

Brown and Campbell both assumed that Cs-137 was uniformly distributed with depth in cultivated land. Some of their assumptions were not valid; for example, the tree canopy redistributes Cs-137 (Bunzl et al., 1989) and different plant species absorbed Cs-137 at different rates (Greger, 2004). However, the research provided valuable insight into field methods. Brown et al. (1981b) introduced the Gravimetric Approach to quantify the soil erosion using:

$$Y = 10\,\frac{A_{ref}-A}{C_S T} \tag{3}$$

where Y is the average soil loss (t ha^{-1} yr^{-1}), A_{ref} is the Cs-137 inventory at the reference site (Bq m^{-2}), A is the Cs-137 inventory for eroded area (Bq m^{-2}), Cs is the mean Cs-137 concentration of surface soil within the eroded area (Bq kg^{-1}), and T is the time elapsed since initiation of Cs-137 accumulation (yr).

The average depth of accumulated sediment was calculated by dividing estimated depletion of Cs-137 activity by soil bulk density and the concentration of Cs-137 in the topsoil. After comparing the results from the Cs-137 method and volumetric estimates, they concluded that Cs-137 could be used to estimate the long-term average soil erosion and deposition rates. Lowrance et al. (1988) further changed the Gravimetric Approach method. They used undisturbed forest as their reference site to estimate soil erosion and deposition rates in cultivated land. Lowrance et al. (1988) found deposition rates to be much higher than the erosion rates for their study area.

A limitation of the Gravimetric Approach is the use of the average soil erosion over the period of record combined with the current Cs-137 content, which will overestimate soil erosion. Another limitation was the model did not predict the deposition rates. In contrast, Ritchie et al. (1975) used Cs-137 to predict deposition rates in a Mississippi valley, which compared favorably with survey data. Robbins and Edgington (1976) built a mathematical model to predict the vertical distribution of deposited Cs-137 and Pb-210 in lake sediments.

2.1.3 Development of the modern Cs-137 conversion models

After the 1980s, additional models were developed to predict soil erosion and deposition rates using Cs-137. Martz and De Jong (1987) used Cs-137 to predict the soil erosion by water and wind for cultivated land in Canada based on grid sampling of a 1.8 km^2 cultivated watershed. They calculated the net soil erosion and deposition, which was the difference between total soil losses minus the total soil gain using:

$$E_{net} = D_p \rho_b \frac{0.95R_c - R_s}{0.95R_c} \qquad \text{For erosion sites} \qquad (4)$$

$$E_{net} = -\rho_b (D_e - D_p) \qquad \text{For deposition sites} \qquad (5)$$

where E_{net} was the net soil erosion (kg m^{-2}), ρ_b was the average bulk density (kg m^{-3}) of surface soil, D_p was the cultivation layer thickness (0.1m), R_c was the mean Cs-137 fallout input (Bq

m^{-2}) at the reference site, R_s was the Cs-137 activity (Bq m^{-2}) at the sampling site, and D_e was the effective depth (m) to which Cs-137 was present. Rc was multiplied by 0.95 to account for soil loss from snow drifting and deep tillage (Jong et al., 1982). Walling et al. (1986b) used a concept budget model to estimate sediment yield at a basin scale (Figure 3). They suggested that with detailed information, Cs-137 could be used to estimate the sediment yield for a basin scale and the mobility of sediment within the watershed.

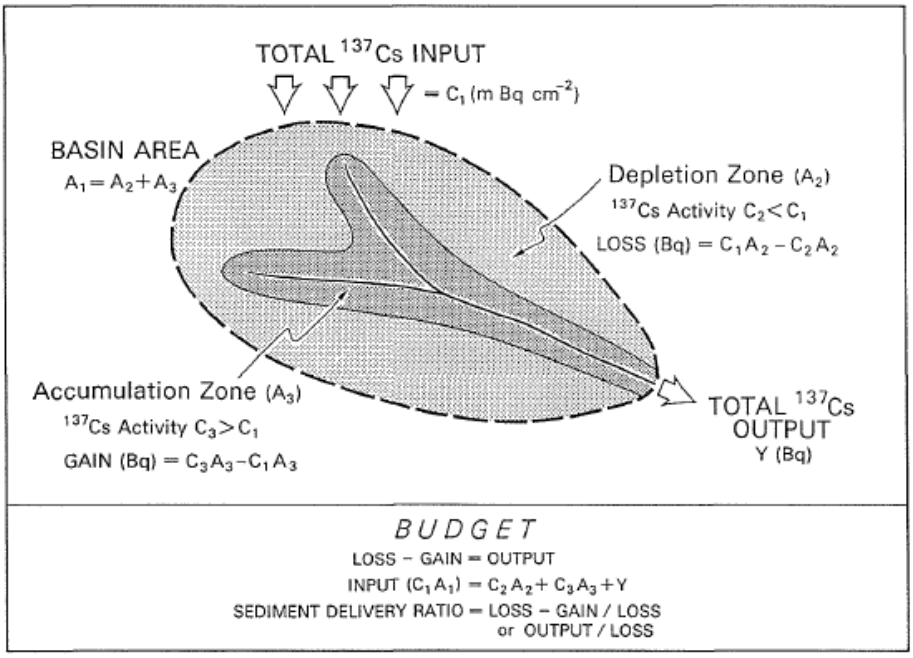

Figure 3 Concept budget model for predicting C-137 movement (Walling et al., 1986b).

Cs-137 has become a useful tool to trace sediment movement, sediment dating and predict sedimentation rates for lakes and reservoirs. Prior research has primarily focused on methods to improve using Cs-137 to estimate soil erosion and deposition. Thus, Cs-137 has become an accepted tool to estimate soil erosion and deposition rates, their spatial distribution, as well as reflecting the effects of topography and land use (Gaspar et al. 2013). The most notable advance was the development of mathematical models to translate measured Cs-137 soil concentrations to

soil erosion and deposition rates. Kachanoski (1987) developed the Proportional Model to predict soil erosion rates of the form:

$$E = \frac{M_s(C_i - C_f)}{(t_i - t_f)C_i} \quad (6)$$

where E is predicted erosion rate (kg m^{-2} yr^{-1}), M_s is specific mass of the plow layer (kg m^{-2}), t_i is the time of initial sampling (yr), t_f is the final sampling time (yr), C_i is the initial total soil Cs-137 corrected for decay time t_i (yr), and C_f is the final total soil Cs-137 corrected for decay time t_f (yr). Kachanoski (1987) recommended adding the temporal changes of Cs-137 to improve the model predictions.

Cs-137 is normally adsorbed onto soil fine particles, i.e. silts and clay. Without accounting for this adsorption, soil erosion rates will be overestimated due to the selective deposition of larger particles. He and Walling (1996) studied Cs-137 adsorption by different soil particles, and found that the concentration of Cs-137 on different size fractions was highly related to the specific surface areas (SSAs) of the fractions. They used the ratio of SSA of mobilized sediment and the original soil to establish the Particle Size Correction Factor (Z), which was used in the Proportional Model to correct for the effects of particle size on soil erosion. The Proportional Model was the most widely used model to predict soil erosion and deposition for cultivated land using Cs-137. The model can also be in the form:

$$Y = 10\ \frac{B\,dX}{100TZ} \quad (7)$$

The limitation of this model was not accounting for newly deposited Cs-137 over time and the subsequent mixing by tillage. When building the Z, it was reported that when the sand proportion increased, the absorption of Cs-137 by sand also increased (He and Walling, 1996). Based on the assumptions of the Proportional Model, the sediment deposition rate can be estimated using:

$$Y' = 10\ \frac{B\,d\,X'}{100\,T\,Z'} \quad (8)$$

$$X' = \frac{(A_{ref} - A)}{A_{ref}} \times 100 \quad (9)$$

where Y is mean annual soil loss (t ha^{-1} yr^{-1}), d is depth of the plow or cultivation layer (m), B is bulk density of soil (kg m^{-3}), X' is percentage increase or reduction in total Cs-137inventory, T is time elapsed since the initiation of Cs-137 accumulation or the commencement of cultivation, whichever is later (yr), A_{ref} is the local Cs-137 reference inventory (Bq m^{-2}), A is measured total Cs-137 inventory at the sampling point (Bq m^{-2}), Z is particle size correction factor for erosion, and Z' is particle size correction factor for deposition.

The Proportional Model is a simple and easy method since it only needs the depth of the tillage layer, and Cs-137 soil concentrations for the erosion/deposition sites and the reference sites. However, this model assumes uniformly distributed Cs-137 in the tillage layer, and the concentration of Cs-137 is constant with time. In fact, new Cs-137 deposits on the surface through precipitation, mixed by plowing, and then removed by erosion plow. Moreover, the tillage depth is typically constant for a given field and thus as soil erosion occurs plowing introduces new low concentration Cs-137 soil at the bottom of the plow depth. Therefore, the model would underestimate the erosion and deposition rates.

Mass-balance models attempt to overcome the limitations of proportional models by accounting for the decay of Cs-137 through time, continuous input of Cs-137 through precipitation and the mixing of soil from below the original plow layer. The original mass-balance model was developed for cultivated land by Kachanoski and de Jong (1984) using the equation:

$$\frac{\partial A_t}{\partial t} = D_t - E_t K_2 C_t - K_1 A_t \quad (10)$$

where A_t is the total Cs-137 in plow layer (Bq m^{-2}), E_t is the average erosion rate (kg m^{-2} yr^{-1}), K_1 is the radioactive decay constant for Cs-137 (0.023 yr^{-1}), K_2 is the enrichment coefficient, C_t is the concentration of Cs-137 in the plow layer (Bq kg^{-1}), and D_t is the average atmospheric

deposition rate of Cs-137 (Bq m^{-2} yr^{-1}). This model is only suitable for areas that have soil erosion rates between 0.5 to 10 kg m^{-2} yr^{-1} and requires a simulation period of 15 to 20 years to achieve relative errors less than 20% (Kachanoski and de Jong, 1984). The model was further modified by Zapata (2002):

$$\frac{dA(t)}{dt} = I(t) - \left(\lambda + \frac{R}{d_m}\right)A(t) \quad (11)$$

where A(t) is cumulative Cs-137 activity per unit area (Bq m^{-2}), t is time since the onset of Cs-137 fallout (yr), R is erosion rate (kg m^{-2} yr^{-1}), d_m is the average plow depth represented as a cumulative mass depth (kg m^{-2}), λ is decay constant for Cs-137 (yr^{-1}), and I(t) is the annual Cs-137 deposition flux at the time t (Bq m^{-2} yr^{-1}).

Based on the mass-balance model, Zhang et al. (1990) created a simplified mass-balance model for cultivated land from loess regions of China in the form:

$$X = Y_R\left(1 - \frac{\Delta H}{H}\right)^{N-1963} \quad (12)$$

where X is the measured caesium-137 amount in profile (Bq m^{-2}), Y_R is the base level input in the reference site (Bq m^{-2}), ΔH is depth of annual soil loss (t ha^{-1} yr^{-1}), H is the depth of plow layer (cm), and N is the year of sampling (yr). Their model assumed:

i. The total Cs-137 input occurred in 1963,
ii. The eroded soil is replaced by soil below the original plow depth,
iii. Erosion rates are constant over time. and
iv. The content of Cs-137 is not be affected by plant uptake and fertilization.

Erosion sites were determined by comparing the total Cs-137 from the sampling point to the local reference inventories. A limitation of this method is the total Cs-137 is assumed to be equal to the Cs-137 deposited in 1963, which is not realistic. In addition, it does not account for newly deposit Cs-137, which would be removed before mixing in the plow layer.

Walling and He (1999) improved the original mass-balance model into a comprehensive model, referred to as the refined or improved mass-balance model. The original mass-balance model assumed that the newly deposited Cs-137 was well mixed in the plow layer, and did not account for the temporal input of Cs-137. The improved model accounted for both erosion and deposition sites, with the governing equations:

$$\frac{dA(t)}{dt} = (1 - \Gamma)I(t) - \left(\lambda + Z\frac{R}{d}\right)A(t) \quad (13)$$

$$A_{c,ex} = \int_{t0}^{t} R'C_d(t')e^{-\lambda(t-t')}dt' \quad (14)$$

where A(t) is the cumulative Cs-137 activity (Bq m^{-2}), R is the erosion rate (kg m^{-2} yr^{-1}), d is the cumulative mass depth representing the average plow depth (kg m^{-2}), λ is a decay constant for Cs-137 (yr^{-1}), I(t) is the annual Cs-137 deposition flux (Bq m^{-2} yr^{-1}), Γ is percentage of the freshly deposited Cs-137 fallout removed by erosion before being mixed into the plow layer, Z is a particle size correction factor, $A_{c,ex}$ is the excess Cs-137 inventory (Bq m^{-2}), R' is the deposition rate (kg m^{-2} yr^{-1}), $C_d(t')$ is the Cs-137 concentration of deposited sediment at the year t' (Bq kg^{-1}), t is the sampling year (yr).

Compared to the simplified mass-balance model, the improved mass-balance model accounted for the temporal variation of Cs-137 input to the surface soil. This model also used the total input Cs-137 instead of using only the Cs-137 in 1963. Although the improved mass-balance model considered the soil mixing by tillage, this model did not take into account the movement of sediment within the watershed. Research showed that soil redistribution from the tillage erosion could not be neglected in the cultivated land especially in hilly areas (Li et al., 2006; Tiessen et al., 2009). Walling and He (1999) developed an improved mass-balance equation accounting for soil redistribution by tillage. For the erosion sites, the equations are:

$$\frac{dA(t)}{dt} = (1 - \Gamma)I(t) + R_{t,in}C_{t,in}(t) - R_{t,out}C_{t,out}(t) - R_wC_{w,out}(t) - \lambda A(t) \quad (15)$$

$$R = R_{t,out} - R_{t,in} + R_w \quad (16)$$

And for deposition sites the equations are:

$$\frac{dA(t)}{dt} = I(t) + R_{t,in}C_{t,in}(t) - R_{t,out}C_{t,out}(t) + R'_w C_{w,out}(t) - \lambda A(t) \quad (17)$$

$$R = R_{t,out} - R_{t,in} - R'_w \quad (18)$$

where A(t) is the total Cs-137 inventory at time t (Bq m^{-2}), t is the time (yr), $R_{t,in}$, $R_{t,out}$ and R_w are the erosion rates caused by tillage input (soil taken into the field by tillage), tillage output (soil taken away from the field by tillage) and water (kg m^{-2} yr^{-1}), respectively, R is the net erosion rate (kg m^{-2} yr^{-1}), R'_w is the water deposition rate (kg m^{-2} yr^{-1}), $C_{t,in}$, $C_{t,out}$ and $C_{w,out}$ are the Cs-137 concentrations of the sediment associated with tillage input, tillage output and water output (Bq kg^{-1}), respectfully, $C_{w,in}$ is the Cs-137 concentration of the sediment input from water deposition (Bq kg^{-1}), λ is the decay constant for Cs-137 (yr^{-1}), and Γ is percentage of the freshly deposited Cs-137 fallout removed by erosion before being mixed into the plow layer. This model is expected to be more realistic than the other mass-balance models, but is more complicated and requires additional detailed data. Walling and He (1999) compared the proportional model, the original mass-balance model, the improved mass-balance model and the mass-balance model incorporating soil movement by tillage. Figure 4 presents their findings, which show a similar trend with the different models. However, the models predicted different soil redistribution rates at the far upslope areas and the toe.

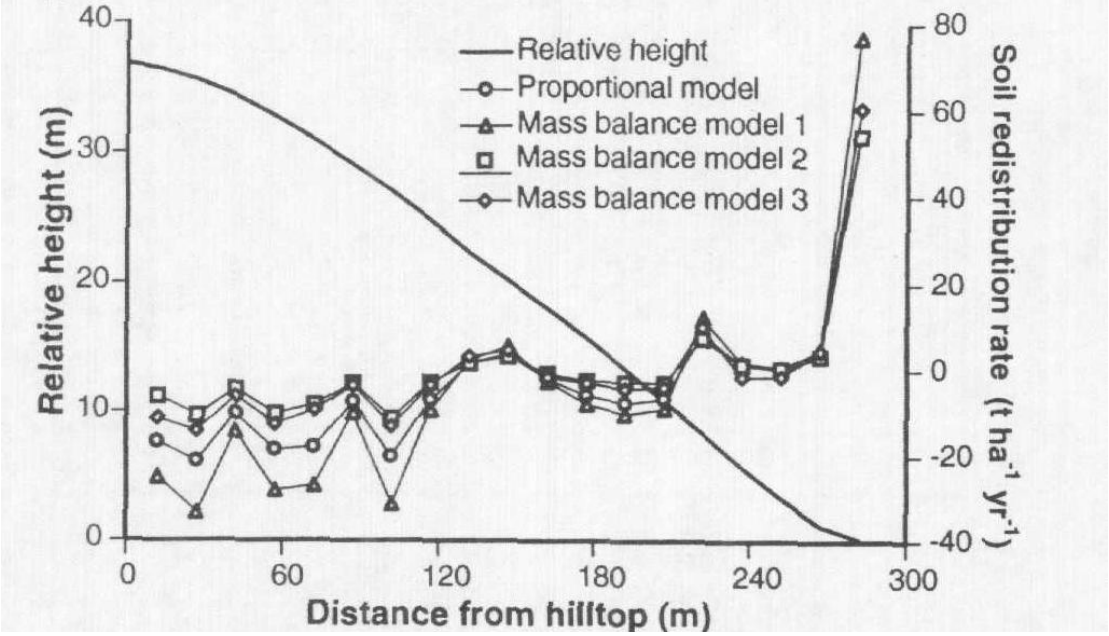

Figure 4 Hill slope erosion distribution predictions from different Cs-137 conversion models for cultivated land: 1) original mass-balance model, 2) improved mass-balance model, and 3) mass-balance model incorporating soil movement by tillage (Walling and He, 1999).

The vertical distribution of Cs-137 in an undisturbed soil is quite different from cultivated land. In an undisturbed soil, Cs-137 concentrates at the surface and typically decreases exponentially with depth (Walling and Quine, 1992). Methods to estimate soil erosion and deposition rates for undisturbed soils using Cs-137 include the profile distribution and the diffusion and migration models. The profile distribution model was developed using the same assumptions as the simplified mass-balance model, and thus may overestimate the soil erosion rates. The profile distribution model also assumes that the vertical distribution of Cs-137 in undisturbed soil decreases exponentially with depth. However, current undisturbed soil profiles will typically have a peak Cs-137 concentration a few centimeters below the soil surface as a result of vertical migration and biological processes (He and Walling, 1997). This may also be the

result from lower Cs-137 atmosphere inputs after the 1980s, with the exception of nuclear plant accidents (Owens et al., 1997).

He and Walling (1997) used measured data to build a vertical soil migration model for Cs-137. By comparing a measured Cs-137 profile with a reference site profile(s), the soil loss can be predicted. This model was further used to establish the diffusion and migration model. Walling and He (1999) compared the two models for undisturbed soil (Figure 5). The results from the two models were significant different. The authors argued that the differences may due to that the diffusion and migration model can reflect the effects of particle size, while the profile distribution model cannot. However, the diffusion and migration model needs more information and high quality input data, because the model is sensitive to its parameters, such as D (diffusion coefficient), V (downward migration rate of Cs-137), and H (depth of plow layer).

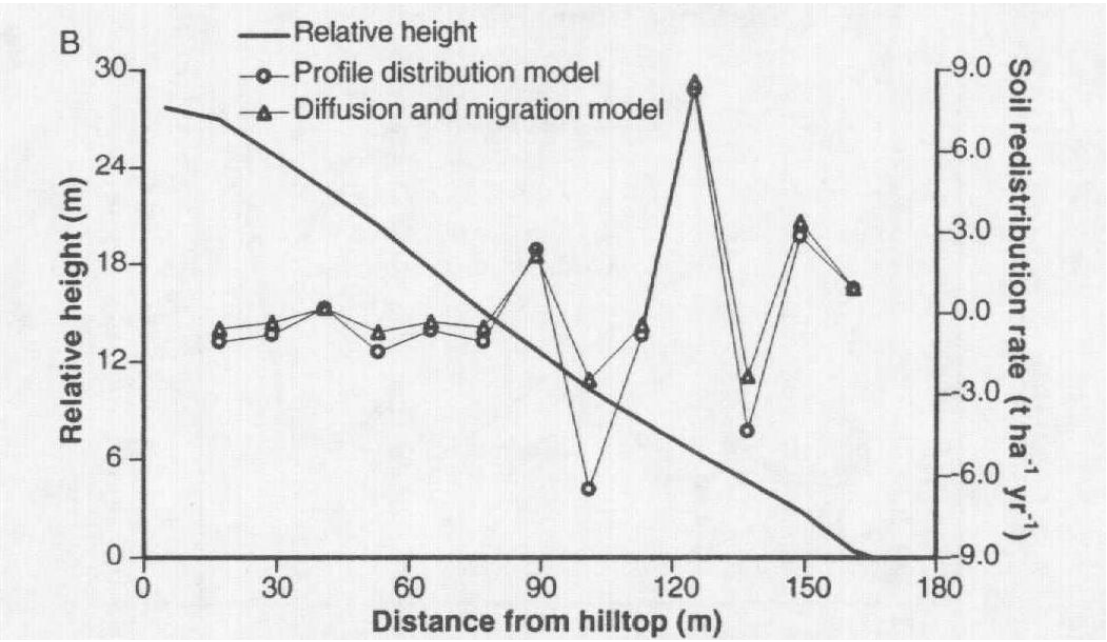

Figure 5 The soil erosion rates calculated using two different converting models for rangeland: 1) Profile distribution model, 2) diffusion and migration model (He and Walling 1999).

Since the profile distribution model was oversimplified and the diffusion and migration model was difficult to use. Zhang et al. (2008) developed a simplified Cs-137 transport model to estimate soil erosion rate for undisturbed land. In this model, only the diffusion of Cs-137 was considered, because the migration rate was tested to be small (Shinonaga et al., 2005). Soil erosion rate was estimated using:

$$A_{rm(T)} = \int_{H}^{+\infty} \frac{A_{rm(T-1)} e^{-\lambda}}{\sqrt{\pi DT}} e^{\left(-\frac{z^2}{4DT}\right)} dz \quad (19)$$

where $A_{rm(T)}$ is the remained Cs-137 inventory in profile in the sampling year (mBq cm^{-2}), T is the time from 1963 (yr), H is the annual soil loss depth during the period from 1963 to the sampling year (cm), λ is the Cs-137 decay rate (0.023 yr^{-1}), z is the depth (cm), D is the effective diffusion coefficient (cm^{-2} yr^{-1}).

This model improved the profile distribution model. Profile distribution model overestimated the soil erosion rates. From the new model, the soil erosion rate was 56.2 to 57.9% of the old model. However, the total deposition of Cs-137 was also assumed to be in 1963 as the profile distribution model. It also assumed that the erosion rate was similar each year. The data used to estimate some of the parameters were measured in China in empirical forms, which may not be used for other areas.

To note that these models did not considered the Cs-137 input from the nuclear accident at Chernobyl in 1986. About 10% to 16% more of the Cs-137 was put into the environment from this accident in Europe (Matisoff and Whiting, 2011). However, little of this Cs-137 was detected in North America (Roy et al., 1988) and near zero of the Cs-137 was transferred from atmosphere (Quine, 1995). Accordingly, the above models can be used in the United States without considering the effects of the Chernobyl accident.

Li et al. (2007) conducted a sensitivity analysis on the conversion models for cultivated land and showed that the predicted total erosion rates were sensitive to both the proportion of the annual Cs-137 input (γ) and the particle size correction factor (Z), and not sensitive to the relaxation mass depth of the initial distribution of fallout Cs-137 (H). However, within reasonable γ and Z ranges, the erosion predictions varied by less than 10%. Theocharopoulos et al. (2003) also conducted a sensitivity analysis and found that the plow depth was a crucial input parameter for all the models. The other sensitive parameters were H and γ for the Mass Balance Model II and III, and the tillage flux constant for the Balance Model III.

As can be seen from the review of converting models, to accurately using Cs-137 to calculate soil erosion or deposition rates, correctly obtaining Cs-137 inventory is necessary. The input of Cs-137 can be measured from the reference sites. Selecting the reference sites was the key to successfully using the Cs-137 method (Walling et al., 1986a). The basic principles for selection a reference site include:

i. No soil erosion or deposition in the reference sites, and no upslope flow. The Cs-137 from the reference sites should only be influenced by the atmospheric inputs.
ii. Have continuous vegetation cover since the 1950s.
iii. Grassland or low herb land is the best. Forest sites can be used. However, the precipitation can be redistributed by tree canopy and stem. The forest has been found to have more Cs-137 than adjacent grassland, which will overestimate the soil erosion rates (Kuhn et al., 1984). The adsorption and absorption of Cs-137 by forest plant species would reach up to 10.1% of the total Cs-137 (Noboru et al., 1969).
iv. The reference sites should be in or close to the study area.
v. For a large-scale study, multiple reference sites should be determined. Walling and Quine (1990) showed the Cs-137 distribution in different soil types (Figure 6). Owens et al. (1996) also gave the distribution of Cs-137 for different soil types in England (Figure 7). Their

results indicated that the migration or diffusion of Cs-137 is different according to the soil types.

vi. The Cs-137 in the reference sites should be compared to the available national or global-level deposition data.

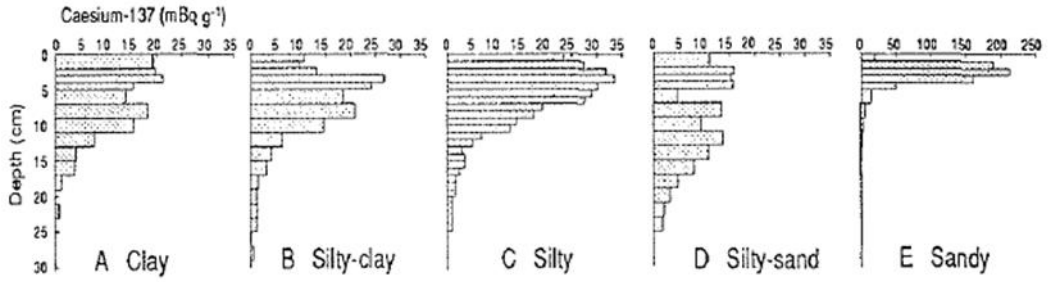

Figure 6 Cs-137 vertical distributions for different soil texture in undisturbed soil (Walling and Quine, 1990).

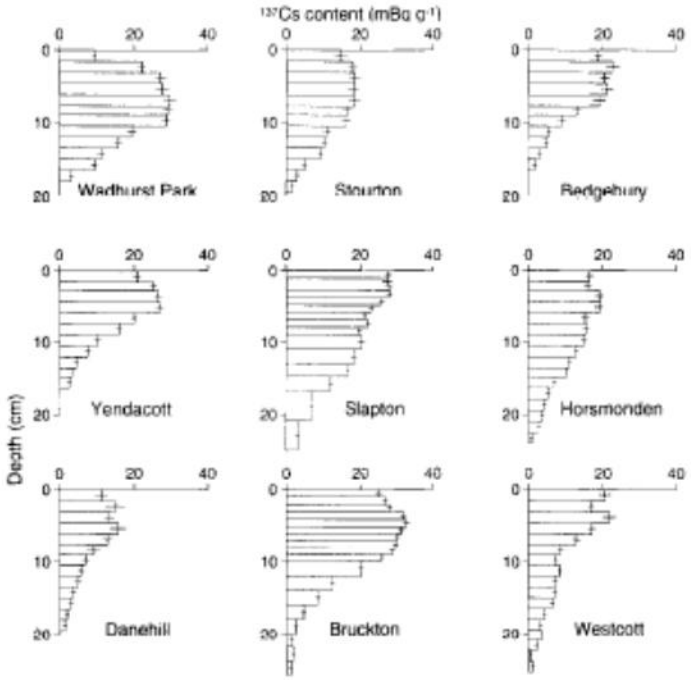

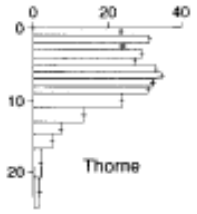

Figure 7 Cs-137 vertical distributions for different soil types in non-eroding uncultivated land (Owens et al., 1996).

However, it is often difficult to find a good reference sites. For the places where it is difficult to find a good reference site, the Cs-137 inventory can be calculated using the model developed by Owens et al. (1996). This mathematical model can be used to estimate the Cs-137 content at the soil surface of stable, non-eroding uncultivated land from the initiation of Cs-137 fallout in the 1950s to the present day. A linear model was also built to calculate the Cs-137 inventory using observed precipitation (Basher, 2000). The problems associated with the variability of Cs-137 inventories at references sites has been discussed and reviewed by Sutherland (1996). Sutherland (1996) collected reference sites information from 70 articles, and discussed the sampling methods used in those articles, and concluded that a minimum of 11 independent samples should be obtained to achieve an error of 10% at a 90% confidence level. Sutherland (1996) also provided the number of samples needed for different levels of variation with an allowable error of 10% at 90% confidence (Figure 8). The number of samples was summarized by Zapata (2002) in Table 1.

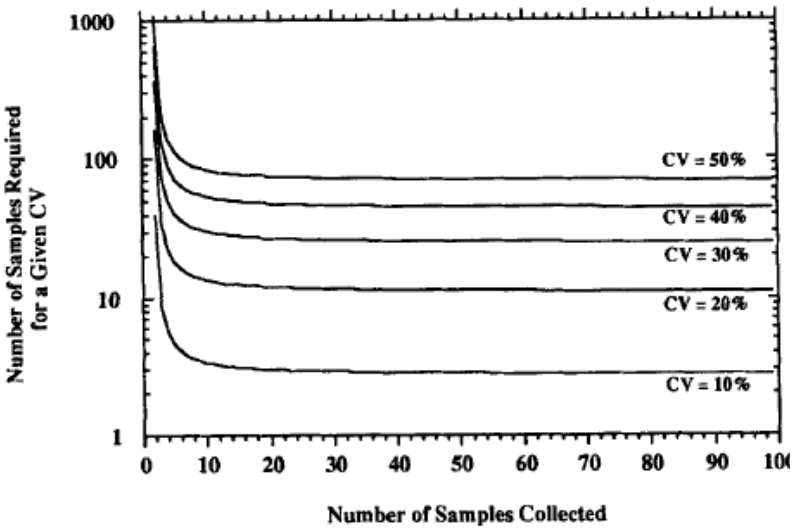

Figure 8 Number of samples needed for different levels of variation with an allowable error of 10% at 90% confidence (Sutherland, 1996). CV is the coefficient of variation.

Table 1 Number of samples needed to achieve a power of 0.80 using a two-sample, two-tailed T-test (Zapata, 2002).

Effective Size (% real difference between means)	Probability of Type I Error (α)			
	0.01	0.05	0.10	0.20
	Number of samples needed for a power of 0.80			
5	376	253	199	145
10	96	64	51	37
15	44	29	23	17
20	26	17	14	10
25	17	12	9	7
30	13	9	7	5
40	8	6	4	3
50	6	4	3	3

2.1.4 Advantages and Limitations of the Cs-137 Method

The advantages and limitations of the Cs-137 method have been discussed by a number of researchers (Sutherland, 1996; Zapata, 2002; Mabit and Fulajtar, 2007; Mabit et al., 2008). The advantages of this method include:

i. Cs-137 can be used to predict medium-term (30 to 40 years) average soil erosion rates for different land scales; extreme events will affect results less.
ii. Due to the wind erosion, it is difficult to directly measure the sediment erosion from cultivate land (Campbell, 1983). When estimating soil erosion or deposition rates, the method can include the influence of both water and wind erosion. It can also reflect the impacts of human and environmental change.
iii. Based on the single point sample; thus minimizing disturbance of the study area.
iv. Provides both the erosion and deposition rates and the spatial distribution for a hillslope or watershed.
v. Sampling is easy and can be cost effective.
vi. Sheet erosion can be included in the predicted soil loss.

Limitations of the Cs-137 method include:

i. Cs-137 decays with time, and thus the Cs-137 in the southern hemisphere is low and needs more time to analysis using gamma analyses.
ii. Nuclear plant accidents can affect the total input globally. This input should be considered when using Cs-137 method; however, most conversion models did not consider this.
iii. May have difficulties when used to estimate the short-term changes caused by land use change or land management.
iv. Predictions highly depend on the measurement at reference sites. Appropriate reference sites are difficult to find for most areas.
v. Gamma spectrometry is expensive.

2.2 Fingerprinting / Source tracking method

Knowing the source for the sediment in rivers and reservoirs is an important for water resource management (Dearing et al., 1990). Collins and Walling (2004) suggested that sediment sources could be estimated indirectly by using soil erosion measurements and directly using the fingerprinting method. The fingerprinting method uses the soil physical and chemical differences within a watershed to calculate the relative contribution of each soil to the sediment in the channels.

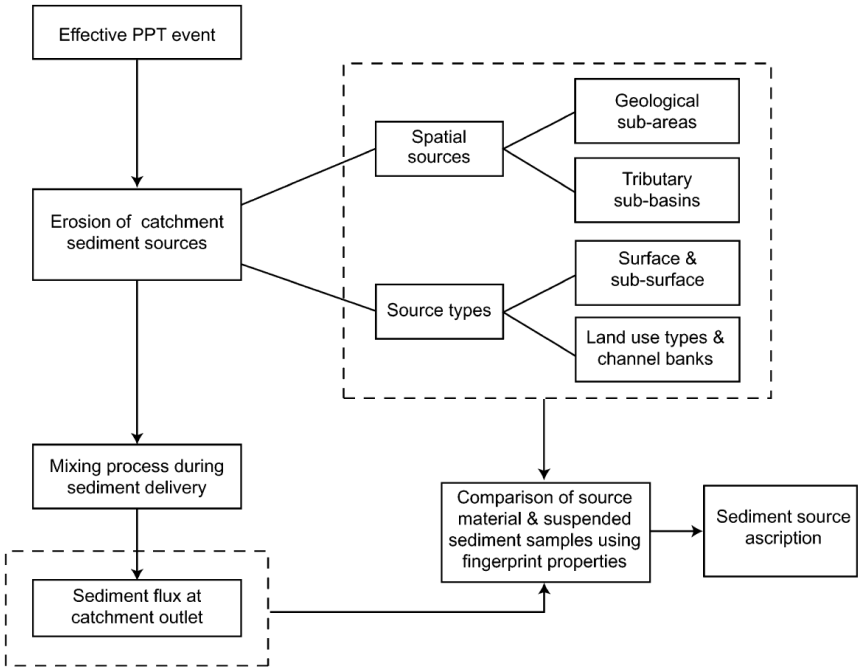

Figure 9 The concept model for fingerprinting method (Collins and Walling, 2002).

Figure 9 is a conceptual model for the fingerprinting method developed by Collins and Walling (2002). To use the fingerprinting method, sediment sources for the whole watershed or study area must be categorized. The sediment sources can be categorized according to their physical and chemical differences, which include land use, soil types (particle size, organic matters and chemical elements), radionuclides, minerals, geochemical, etc (Collins et al., 1997b). Next,

statistic methods are used to select parameters that reflect the differences. Walling et al. (1999) used the Kruskall-Wallis H-test to select elements that were significant different between the sources, and then use the Discriminant Function Analysis (DFA) to choose the least number of chemicals needed to present the most acceptable variance. The stepwise selection algorithm, Wilks' lambda or U-statistic, was chosen for the DFA. Normally, more than one parameter should be selected (Peart and Walling, 1986). The next step is to use a mixing model to calculate the contribution of each source type. Koiter et al. (2013) summarized the publications that used the fingerprinting method to predict sediment sources. Figure 10 illustrates the dramatic increase in the use of the fingerprinting method in recent years.

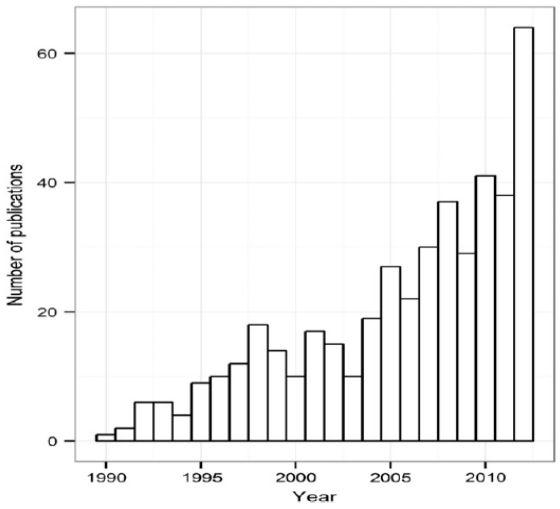

Figure 10 Number of publications using the fingerprinting method between 1990 and 2013 (Koiter et al., 2013).

To calculate the source contribution for the sediment, the mixing model was selected. The original mixing model was (Long et al., 2012):

$$S_k = \sum_{i=1}^{n} S_{ki} b_i \ (k = 1 \ldots n-1) \tag{20}$$

$$\sum_{i=1}^{n} b_i = 1 \quad (21)$$

where S_k is the concentration of k type of tracer in the sediment, S_{ki} is the concentration of k type of tracer in i type of soil sources, b_i is relative contribution from i type of source soil.

In reality, chemicals are more absorbed to fine soil particles, and isotopes like Cs-137 and Pb-210 are associated with the organic fraction (Wallbrink et al., 1997). Therefore, the chemical concentrations should be corrected based on particle size and organic matter. Mizugaki et al. (2006) developed the following equation to calculate the radionuclide activity associated with the soil samples:

$$C_m = \frac{C_{total} - C_{om} OM}{1 - OM} \quad (22)$$

where C_{total} is the total radionuclide activity associated with the sediment or potential source material, C_{om} is the radionuclide activity associated with the organic fraction, OM is the organic matter content of the sediment or potential source material. For this method, the organic matter must be extracted from soil samples and tested for radionuclide activity. Collins et al. (1997a) created an organic carbon content correction factor to reflect the effect of organic matter for all chemical concentration in the soil samples. The organic carbon content correction factor was the ratio of sediment sample organic carbon content to mean organic carbon content for each source type.

Particle size corrections were also built for isotopes and other chemicals. He and Walling (1996) developed the following equation to estimate the particle size correction factor, Z:

$$Z = \left(\frac{S_{ms}}{S_{sl}}\right)^{v} \quad (23)$$

where S_{ms} and S_{sl} are the SSAs of the mobilized sediment and original soil, respectively, and v was a constant with a value of 0.65 for Cs-137 and 0.76 for Pb-210. This equation was created based on data from cultivated soil from Jackmoor Brook, Devon, UK.

Collins et al. (1997a) used the ratio of sediment sample SSA to mean SSA for each source type as the particle size correction factor. Collins et al. (2010) also studied the influence of within-source variability of tracer property values and the discriminatory power of those properties. They added weighting factors representing the within-source variability of fingerprint property (SV_{si}) and the tracer discriminatory weighting (W_i) to reduce the uncertainty ranges in the sediment source contributions. SV_{si} was estimated using the inverse of the root of the variance associated with each fingerprinting property measured for each source. W_i was based on information on the relative discriminatory efficiency of each individual tracer included in any given composite fingerprint provided by the results of the DFA. However, since organic matter was also correlated with the particle size, when using both particle size and organic matter corrections at the same time, the results will overcorrect (Motha et al., 2004).

The fingerprinting method only needs a small amount soil and can be used for different scales studies. The sampling is easy and quick, and the channel bank and gully erosion can also be predicted (Zhang et al., 2007). With detailed measurement, the sources for long-term sediment and each discharge can be predicted. Froehlich and Walling (2005) studied a30-year data set for a mountain basin area. They used the fingerprinting method, and successfully predicted the potential source materials for different rainfall intensities. However, the fingerprinting method is under two assumptions: first, there are significant differences among the physical or chemical properties of the source types; and second these characters can be reflected in the certain sediment properties. If there is no significant difference among the soil properties, the method cannot be used. Isotopes are mostly used by the fingerprinting method to identify the different source types due to their strong adsorption with soil particles and significant different

concentrations in sources types (Long et al., 2012). One problem for using isotopes for this method is to collected adequate amounts of suspended sediment samples. Some researchers pumped liters of water and extract the suspended sediment, although it is difficult for a large watershed or many rainfall events (Motha et al., 2003, Mizugaki et al., 2008). Sediment traps or samplers, and flood plain, lakes, or channel bed sediment were often used as the suspended sediment (Phillips et al., 2000, Walling et al., 2008, Wilson et al., 2008). Another disadvantage of the fingerprinting method would be the limitation for the number of source types. Lees (1997) manually mixed the soil sources and then using the fingerprinting method to calculate the source contribution. The results showed that the fingerprinting method predicted the two sources best, and when the number of sources increased from three to six, the fail chances increase from approximately 25 to 100%. Lees' results are given in Figure 11.

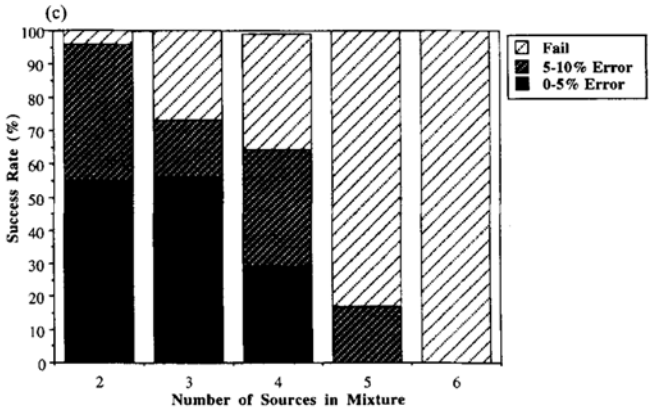

Figure 11 The fail rates for the mixing experiments regarding different number of sources - comparing fingerprinting method and the actual mixing proportion (Lees, 1997).

2.3 Soil erosion models

Soil erosion models are important tools for quantification of soil erosion and evaluating soil conservation practices. Use of soil erosion model is low-cost and faster method compared to

field measurement, especially for large areas. The main spatial scales for soil erosion models are hillslope or plot scale, small watershed scale, and basin or region-scale.

2.3.1 Field scale models

The earliest soil erosion model used only slope and slope length to calculate soil loss for the soil erosion study plots (Zingg, 1940). Smith (1941) added the cover factor (C) and conservation support practice factor (P) into the model, and built the basis for the Universal Soil Loss Equation (USLE) (Wischmeier, 1959). The USLE was developed using plot data to predict gross erosion at the field scale. In 1997, the Agriculture Handbook No.703 published the Revised USLE (RUSLE) (Renard et al., 1997). USLE and RUSLE have been the most widely used soil erosion models. The first process-based model was Chemicals Runoff Erosion in Agricultural Management Systems (CREAMS) (Knisel, 1980) followed by the Erosion-productivity Impact Calculator (EPIC) model. Another process-based model was Misra et al. (1996), developed to predict soil erosion and deposition for a single event.

2.3.2 Small watershed scale models

Development of soil erosion models for small watershed scale began in the 1980s. Beasley el al. (1980) built the Areal Nonpoint Source Watershed Environment Response Simulation (ANSWERS), which was a distributed parameter model. Arnold et al. (1990) published the SWRRB model to predict the sediment yield from rural watersheds. Based on SWRRB, the Soil and Water Assessment Tool (SWAT) was developed to predict the water resource and the nonpoint-source pollution at a basin scale in the early 1990s (Williams et al., 1999). The sediment model used in SWAT was the Modified USLE (MUSLE). MUSLE used used data collected at watershed outlets and the rainfall energy factor was replaced by the product of runoff volume and peak discharge to predict sediment yield.

2.3.3 Both field and small watershed scales models

SLOSS was a process-based model of erosion and deposition, which was used in the Hydrology and Sedimentology Watershed Model II (SEDIMOT) model (Wilson et al., 1984). The SEDIMOT II model was developed to estimate the hydrology and sedimentology of small watersheds to predict sediment yield. This model considered the particle size distribution and the effects of three sediment control structures (including detention ponds, grass filters, and porous check dams). The European Soil Erosion Model (EUROSEM) was also a dynamic distributed model applied at both field and watershed scales (Morgan et al., 1998) predicting rill and interill erosion for a single storm. Another processed based model for both field and watershed scales was Water Erosion Prediction Project (WEPP).

Starting in 1985 the United States Department of Agriculture (USDA) developed WEPP, a process-based soil erosion model to replace the USLE (Foster and Lane, 1987). The first official version of WEPP was published in 1995, WEPP95 (Foster and Nearing, 1995). Updated WEPP versions were published continually and the latest version was released in August 2012 (USDA, 2012). Although the WEPP MS Windows interface can be used to simulate both hillslope and watershed scales, it was difficult to build models for large areas. Therefore, GeoWEPP was created and released in 2001 (Renschler et al., 2002). GeoWEPP linked the WEPP with the Geographic Information Systems (GIS), which allowed the users to use the digital input data directly. A Web-based interface without the GIS can also be accessed through the National Soil Erosion Research Laboratory (Flanagan et al., 2004). Cocbrane and Flanagan (1999) compared the manual WEPP and the GeoWEPP and no significant differences in the predictions.

Flanagan and Laflen (1997) briefly introduced the main components of the WEPP model. Evaluations of the WEPP performance were done by comparing predictions to observed data or

other soil erosion models. Zhang et al. (1996) evaluated the WEPP hillslope model for cultivated land. Field measured runoff and soil loss data from 556 plot-years with 34 cropping scenarios were used to compare the results predicted from WEPP hillslope model. Their results showed that for measured runoff less than 5 mm, WEPP overestimated runoff by 38% for optimized K_b and 28% for estimated K_b; for measured runoff equal or larger than 5mm, WEPP underestimated the runoff by 8% for optimized K_b and 28% for estimated K_b. However, WEPP predicted the average runoff adequately. For soil loss, the model overestimated 65 to 95% of the years when soil loss was less than 0.5 kg m^{-2}, and underestimated 10% of the years when soil loss was larger than 10 kg m^{-2}. When soil loss was between 0.5 and 10 kg m^{-2}, the model predicted reasonably well. Other research gave the similar results (Jetten et al., 1999, Jetten et al., 2003, Pieri et al., 2007).

Tiwari et al. (2000) compared the Nash Sutcliffe model efficiency using 1,600 plot-years data from 20 locations. Although, their results indicated that all the three models (USLE, RUSLE and WEPP) predicted the average annual soil loss very well, the USLE and RUSLE had higher model efficiency compared to WEPP. However, almost all the measured data used in this study were used to build USLE and RUSLE and WEPP was uncalibrated. Laflen et al. (2004) reviewed the evaluations for WEPP and discussed the findings using the new statistical method developed by Nearing (2000). In this study, they concluded that all models would perform well for some locations and not for others; WEPP performed as well as the USLE or RUSLE when uncalibrated. Moreover, WEPP can be used for situations that USLE or RUSLE cannot be used, such as a single event. Research also was done to compare WEPP to other soil erosion models (EPIC and ANSWERS), and the results showed that the overall results from WEPP were better (Bhuyan et al., 2002; Stolpe, 2005).

2.3.4 Basin or region scale models

De Jong et al. (1999) built the distributed regional soil erosion model, SEMMED, for the Mediterranean region. SEMMED combined GIS and RS techniques. Also in the Mediterranean area, Kirkby et al. (1998) used the MEDRUSH model to predict soil loss for uncultivated land at a large scale to estimate the long-term effects of vegetation on soil erosion.

2.3.5 Comparing soil erosion models to Cs-137 method

Busacca et al. (1993) compared the Cs-137 method to RUSLE for cultivated areas, and showed that the erosion and deposition patterns predicted by the Cs-137 method coincided with observed landforms. The net erosion predicted by RUSLE was significantly higher compared to the Cs-137 method. The differences may have been caused by the high Cs-137 concentrations measured at the reference site. On the contrary, Turnage et al. (1997) showed that the Cs-137 method predicted lower net erosion compared to RUSLE for three land use types (crop, grass and forest) and the predicted deposition trend was reasonable. Turnage et al. (1997) suggested that the Cs-137 included the erosion from tillage and gully erosion may be the reason the Cs-137 method had higher net erosion loss. Belyaev et al. (2005) used the Cs-137 method to evaluate the Russian version of USLE. Their results showed that Cs-137 estimated higher net erosion compared to the USLE, but coincided with measured survey data. Martinez et al. (2009) also compared the Cs-137 method with the USLE and the process-based model SIBERIA in Australia. They reported that both the Cs-137 method and SIBERIA predicted soil losses similar to observed data, while the USLE overestimated soil loss significantly. Sparovek et al. (2000) compared the mean and spatial erosion and deposition predicted by USLE, WEPP and Cs-137 method. Their results indicated that USLE predicted the highest erosion rates due to the long and S-shaped slopes. WEPP predicted the lowest

average erosion and its predicted erosion and deposition patterns were reasonable. However, the Cs-137 method reflected all factors that affect erosion like road, gullies, plowing, etc.

Other studies also evaluated differences between the Cs-137 method and the erosion models (Onori et al. 2006, López-Vicente et al. 2008). Because the uncertainties in both the Cs-137 method and erosion models (sampling, reference sites, model parameters, calibration, etc.) and their different erosion processes (e.g. if include gully, tillage, wind effects), it is hard to say which method was better. Bacchi et al. (2003) compared the predicted spatial distribution using the Cs-137 method, USLE and WEPP on a hillslope, which started as a cultivated and was clatter converted to a pasture buffer strip. The results showed that the WEPP predicted the classical water erosion pattern of increasing erosion from the top to the bottom of the hillslope and deposition in the pasture buffer. Bacchi et al. (2003) indicated that WEPP was sensitive to the change of the landcover. USLE cannot predicted deposition and was more sensitive to changes in slope steepness and slope length. The Cs-137 method accounted for deposition, but showed the spatial distribution of erosion and deposition quite differently since the Cs-137 method reflected actual historical influences from the road, terrace construction or maintenance, or plowing operations.

The Cs-137 method has been used to validate spatially distributed models (Sidorchuk and Golosov, 1996). He and Walling (2003) used the Cs-137 method to validate four spatial distributed models: AGNPS, ANSWERS, a topography-based sediment delivery model, and a topography-driven soil erosion model. Their results showed a low agreement between the predicted and observed values. Stefano et al. (2005) successfully validated the spatially distributed sediment delivery model using Cs-137 for a forested basin. They built an empirical model to estimate erosion and deposition using Cs-137 based on the measured data at the basin outlet. The results showed a good agreement at both the hillslope and basin scales. Stefano et al. (2005) indicated that the proper application of the conversion models for Cs-137 method were

an important factor to successfully applying Cs-137 method. Although the Cs-137 method may not always be applied successfully to validate erosion models, it showed potential to provide spatial distributed data to help improve erosion models (Quine, 1999).

CHAPTER III

METHODOLOGY

This chapter provides an overview of the sampling methods, equipment and the soil erosion models, which were used in this research. Soil sampling included surface soil sampling in cultivated land, rangeland and stream channels. Gamma spectrometry, used for testing Cs-137, is also described. Several soil erosion models used to calculate soil erosion rate and sediment investigation are detailed, which were compared to isotope based erosion predictions.

3.1 Fingerprinting method soil sampling

3.1.1 Surface soil sampling for cultivated land and rangeland areas and gullies

Surface soil samples were taken based on soil-land cover categories, which were created by overlaying a SSURGO soil map (Soil Survey Geographic database, 2008) and an NLCD landcover map (National Land Cover Dataset, 2001). There were eleven SSURGO soil types after aggregating slope categories. Soil types are shown in Table 2 and the spatial distribution is given in Figure 12. Five land cover categories were used after creating a rangeland category by combining deciduous forest, evergreen forest and grassland/herbaceous land cover categories (Figure 13 and Table 3). The two primary land cover categories, rangeland and cultivated, were sampled (Figure 14). Although the land cover map was based on 2001 data, land cover did not change in Bull Creek watershed prior to sampling.

Aluminum rings 5 cm in diameter and 2.5 cm deep were used to collect surface soil samples (Figure 15). Each sample was a mixture of 30 sub-samples taken randomly from a contiguous area for each land cover category. Areas larger than 30 ha were subdivided into areas less than 20 ha. Gully soil samples were taken from the top to the bottom of the gully bank face at 10 cm increments. Two gully samples were taken for each channel reach; only one sample was taken at the gully head for channel reach less than 400 m (Figure 16). The location of the sampling areas is given in the Appendix. Soil and landuse maps were uploaded into the GPS (MobileMapper MC-08504-00, Magellan) to help locate the sampling area.

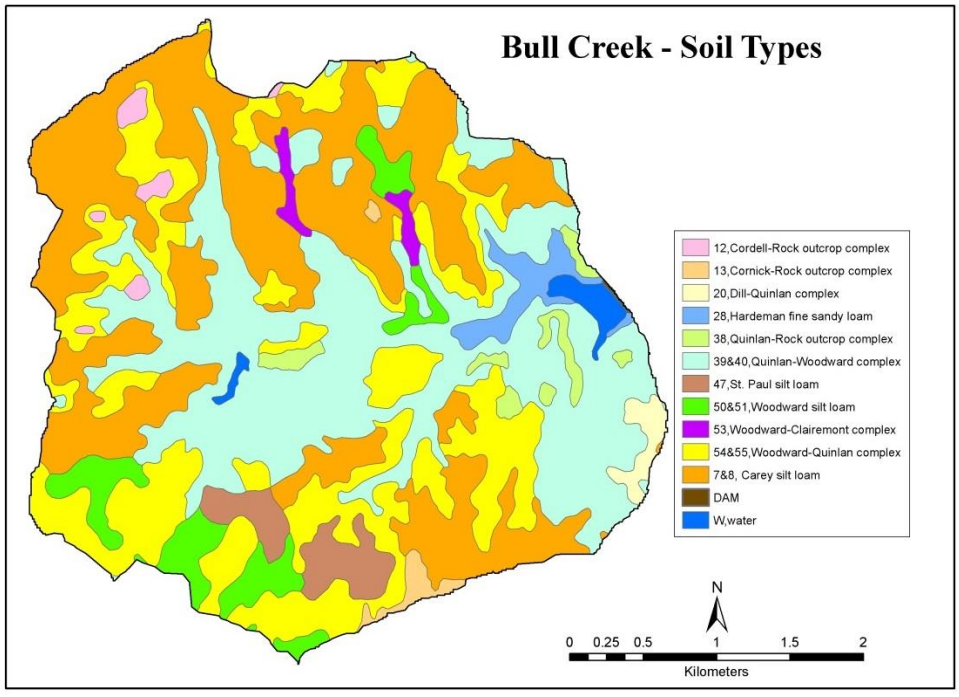

Figure 12 Soil map for the Bull Creek watershed (SSURGO 2.2).

Table 2 SSURGO soil types for the Bull Creek watershed (SSURGO 2.2, 2008)

MUKEY	Soil Types	Area (%)	Combined Area (%) *
7	Carey silt loam, 1 to 3 percent slopes	6	32
8	Carey silt loam, 3 to 5 percent slopes	25	
12	Cordell-Rock outcrop complex, 2 to 15 percent slopes	1	NA
13	Cornick-Rock outcrop complex, 1 to 12 percent slopes	1	NA
20	Dill-Quinlan complex, 3 to 5 percent slopes	1	NA
28	Hardeman fine sandy loam, 3 to 5 percent slopes	2	NA
38	Quinlan-Rock outcrop complex, 8 to 20 percent slopes	2	NA
39	Quinlan-Woodward complex, 3 to 5 percent slopes, eroded	6	29
40	Quinlan-Woodward complex, 5 to 12 percent slopes	24	
47	St. Paul silt loam, 1 to 3 percent slopes	3	NA
50	Woodward silt loam, 1 to 3 percent slopes	2	5
51	Woodward silt loam, 3 to 5 percent slopes	3	
53	Woodward-Clairemont complex, 0 to 12 percent slopes	1	NA
54	Woodward-Quinlan complex, 1 to 3 percent slopes	1	23
55	Woodward-Quinlan complex, 3 to 5 percent slopes	22	

*Areas not combined are marked as NA.

Table 3 Land cover categories for the Bull Creek watershed based on NLCD (2001)

Record Number	Name	Area (km^2)	Area (%)	Combined Area (%)*
11	Open Water	0.16	1	NA
21	Developed, Open Space	0.62	5	NA
22	Developed, Low Intensity	0.01	0.05	NA
41	Deciduous Forest	0.11	1	44
42	Evergreen Forest	0.15	1	
71	Grassland/ Herbaceous	5.56	42	
82	Cultivated Crops	6.73	50	NA

* Areas not combined are marked as NA.

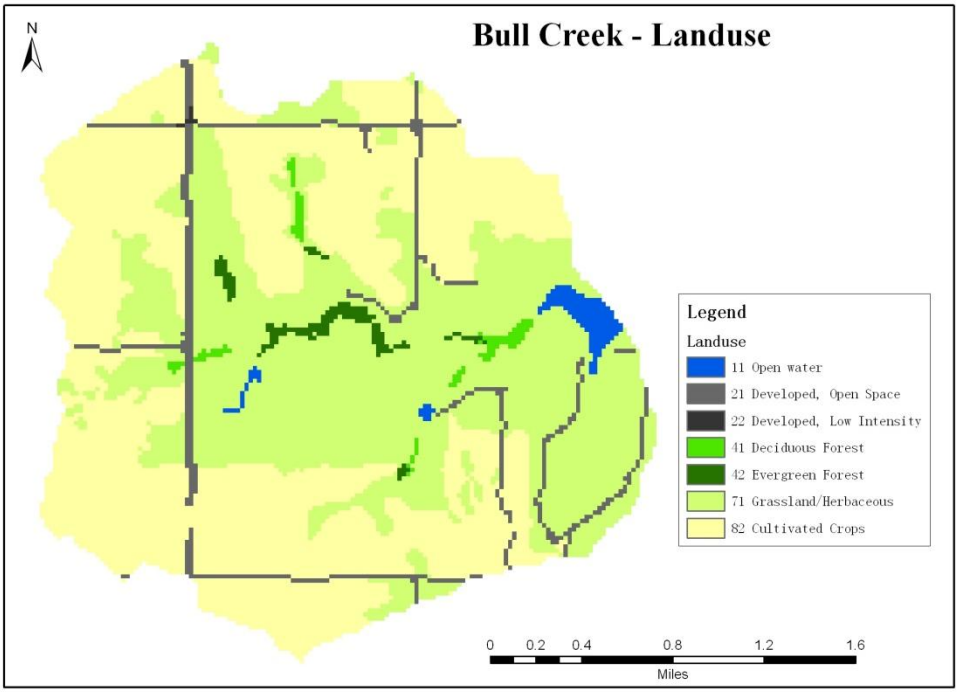

Figure 13 Land cover map for Bull Creek watershed (NLCD).

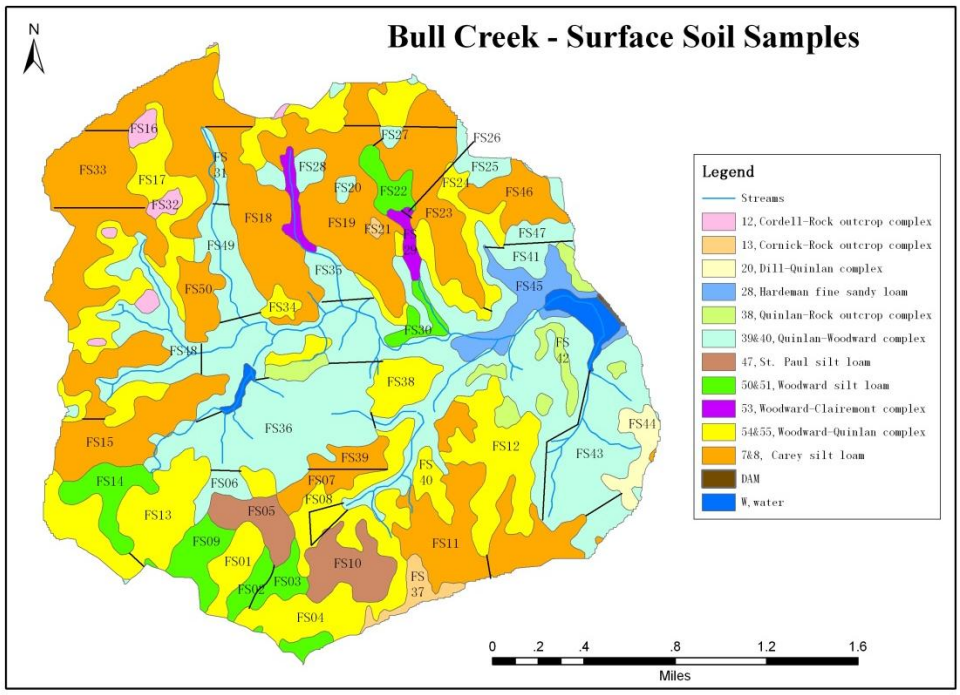

Figure 14 Soil sampling groups for the Bull Creek watershed (background map is SSURGO 2.2 soil map).

Figure 15 Rangeland surface soil sampling using a soil ring.

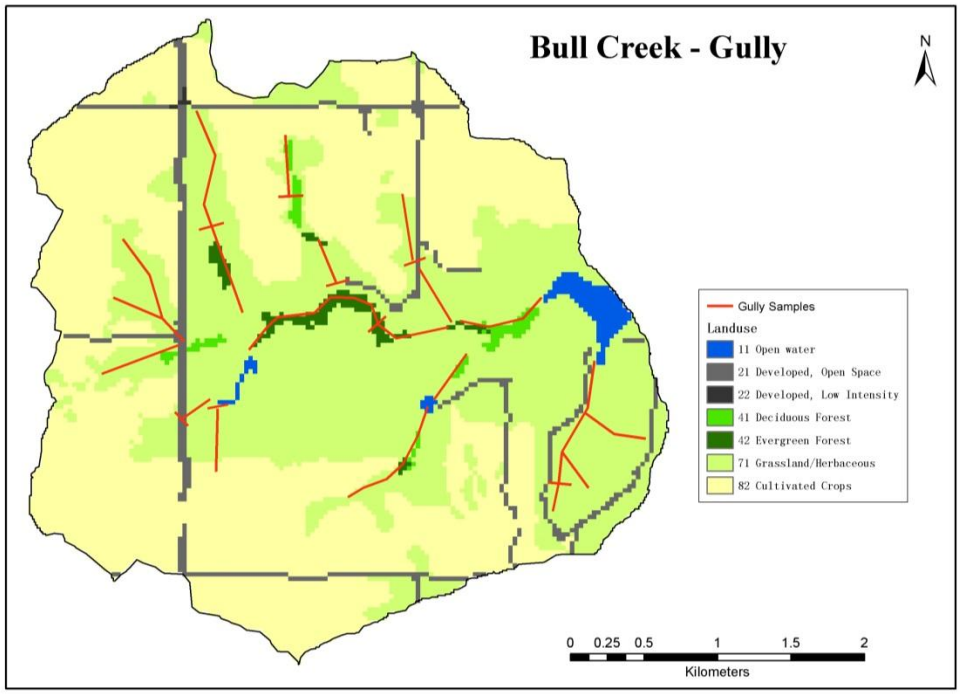

Figure 16 Channel locations of gully sampling for the Bull Creek watershed (background map is SSURGO 2.2 soil map).

3.1.2 Sediment traps and automatic samplers

Sediment traps are a simple and effective method to collected sediment for the fingerprinting method (Phillips et al., 2000, Russell et al., 2000, Walling et al., 2008). In this study, sixteen sediment traps were used to collect data for each rainfall event, and among the sixteen sediment traps, six traps were selected for the fingerprinting method. The sediment traps were located at the end of the gullies were soil samples were taken. The ends of the gully were located at the confluence of a stream channel. Figure 17 illustrates the location of the sediment traps. Figure 18 and Figure 19 illustrate the sediment trap installation; the sediment traps were placed at the bottom of the stream channels and secured using steel bars. Two auto-samplers were also installed in the main stem to collect the runoff and sediment data. However due to the pipe damage from animals, none of these data were usable.

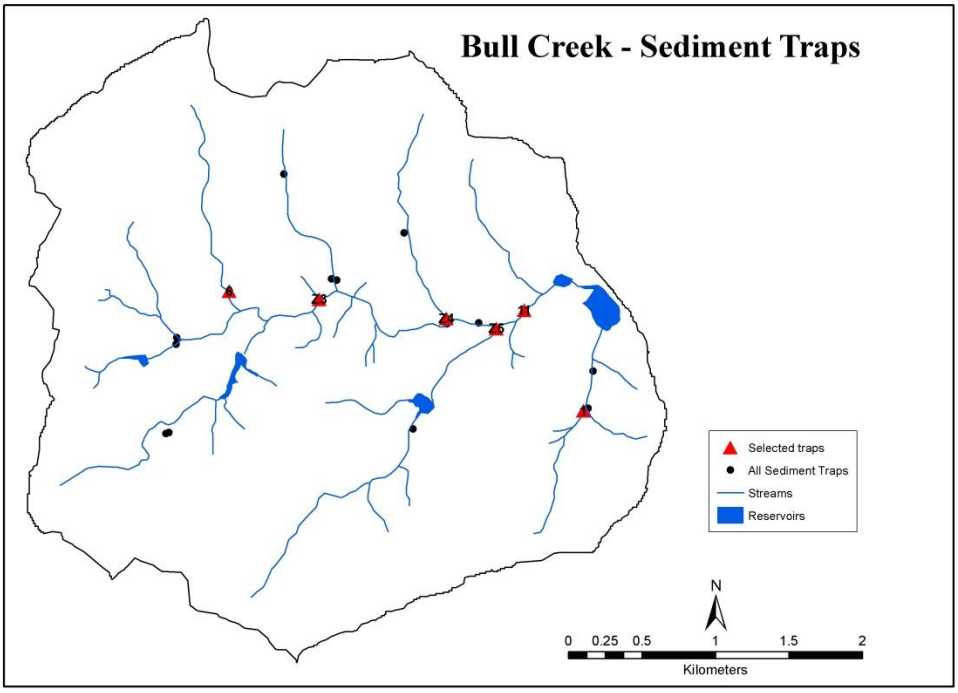

Figure 17 Location of sediment traps and reservoirs sampled in Bull Creek watershed.

Figure 18 Sediment trap installation in the Bull Creek watershed.

Figure 19 Sediment trap installation in a dry stream channel in the Bull Creek watershed.

3.2 Cs-137 soil sampling

3.2.1 Transect soil sampling

A small watershed in the southeast corner of the Bull Creek watershed was selected to collect soil samples along transects (Figure 20). This subwatershed was selected since the area was primarily rangeland and did not have terraces, which disturbed the soil surface and relocated soil. Sampled transect had the same soil and land cover, and the slope and curvature could change along the slope but not across the slope. The Landform Classification (Pennock et al., 1987) in Figure 21, the Topographic Wetness Index (TWI) (Moore et al., 1993) in Figure 22 and slope in Figure 23 were used to help identify typical hillslope. The sampled hillslopes were required to have a uniform slope across the hillslope, which translated into the same TWI across the slope. The landform map was used to help identify convex, concave and relatively flat hillslopes. Transects extended from the top of the slope to the foot or where they reached a gully or road.

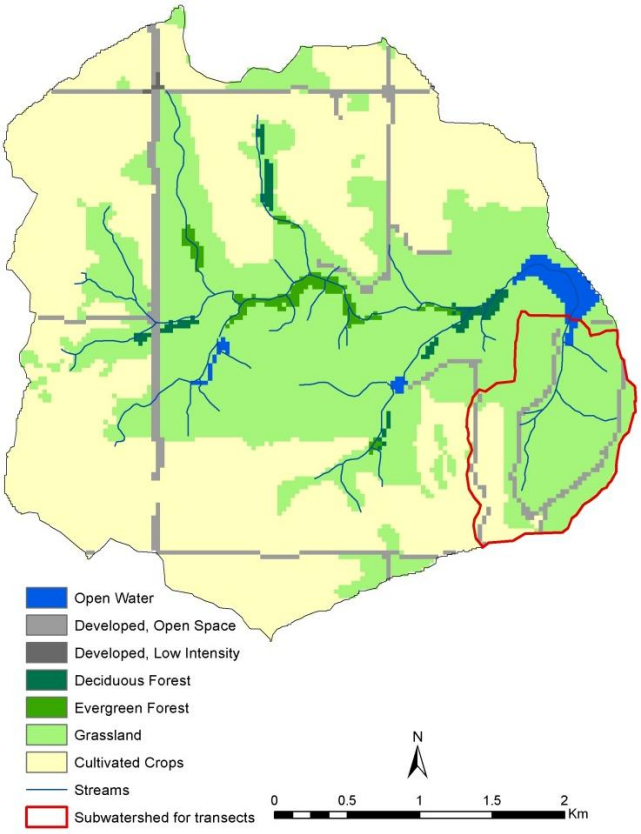

Figure 20 Transect soil sampling subwatershed location in the Bull Creek watershed.

Figure 24 shows the locations of the selected transects, with the geographic locations provided in the Appendix. Transects numbers 1 to 10 were in rangeland and transect number 11 was in cultivated land. Transect 3 was out of the watershed on the map. However, since it was adjacent to our watershed and had the same soil type and land use, it was also sampled for this study. Figure 25 is a photo of transect number 1. Along each transect, soil samples were taken at the slope steepness change points, which resulted in three or four sampling locations per transect. The soil cores were collected using a hydraulic coring device, which was mounted on the side of a truck (Figure 26). At each sampling point along the transect, a 5.0 cm diameter probe was used to take 30 cm soil cores, which were divided into four sub-samples at 5.0 cm increments. Next, six additional soil cores were taken at one-meter increments perpendicular to

the transect; three samples to the right and three samples to the left of the transect. Next, the seven samples were composited by five cm sub-samples, and analyzed for Cs-137 activities, and soil bulk density.

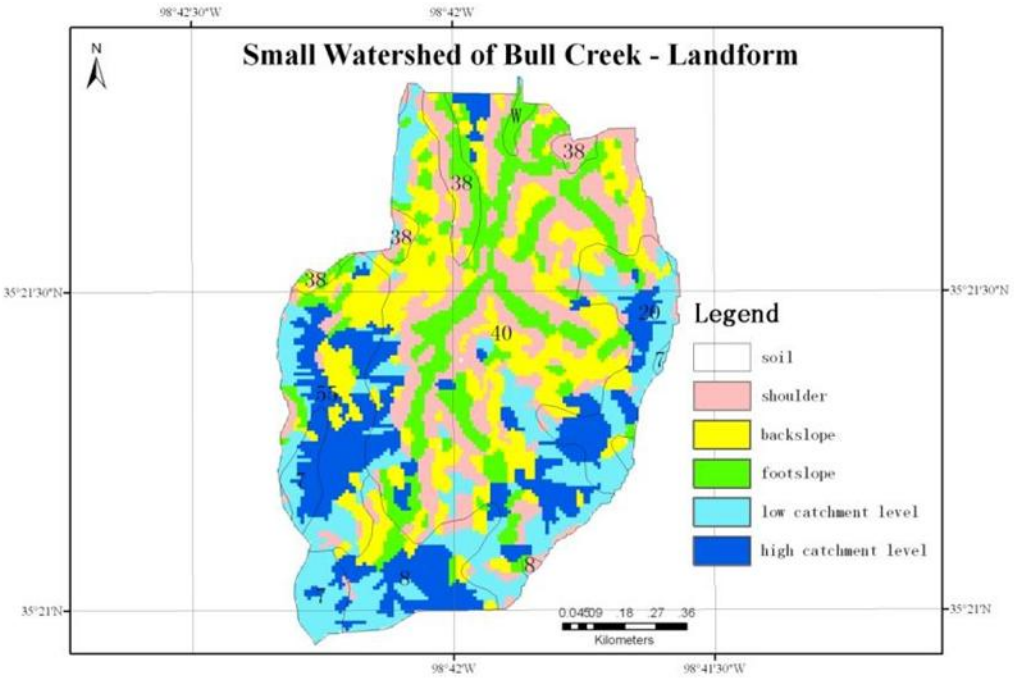

Figure 21 Landforms for the Bull Creek sub-watershed (labels are soil type numbers).

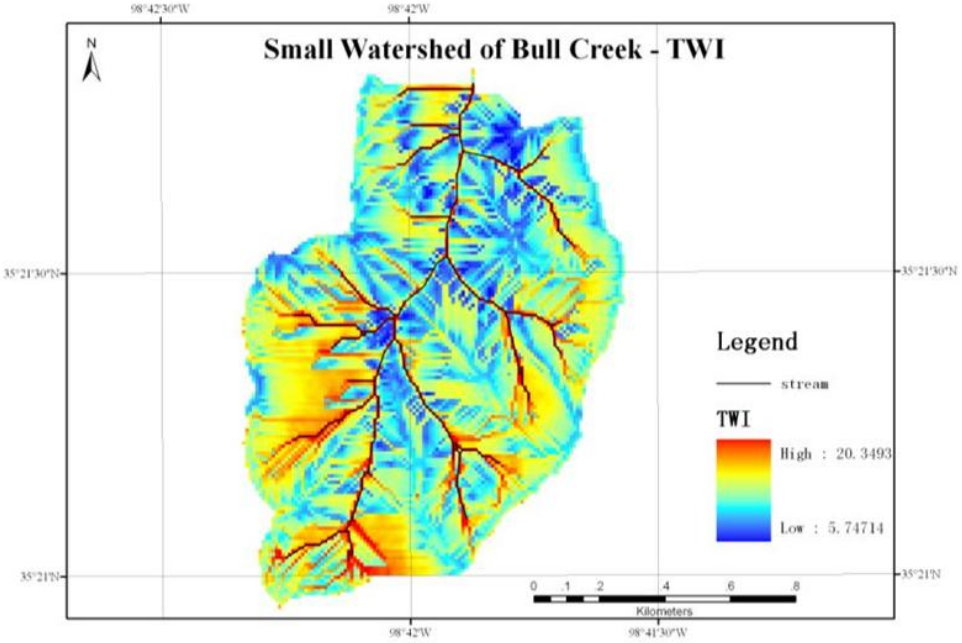

Figure 22 Topographic Wetness Index for the Bull Creek sub-watershed.

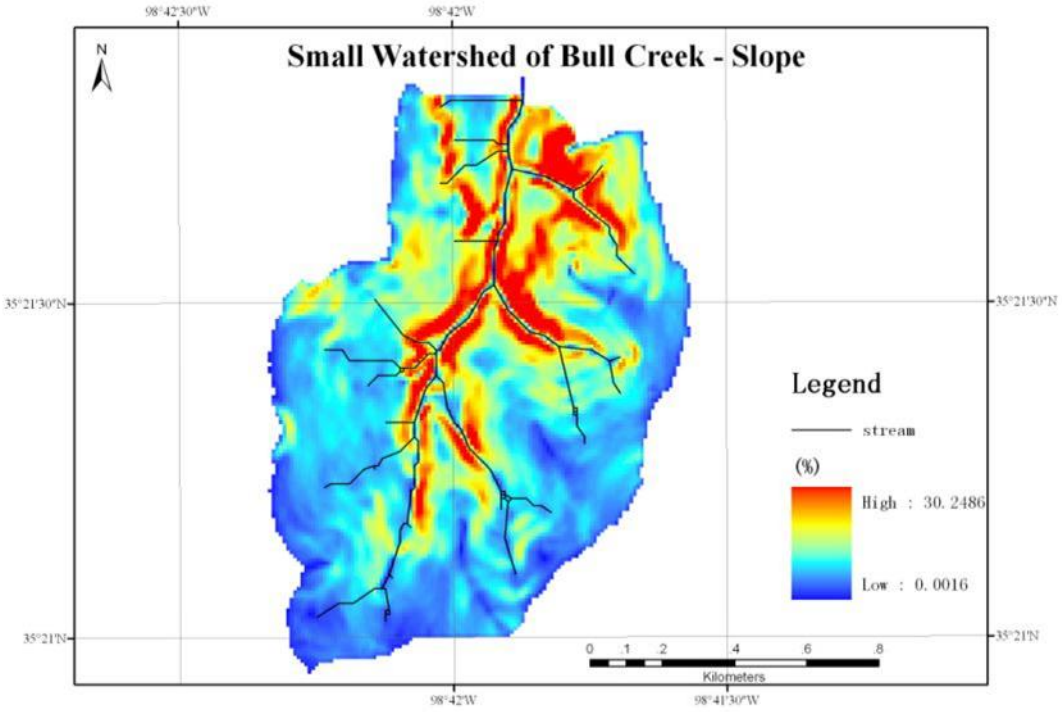

Figure 23 Slope steepness (%) for the Bull Creek sub-watershed.

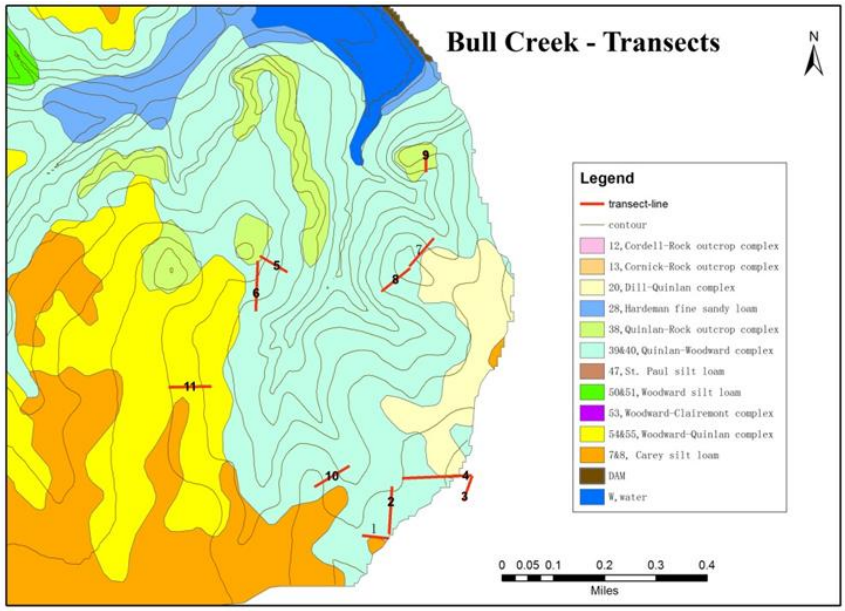

Figure 24 Eleven selected transects in the Bull Creek sub-watershed (background map is soil type map from SSURGO 2.2).

Figure 25 Transect one in Bull Creek watershed (white flags represent the center point where seven sub-samples were taken).

Figure 26 Truck mounted soil probe used to take soil cores along transects.

3.2.2 Reference sites

A reference site was a location where the soil erosion and deposition were assumed negligible. Therefore, Cs-137 activity in the reference site represents the total Cs-137 input for the area. Soil erosion or deposition rates were calculated based on the ration of the sampled Cs-137 activity to that of the reference site. Ideally, reference sites will have no soil erosion and deposition, and have the same amount of rainfall and Cs-137 deposition as the soil sampled areas. For the Bull Creek watershed, suitable reference locations were not available within the watershed and thus locations near the watershed were identified. Two reference sites were selected. The first site was located 2.0 km east of the Bull Creek watershed (N98°40′24.789″, W35°20′41.086″) and was a grassed field in the Town of Colony, Oklahoma that had not been tilled (Figure 27). The second reference site was located 24 km southeast of the Bull Creek watershed (N98°28′55.841″, W35°13′22.996″) and was a state park which has not been disturbed since 1960s (Figure 27).

Figure 28 illustrate the soil sampling method used at the reference sites. A large 45 cm diameter metal ring was pressed into the soil, which had reference marks at increments of 2.5 cm depths. A 5 cm diameter 2.5 cm deep ring was then pushed into the soil in the center of the larger ring, which was removed and used to measure soil bulk density. Next, 2.5 cm of soil was removed from within the large metal ring. This process was repeated at 2.5 cm increments to a total depth of 30 cm. Soil samples at each 2.5 cm depth were analyzed for Cs-137 activity. An additional 15 soil cores 2.4 cm in diameter and 30 cm deep were taken at each reference site using the hydraulic soil probe. Each 30 cm soil core was analyzed separately for Cs-137.

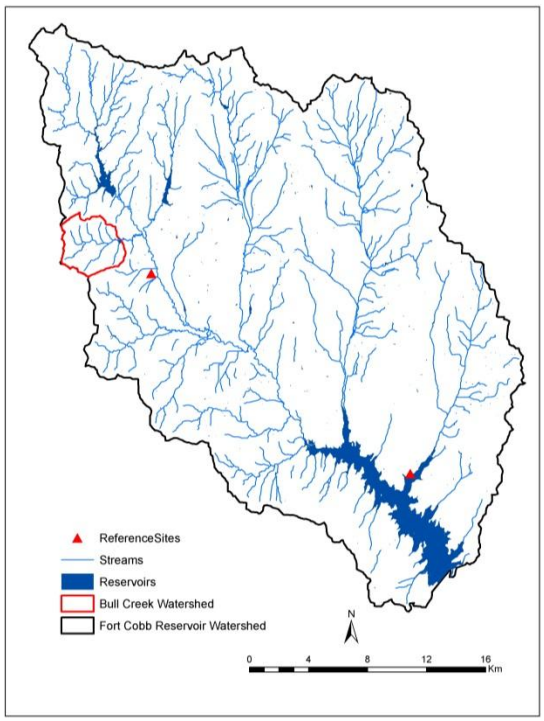

Figure 27 Locations of the two reference sites for Bull Creek.

Figure 28 Reference site soil sampling protocol photographs.

3.3 Soil analysis

3.3.1 Measuring Cs-137 using Gama Spectrometry

The Cs-137 activity of the soil samples was tested by the School of Geography, Beijing Normal University in Beijing, China. Cs-137 activity was measured using gamma Spectrometry using an ORTEC GMX50P4, which used a high purity germanium (HPGe) detector. The detector dimensions were 70 mm in diameter, 30 mm long, 3850 mm^2 area, with a 0.50 mm beryllium absorber layer and a Digital Portable Multichannel Analyzer type DSPEC-jr-2.0. The useful energy range was from 3 keV to 10 MeV, with an energy resolution less than 2.2keV at 1.33 MeV (Co-60) and less than 800eV at 5.9 keV (Fe-55). The peak to Compton ratio (Co-60) was 58:1 and the relative photo peak efficiency was 50% (Radu et al., 2009; ORTEC, 2011).

The process used to test Cs-137 activity was based on the germanium receiving the signal corresponding to the gamma photons being emitted by Cs-137. The detector crystal sends a signal to the Multi-Channel Analyzer (MCA) system, where the emission counts are plotted against the radionuclide energies. The ORTEC MAESTRO Multichannel Analyzer Application Software is used to convert the peak-count information to specific activities (Bq Kg^{-1}) using calibration procedures by Zapata (2002). Becquerel (Bq) is the activity unit or rate of nuclear transformation of radionuclides, i.e. the number of nuclear disintegrations per second. The energy used to test the Cs-137 was 661.66 keV. The counting error of main gamma line was 0.39% with 1σ errors indicated (ORTEC, 2003). Table 4 shows the count rates for Cs-137 based on the sample distances to the HPGe detector (Radu et al., 2009).

Table 4 Cs-137 count rates for different sample distances to the HPGe detector (Radu et al., 2009) for an ORTEC GMX50P4.

Radionuclide	Energy (keV)	Count Rate (counts per second)				
		Distance from Sample (mm)				
		20	50	100	150	200
Cs-137	661.66	101.12	40.90	38.94	11.59	5.27

The peak width was calculated using the Gaussian peak function estimated using:

$$\text{Gaussian} = \text{Ampl} \cdot \exp\left(-\frac{(\text{x}-\text{Pos})^2}{\text{Width}^2}\right) \tag{24}$$

where the Ampl was the amplitude of the peak, Pos was the position of the centroid, x was the channel number, and Width was the peak width parameter. The actual value was determined by the tested peak count or the Cs-137 activity in the soil sample. The full width at half-maximum (FWHM) was calculated using:

$$\text{FWHM} = 2 \cdot \text{Width} \cdot \sqrt{\log(2)} \tag{25}$$

Width for the Cs-137 peak width was approximately 1.4 keV, giving a FWHM of approximately 1.5 keV (Wei, 2007). Pasternack and Harley (1971) computed the lower limit of detection (LLD) for the multi-channel gamma ray spectrometer based on testing and background time, with their results given in Table 5. The background time used to test the soil samples was greater than 30 min and less than 1000 min. The LLD was lower when the background time was longer. The reported minimum detectable activity of Cs-137 for the HPGe detector was 1Bq kg^{-1} (Kannan et al., 2002). The gamma spectrometry was shielded by two 7.6 cm thick lead boxes, which minimized outside effects.

Table 5 LLD (lower limit of detection) computed by Pasternack and Harley (1971) for an ORTEC GMX50P4

Nuclide	Estimated Activity ± standard error (Bq)	LLD (Bq)
	Zero activity, sample counting time 30min, background 30min	
Cs-137	0±0.16	0.56
	Zero activity, sample counting time 30min, background 1000min	
Cs-137	0±0.11	0.37

The mass of soil sample used for the gamma spectrometry was between 300 and 400 g and each sample was tested for 3.3 to 23.3 hours; the time was sample dependent. These parameters were selected by Beijing Normal University with the purpose of achieving the maximum peak activity with a relative error less than 10% (Xie et al., 2010). There were two additional constraints when calculating the Cs-137 activities. First, when the measured error was greater than the net area, the activity was set to zero. Second, when the measured net area was zero or negative, then the activity was set to zero.

3.3.2 Fingerprinting Method Soil Sample Analysis

Geochemical properties were tested by the University of Georgia Laboratory of Environmental Analysis. Soil samples were analyzed using a Perkin Elmer Elan 9000 inductively coupled plasma mass spectrometry (ICP-MS). To prepare the soil samples for the ICP-MS, they were digested using the EPA Method 3050B for acid digestion of sediments and sludges. Walling et al. (2000) analyzed the particle size of the suspended sediment for two basins and found that more than 95% of the suspended sediment was less than 63 μm. Therefore, only soil particles less than 63 μm were tested for the fingerprinting method to mimic the selective transportation of fine particles and the enrichment of fine particles in the sediment. The detailed acid extraction procedures are given in the Appendix. The chemical elements tested included Li, B, Na, Mg, Al, P, Ca, V, Mn, Co, Cu, Zn, As, Sr, Cs-133, Ba, Pb, U-238, Si, Ti, Ge, Br, Zr, Nb, Mo, Sn, and Hf.

3.4 Water Erosion Prediction Project (WEPP)

The WEPP model was used to help evaluate the utility of the Cs-137 and Fingerprinting methods. The WEPP hillslope and WEPP watershed models were used to calculate the soil loss for the transects and the entire Bull Creek watershed, respectively.

The WEPP erosion components calculate both the rill and interrill erosion. The continual sediment movement in a rill was described as:

$$\frac{dG}{dx} = D_r + D_i \quad (26)$$

where G was the sediment load in the flow down a hillslope (kg s^{-1} m^{-1}), x was the distance downslope (m), D_i was the interrill sediment delivery rate to the rill (kg s^{-1} m^{-2}), D_r was the rill detachment or deposition rate (kg s^{-1} m^{-2}).

The WEPP interrill erosion results from rainfall splash. The interrill sediment delivery rate D_i was estimated using:

$$D_i = K_i I_e^2 G_e C_e S_f \quad (27)$$

where K_i was the interrill erodibility (kg s^{-1} m^{-4}), I_e was the effective rainfall intensity (m s^{-1}), G_e was a ground cover effect adjustment factor, C_e was a canopy cover effect adjustment factor, and S_f was a slope adjustment factor. The slope adjustment factor was calculated using:

$$S_f = 1.05 - 0.85\exp(-4 \sin B) \quad (28)$$

where B was the interrill slope angle.

For rill erosion, detachment and deposition were calculated separately. When the flow shear stress exceeds the critical threshold value on the soil and the sediment transport capacity is larger than the sediment load, detachment occurs. The detachment rate D_r (kg s^{-1} m^{-2}) can be expressed as:

$$D_r = K_r(\tau - \tau_0)(1 - \frac{G}{T_c}) \quad (29)$$

where K_r was the adjusted rill erodibility parameter (s m^{-1}); τ was the flow shear stress (Pa), τ_0 was the critical flow shear stress (Pa), and T_c was the flow sediment transport capacity (kg s^{-1} m^{-1}). The transport capacity was calculated using:

$$T_c = k_t \tau^{1.5} \quad (30)$$

where k_t was the transport coefficient ($m^{0.5}$ s^2 $kg^{-0.5}$).

In WEPP, rill deposition occurs when the sediment load exceeds the sediment transport capacity. The deposition rate can be expressed as:

$$S_r = BV_{eff}(T_e - G)q^{-1} \quad (31)$$

where S_r was the rill deposition rate (kg s^{-1} m^{-2}), B was the rainfall-induced turbulence factor (default is 0.5), V_{eff} was the effective particle fall velocity (m s^{-1}), q was the flow discharge per unit width (m^2 s^{-1}).

3.4.1 WEPP Hillslope Model for Rangeland and Cultivated land

The WEPP Windows Interface Version September 17, 2012, which was developed by the USDA-ARS and Purdue University, was used to develop hillslope models for each transect. An example model setup for rangeland transect 6 is given below. Examples of the plant coverage changes along the slope for transect 6 are given in Figure 29 and Figure 30.

Step 1: Set up the slope profile for the transect in WEPP hillslope model

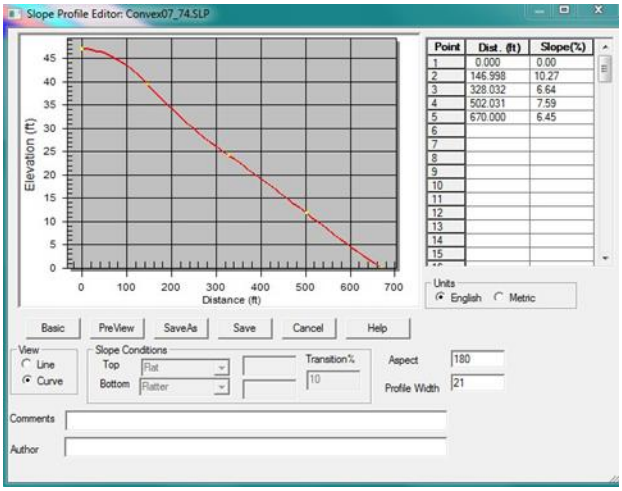

Step 2: Set up the climate for the study area (simulation period is 60 years) in the WEPP hillslope model

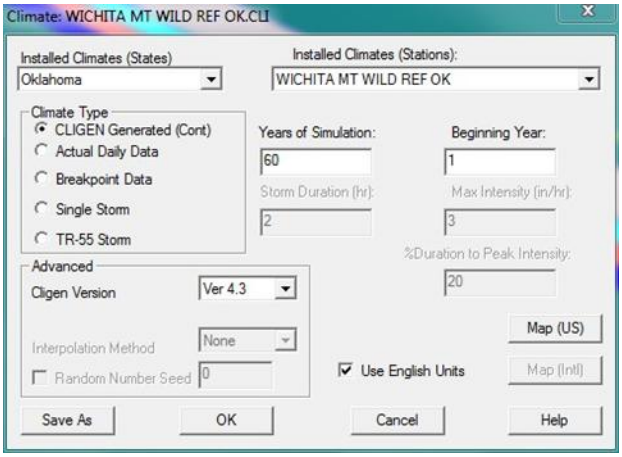

Step 3: Set up the management (divided the hillslope into two segment according to the change of plant coverage) in the WEPP hillslope model

Management		Segment Length (ft)	Average Detachment (t/acre)	Detachment Length (ft)	Average Deposition (t/acre)	Deposition Length (ft)
Rangeland\ Blu		147.0	1.11	147.0	0.00	0.0
Rangeland\ Blu		523.0	1.49	523.0	0.00	0.0

Step 4: Input details about the management for the rangeland in the WEPP

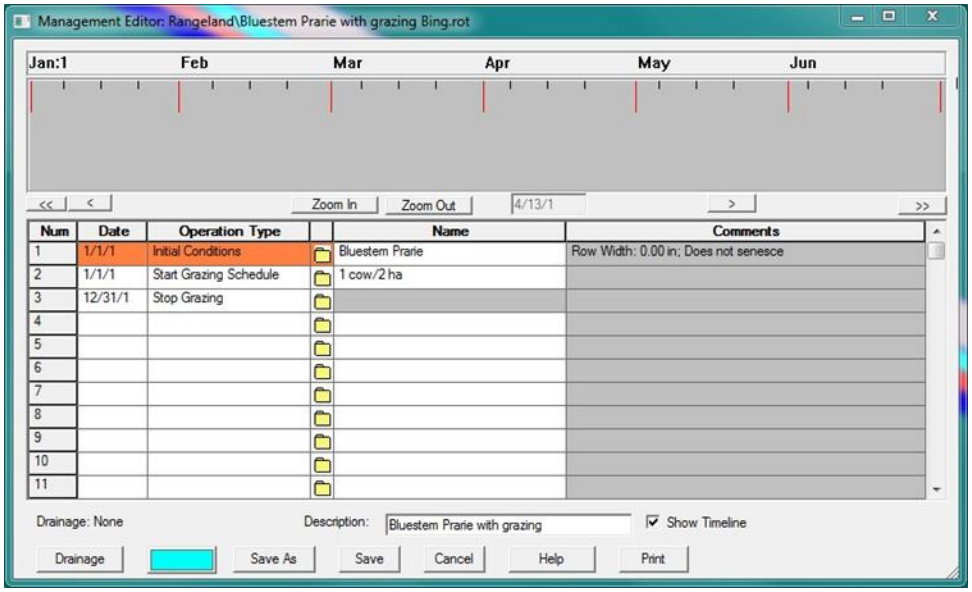

Step 5: Set up the soil parameters in the WEPP

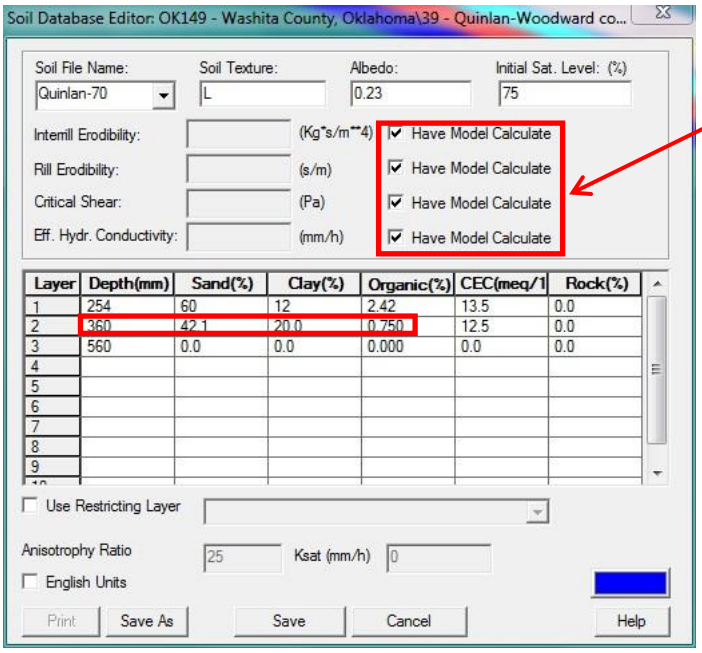

Change the layer to the measured particle size and organic carbon. Let the model calculate the parameters.

Step 6: The overall look of the WEPP hillslope model

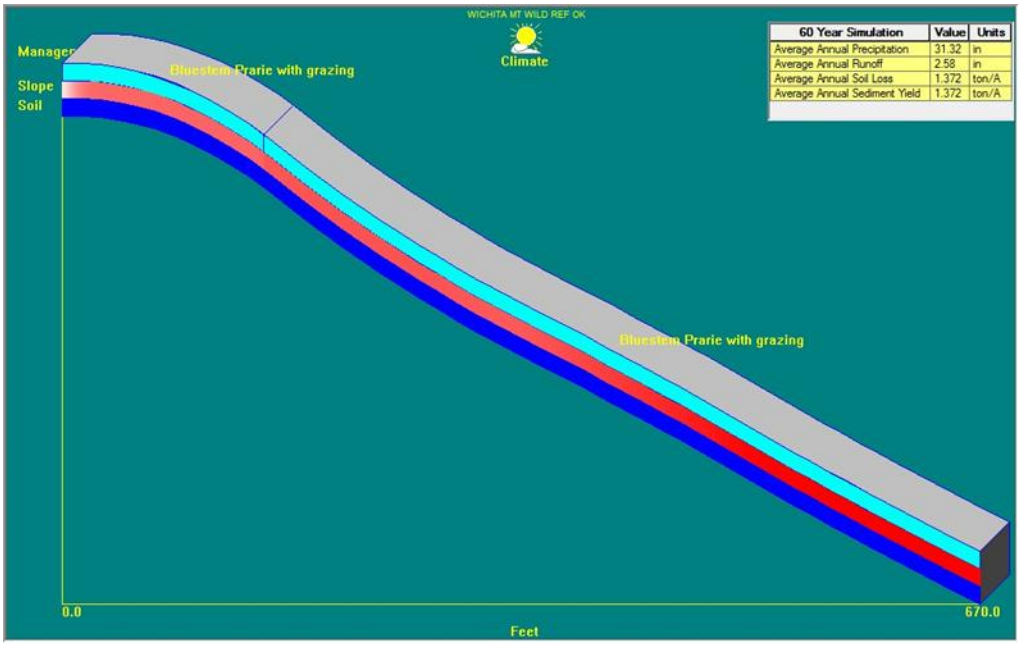

Figure 29 Example of the plant coverage change on top of a transect 6.

Figure 30 Example of the plant coverage from the middle to the bottom of a transect 6.

For the cultivated land (transect 11), there were three terraces from the top to the bottom of the transect. Since terraces cannot be added as a land management in WEPP, the terraces were added to the hillslope by change the slope steepness at specific slope segments. An overview of the cultivated hillslope is given in Figure 31.

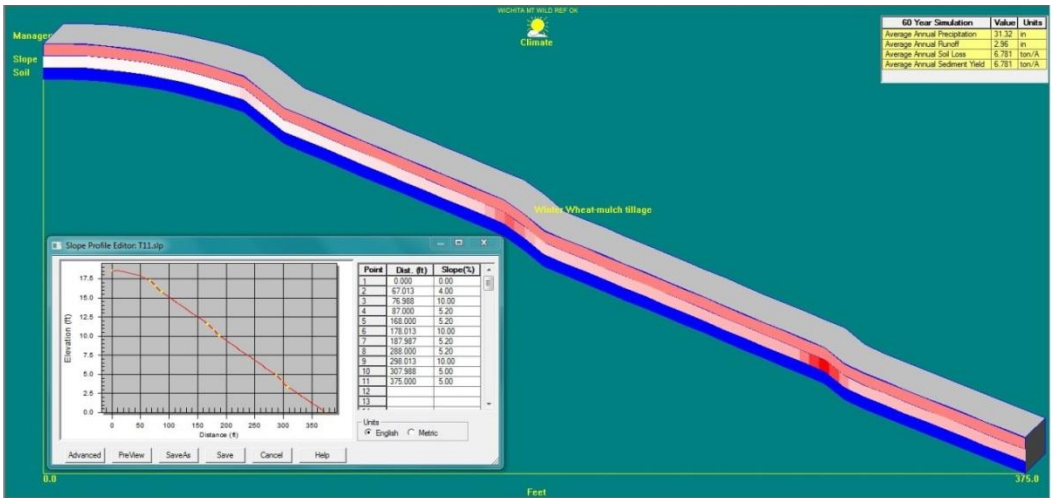

Figure 31 Transect 11 cultivated hillslope with terraces in the WEPP.

3.4.2 WEPP watershed model for the Bull Creek watershed

The current WEPP interface can only accommodate a small watershed, and thus the WEPP watershed model was developed using GeoWEPP 9.x. Ten-meter USGS DEM was used to delineate the watershed boundary and channel network. The critical source area was set to 20 hectares for the entire Bull Creek watershed and 10 for all the subwatersheds. The minimum source channel length was set to 100 meters.

Land management and soil properties were the same as the WEPP hillslope models. The simulation was performed for 60 years using historical weather data. In the watershed model, each hillslope had only one land use and one soil type. All parameters were set up manual except the topographic information. Although the GeoWEPP interface can automatically use the landuse and soil maps to generate the different landuse and soils on a hillslope, software bugs prevented this. In addition, reservoirs cannot be added using the GeoWEPP interface. Steps used to develop the watershed model are given below.

Step 1: Network delineation using 10m DEM in the WEPP watershed model

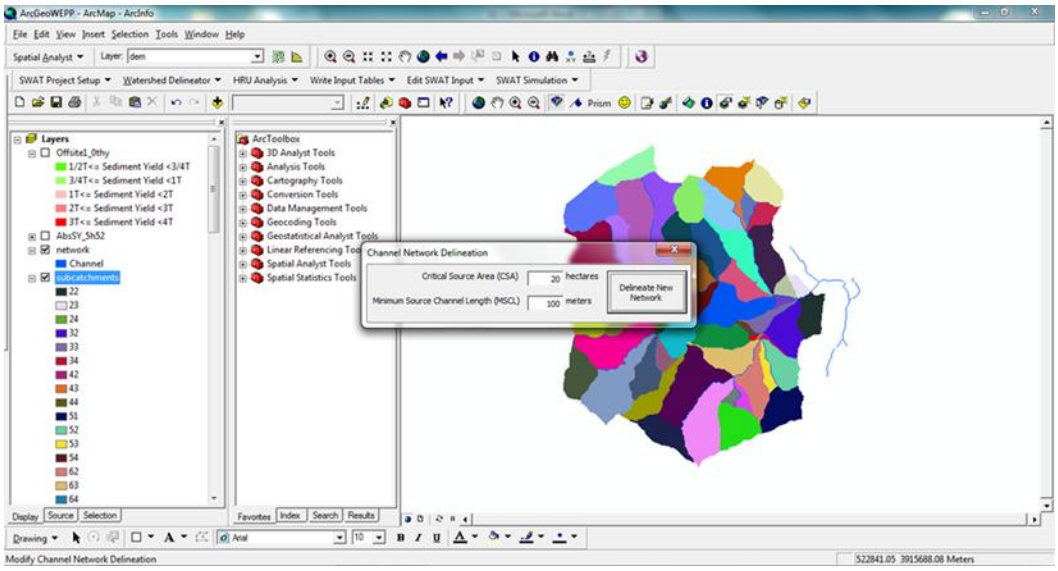

Step 2: Set up the land management in the WEPP watershed model

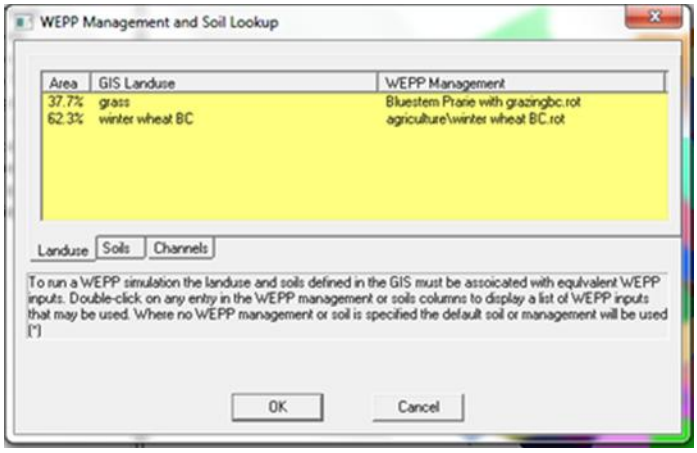

Step 3: Set up soil properties in the WEPP watershed model

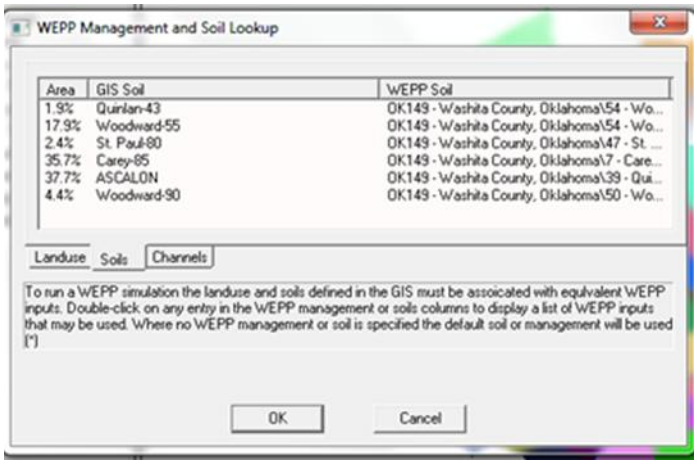

3.5 Cs-137 Conversion models to calculate soil erosion rates, soil redistribution and sedimentation

Cs-137 activity in the soil was converted to soil erosion or deposition rates through conversion models. The Cs-137 vertical distribution in the reference site should first be known, then by comparing the Cs-137 activity in the soil samples to the total Cs-137 inventory in the reference site, the depth of soil loss can be estimated (Figure 32). The conversion models were equations

that present the vertical distribution of the Cs-137 in the soil and relationships between the lost soil depth and the removed Cs-137 fallout.

All Cs-137 conversion models used to predict soil loss were performed using a Microsoft Excel add-in created by Walling at el. (2006). This add-in included the conversion models for both rangeland and cultivated land.

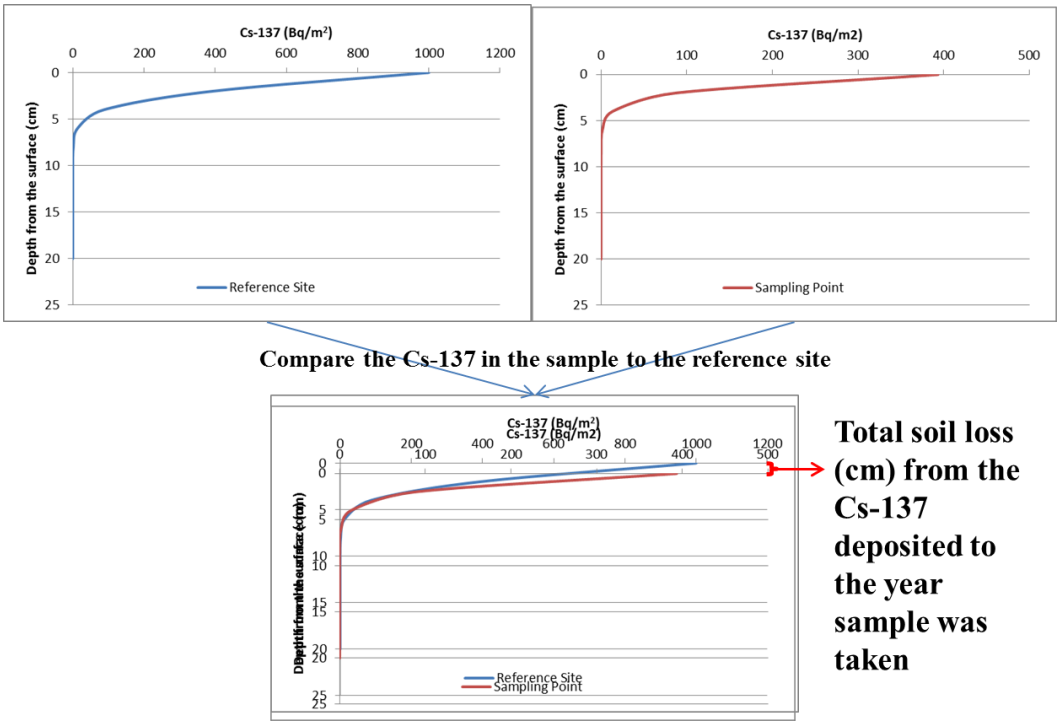

Figure 32 Example of how the Cs-137 activity was converted to soil erosion rate

3.5.1 Rangeland

Conversion models are used to convert the Cs-137 activity to soil erosion or deposition rates. The most commonly used conversion models for rangeland were the Profile Distribution model (Walling and Quine, 1990) and the Diffusion and Migration model (He and Walling, 1997).

3.5.1.1 Profile Distribution model

The Profile Distribution model for an erosion sites was given by:

$$A_h = A\left(1 - e^{-\lambda/h}\right) \quad (32)$$

where A_h was the amount of Cs-137 above the depth h (Bq m^{-2}), h was the coefficient describing profile shape (kg m^{-2}), A was the Cs-137 reference inventory (Bq m^{-2}), and λ was the mass depth from soil surface (kg m^{-2}). The equation can be further modified to the form (Walling and Quine, 1990):

$$R = \frac{10}{(t-1963)Z} \ln\left(1 - \frac{X}{100}\right) h_0 \quad (33)$$

where R was the annual soil loss (t ha^{-1} yr^{-1}), t was the sampling year (yr), X was the percent Cs-137 loss in the total inventory at time t, h_0 was a coefficient describing profile shape (kg m^{-2}).

The profile shape factor (h_0) was the rate of exponential decrease of Cs-137 in the undisturbed sites. The larger h_0, the deeper the Cs-137 migrated vertically in the soil. h_0 was calculated using (Walling and Quine, 1990):

$$h_0 = -\frac{z}{\ln\frac{f(z)}{f(0)}} \quad (34)$$

where f(z) was the surface fallout concentration (Bq m^{-2}), f(0) was the fallout concentration (inventory) at the soil surface (Bq m^{-2}), z was the sampling depth expressed as a cumulative mass above a given depth (m).

3.5.1.2 Diffusion and Migration model

The Cs-137 profile in the non-reference sites was calculated using (He and Walling, 1997):

$$C_u(t) \approx \frac{I(t)}{H} + \int_0^{t-1} \frac{I(t')e^{-R/H}}{\sqrt{D\pi(t-t')}} e^{-\frac{V^2(t-t')}{4D} - \lambda(t-t')} dt' \quad (35)$$

where $C_u(t)$ was the Cs-137 concentration in surface soil with time t (Bq kg^{-1}), t was the sampling time (yr), t' was beginning year for Cs-137 deposition (yr), i.e.1954, I(t) was annual Cs-137 deposition flux (Bq m^{-2} yr^{-1}), H was the depth of plow layer (cm), λ was the decay constant for Cs-137 (yr^{-1}), R was erosion rate (kg m^{-2} yr^{-1}), D was diffusion coefficient (kg^2 m^{-4} yr^{-1}), and V was downward migration rate of Cs-137 in the soil profile (kg m^{-2} yr^{-1}). For an eroding point, if sheet erosion was the primary erosion process, the soil erosion rate was expressed as (He and Walling, 1997):

$$R = \frac{A_{ls}(t)}{\int_0^t Z C_u(t')} e^{-\lambda(t-t')} \tag{36}$$

$$A_{ls}(t) = A_{ref} - A_u(t) \tag{37}$$

where Z was particle size correction factor, $A_{ls}(t)$ was the diminished Cs-137 inventory (Bq m^{-2}) A_{ref} was the Cs-137 reference inventory (Bq m^{-2}) , and $A_u(t)$ was the total measured Cs-137 inventory (Bq m^{-2}). For a depositional point (He and Walling, 1997):

$$R' = \frac{A_{ex}(t)}{\int_{t_0}^{t} C_d(t') e^{-\lambda(t-t')} dt'} \tag{38}$$

$$C_d(t') = \frac{1}{\int_S R dS} \int_S Z' P C_u(t') R dS \tag{39}$$

$$A_{ex}(t) = A_u(t) - A_{ref} \tag{40}$$

where R′ was the deposition rate (kg m^{-2} yr^{-1}), $C_d(t')$ was the Cs-137 concentration of deposited sediment (Bq m^{-2}), and $A_{ex}(t)$ was the excess Cs-137 inventory (Bq m^{-2}).

The diffusion coefficient (D) and the migration rate (V) were used to describe the shape of the vertical distribution of Cs-137. The larger D and V the deeper the Cs-137 migrated vertically in the soil. D and V were calculated using (He and Walling, 1997):

$$V \approx \frac{W_p}{t-1963} \tag{41}$$

$$D \approx \frac{(N_p - W_p)^2}{2(t-1963)} \tag{42}$$

where D was the diffusion coefficient ($kg^2\ m^{-4}\ yr^{-1}$), V was the migration rate ($kg\ m^{-2}\ yr^{-1}$), t was the year when the soil core was collected (yr), W_p was mass depth of the maximum Cs-137 concentration ($kg\ m^{-2}$), N_p was distance between the depth of the maximum Cs-137 concentration and the point where the Cs-137 concentration reduces to 1/e of the maximum concentration (m). D and V were normally in the range of 30-50 $kg\ m^{-2}\ yr^{-1}$ and 0.2-1.0 $kg\ m^{-2}\ yr^{-1}$, respectively.

Cesium-137 was associated with the fine particles in most environments (Sutherland, 1991). The particle size correction factor was used to reflect the selective eroded particles in the sediment. He and Walling (1996) measured the Cs-137 concentration in different particle sizes. They found the Cs-137 concentration had a relationship with particle SSA as:

$$C = 54.6S^{0.75} \qquad \text{for undisturbed land} \tag{43}$$

$$C = 14.5S^{0.65} \qquad \text{for cultivated land} \tag{44}$$

$$Z = \frac{M}{C} = (\frac{S_M}{S_C})^v \tag{45}$$

$$Z' = (\frac{S_D}{S_M})^v \tag{46}$$

where C was the Cs-137 concentration in the soil particle ($mBq\ g^{-1}$) and the S was the SSA for the soil particle ($m^2\ g^{-1}$), Z was the particle size correction factor for erosion area, Z' was the particle size correction factor for deposition area, M was the Cs-137 concentration in the mobilized sediment ($mBq\ g^{-1}$), S_M was the SSA of the mobilized sediment ($m^2\ g^{-1}$), S_C was the SSA for the original soil ($m^2\ g^{-1}$), S_D was the SSA for the deposited sediment ($m^2\ g^{-1}$), v was equal to 0.75 for undisturbed land and 0.65 for disturbed land.

The SSAs were measured for five soil samples (two rangeland, two cultivated, and one sediment) from the subwatershed where the transect samples for Cs-137 method were taken. The SSA was measured using a Micromeritics ASAP 2000 instrument (Micromeritics Instrument, Norcross, GA) at the Laboratory for Environmental Analysis, University of Georgia. The Brunauer-Emmett-Teller (BET) method (Kim and Stucky, 2000) was used with nitrogen as the probe gas.

The annual fallout deposition since 1954 was required by the models. The local Cs-137 deposition flux, I(t), was calculated using (Cambray et al., 1989):

$$I(t) = \alpha I_n(t) \tag{47}$$

where $I_n(t)$ was the Cs-137 deposition flux for the reference station (Bq m^{-2} yr^{-1}), t is time (yr) and α was a scaling factor. The scaling factor was calculated using (Cambray et al., 1989):

$$\alpha = \frac{A_{ref}}{\int_{1954}^{t} I_n(t') e^{-\lambda(t-t')} dt'} = \frac{A_{ref}}{A_n} \tag{48}$$

where A_n is the present total atmospheric fallout inventory for the Cs-137 deposition at the representative station (Bq m^{-2}). This information is the annual flux of Cs-137 started in 1954 and assumed to be zero after 1983. Since there was no available data for the Bull Creek watershed, the default data was used which was included in the program developed by Walling et al. (2006).

3.5.2 Cultivated land

There were four models to convert Cs-137 concentration to soil loss for the cultivated land. They were the Proportional model, the simplified Mass Balance model, Mass Balance model and the Mass Balance model that accounted for tillage.

3.5.2.1 The Proportional Model

The proportional model assumed that the Cs-137 was completely mixed and distributed uniformly in the plow layer. The soil erosion rate was proportional to the loss of Cs-137, which was represented as (Martz and de Jong 1987):

$$Y = 10\frac{BdX}{100T} \tag{49}$$

where Y was the mean annual soil loss (t ha^{-1} yr^{-1}), d was the depth of the plow or cultivation layer (m), B was soil bulk density (kg m^{-3}), X was the percent reduction in total Cs-137 inventory, T was the time elapsed since the initiation of Cs-137 (yr), and A_{ref} was the local Cs-137 reference inventory (Bq m^{-2}). The percent reduction in total Cs-137 inventory was defined as:

$$X= (A-A_{ref})/A_{ref}\times 100 \tag{50}$$

Where A was the measured total Cs-137 inventory at the sampling point (Bq m^{-2}). The deposition rate was calculated using (Martz and de Jong 1987):

$$Y' = 10\frac{BdX}{100T} \tag{51}$$

where Y′ was the deposition rate (t ha^{-1} yr^{-1}), and X was the percent increase in total Cs-137 inventory.

3.5.2.2 Mass Balance Model I (Simplified Mass Balance Model)

Zhang et al. (1990) published a simplified mass balance model that assumed the total Cs-137 fallout occurred in 1963. The equation for calculating soil erosion rate was (Zhang et al., 1990):

$$R = d\left(1 - \left(\frac{A(t)}{A_{ref}}\right)^{\frac{1}{t-1963}}\right) \tag{52}$$

where A(t) was the total Cs-137 inventory in year t (Bq m^{-2}), A_{ref} was the local reference inventory (Bq m^{-2}), d was the plow depth or cultivation layer (m), R was a constant erosion rate (m m^{-2} yr^{-1}), and t was the sampling year (yr). The deposition rates were calculated using:

$$R' = \frac{A_{ex}(t)}{\int_{1963}^{t} C_d(t')e^{-\lambda(t-t')}dt'} = \frac{A(t) - A_{ref}}{\int_{1963}^{t} C_d(t')e^{-\lambda(t-t')}dt'} \quad (53)$$

where $A_{ex}(t)$ was the measured inventory less the local reference inventory (Bq m^{-2}), $C_d(t')$ was the Cs-137 concentration of deposited sediment at year t′ (Bq kg^{-1}), and λ was the decay constant for Cs-137 (yr^{-1}).

3.5.2.3 Mass Balance Model II

The Mass Balance Model II considered the time-variant of Cs-137 input, i.e. Cs-137 deposition on the soil surface prior to mixing in the plow layer. The soil erosion rate, R (kg m^{-2} yr^{-1}), was calculated using (Walling and He, 1999):

$$A(t) = A(t_0)e^{-(ZR/d+\lambda)(t-t_0)} + \int_{t_0}^{t} (1 - Z\gamma(1 - e^{-R/H}))I(t')e^{-(ZR/d+\lambda)(t-t')}dt' \quad (54)$$

where A(t) was the cumulative Cs-137 activity per unit area (Bq m^{-2}), $A(t_0)$ was the Cs-137 inventory at t_0 (Bq m^{-2}), Z was the particle size correction factor, d was the cumulative mass depth representing the average plow depth (kg m^{-2}), λ was the decay constant for Cs-137 (yr^{-1}), t_0 was the year when cultivation started (yr), t was the sampling year (yr), γ was the proportion of the annual Cs-137 input susceptible to removal by erosion, H was the relaxation mass depth of the initial distribution of fresh fallout Cs-137 at the surface of the soil profile (kg m^{-2}), and I(t) was the annual Cs-137 deposition flux (Bq m^{-2} yr^{-1}). A(t) and $A(t_0)$ were represented as (Walling and He, 1999):

$$R = \frac{d}{Z}\left(\frac{(1-\Gamma)I(t)-\frac{dA(t)}{dt}}{A(t)} - \lambda\right) \quad (55)$$

$$A(t_0) = \int_{1954}^{t_0} I(t')e^{-\lambda(t'-t_0)}dt' \quad (56)$$

where Γ was the percent of the freshly deposited Cs-137 fallout removed by erosion before being mixed into the plow layer. Γ was calculated using (Walling and He, 1999):

$$\Gamma = Z\gamma(1-e^{-R/H}) \quad (57)$$

The deposition rate R′ (kg m^{-2} yr^{-1}) was calculated using (Walling and He, 1999):

$$R' = \frac{A_{ex}}{\int_{t_0}^{t} C_d(t')e^{-\lambda(t-t')}dt'} \quad (58)$$

where A_{ex} was the measured total inventory A(t) less the local direct fallout input A_{ref} (Bq m^{-2}). A_{ex} was calculated using (Walling and He, 1999):

$$A_{ex} = \int_{t_0}^{t} R'C_d(t')e^{-\lambda(t-t')}dt' \quad (59)$$

where $C_d(t')$ was the Cs-137 concentration of deposited sediment (Bq kg^{-1}). $C_d(t')$ was calculated using (Walling and He, 1999):

$$C_d(t') = \frac{1}{\int_S RdS}\int_S Z'C_e(t')RdS \quad (60)$$

3.5.2.4 Mass Balance Model III

The Mass Balance Model III accounted for the effects of tillage. Govers et al. (1996) reported that the downslope sediment flux, F_Q in kg m^{-1} yr^{-1}, from a unit contour length was expressed as (Govers et al. 1996):

$$F_Q = \phi \sin \beta \tag{61}$$

where β is the slope angle in degrees, ϕ was a site-specific constant (kg m^{-1} yr^{-1}). Assuming the hillslope can be divided into straight uniform sections, the soil loss, R_t (kg m^{-2} yr^{-1}), by tillage can be expressed as (Walling and He, 1999):

$$R_t = (F_{Q,out} - F_{Q,in}) / L_i = \phi(\sin \beta_i - \sin \beta_{i-1}) / L_i = R_{t,out} - R_{t,in} \tag{62}$$

where L_i (m) was the slope length of the i^{th} segment. $R_{t,out}$ (kg m^{-2} yr^{-1}) and $R_{t,in}$ (kg m^{-2} yr^{-1}) were defined as (Walling and He, 1999):

$$\begin{aligned} R_{t,out} &= \phi \sin \beta_i / L_i \\ R_{t,in} &= \phi \sin \beta_{i-1} / L_i \end{aligned} \tag{63}$$

The total soil loss R_w (kg m^{-2} yr^{-1}) by water erosion was calculated by solving the following equation (Walling and He, 1999):

$$\frac{dA(t)}{dt} = (1 - \Gamma) I(t) + R_{t,in} C_{t,in}(t) - R_{t,out} C_{t,out}(t) - R_w C_{w,out}(t) - \lambda A(t) \tag{64}$$

where $C_{t,in}$, $C_{t,out}$ and $C_{w,out}$ were the Cs-137 concentrations of the sediment associated with tillage input, tillage output and water output, respectively (Bq kg^{-1}). The net erosion rate, R (kg m^{-2} yr^{-1}), was (Walling and He, 1999):

$$R = R_{t,out} - R_{t,in} + R_w \tag{65}$$

For a deposition point, the deposition R'_w (kg m^{-2} yr^{-1}) resulted from water erosion was expressed as (Walling and He, 1999):

$$\frac{dA(t)}{dt} = I(t) + R_{t,in}C_{t,in}(t) - R_{t,out}C_{t,out}(t) + R'_w C_{w,in}(t) - \lambda A(t) \quad (66)$$

where $C_{w,in}$ was the Cs-137 concentration of the sediment input from water-induced deposition (Bq kg^{-1}). The net erosion rate R was:

$$R = R_{t,out} - R_{t,in} - R'_w \quad (67)$$

The Cs-137 concentration of the soil within the plow layer, $C_s(t')$ (Bq kg^{-1}), was expressed as (Walling and He, 1999):

$$C_s(t') = \frac{A(t')}{d} \quad \text{(erosion)} \quad (68)$$

$$C_s(t') = \frac{1}{d}[A(t') - \frac{|R|}{d}\int_{t_0}^{t-1} A(t'')e^{-\lambda t''}dt''] \quad \text{(deposition)} \quad (69)$$

3.5.2.5 Conversion Model Comparison

The conversion models for cultivated land are compared in Table 6. The Proportional Model assumed that the after the Cs-137 was deposited on the soil, it was well mixed in the plow layer, and thus soil loss was directly proportional to the reduction of Cs-137. The Mass Balance models considered the inputs of the Cs-137 and the soil below the original plow layer (assumed no Cs-137) mixed with Cs-137 after soil loss from water erosion. The Mass Balance Model I assumed that all Cs-137 fallout was deposited in the year 1963. Mass Balance Model II improved the Mass Balance Model I by considering the annual Cs-137 inputs and the loss of the freshly deposited fallout due to erosion before it was mixed in the plow layer. Based on the

Mass Balance Model II, Mass Balance Model III added the effects of tillage redistribution of Cs-137.

Table 6 Comparison of the conversion models for cultivated land

Proportional Model	Mass Balance Model		
	I	II	III
Cs-137 completely mixed within the plow layer Soil loss directly proportional to the reduction in Cs-137	Assumes total Cs-137 fallout occurred in 1963	Considers the time-variant fallout Cs-137 input and the fate of the freshly deposited fallout before incorporated into plow layer	Same as Model II, but accounts for soil redistribution by tillage

3.6 Fingerprinting method

3.6.1 Mixing model method

The original mixing model used in the fingerprinting method was calculated using (Long et al., 2012):

$$0 \leq P_s \tag{70}$$

$$\sum_{s=1}^{n} P_s = 1 \tag{71}$$

$$\min \left(\sum_{i=1}^{n} [(C_i - \sum_{s=1}^{m} P_s S_{si})/C_i]^2 \right) \tag{72}$$

where C_i was the concentration of fingerprint property i in the sediment, P_s was the optimized percentage contribution from source category s, S_{si} was the mean concentration of fingerprint property i in source category s, n was the number of fingerprint properties, and m was the number of sediment source categories.

Collins et al. (2010) improved the mixing model by accounting for particle size and organic matter content, which has been widely used. This model will be called Colllins method to separate it from the original mixing model. The form of the model was given as:

$$0 \leq P_s \leq 1 \tag{73}$$

$$\sum_{s=1}^{n} P_s = 1 \tag{74}$$

$$\min \left(\sum_{i=1}^{n} \{[C_i - (\sum_{s=1}^{m} P_s S_{si} Z_s O_s SV_{si})]/C_i\}^2 W_i \right) \tag{75}$$

$$\text{RME} = \left\{1 - [\frac{1}{n} \sum_{i=1}^{n} \{[C_i - (\sum_{s=1}^{m} P_s S_{si} Z_s O_s SV_{si})]/C_i\}^2 W_i] \right\} * 100\% \tag{76}$$

where C_i was the concentration of fingerprint property (i) in the floodplain sediment collected from the sub-catchment outlet, P_s was the optimized percentage contribution from source category (s), S_{si} was the mean concentration of fingerprint property (i) in source category (s), Z_s was the particle size correction factor for source category (s), O_s was the organic matter content correction factor for source category (s), SV_{si} was the weighting representing the within-source variability of fingerprint property (i) in source category (s), W_i was the tracer discriminatory weighting, n was the number of fingerprint properties comprising the optimum composite fingerprint, m was the number of sediment source categories, and RME is the root mean error (%). Z_s was calculated as the ratio of the mean SSA of the floodplain sediment samples to the corresponding mean for each individual source type or spatial source. O_s was the ratio of the organic carbon content of the floodplain sediment samples to the corresponding mean value for each individual source type or spatial source. SV_{si} was estimated using the inverse of the root of the variance associated with each fingerprinting property measured for each source. W_i was based on information on the relative discriminatory efficiency of each individual tracer included in any given composite fingerprint provided by the results of the Discriminant Function Analysis method (DFA). Compared to the original mixing model, the modified mixing model reduced the

uncertainty and narrowed the contribution ranges, which provides an improved estimate of the source contribution.

3.6.2 Delineating sources using the Discriminant Function Analysis (DFA) Method

Collins et al. (1997a) discussed using statistical tests to select chemical properties to include for the fingerprinting method. The stepwise DFA was used to identify chemicals to best delineate differences among sediment sources. The DFA was only used to select properties for mixing models. However, the DFA can be used directly to predict the source contributions, which may overcome some of the limitations of the fingerprinting method. For example, when the number of sources is more than two, mixing models predict one or more source contributions as zero. Using DFA to predict source contributions directly has not been published to date. When applying the DFA to the fingerprinting method, the closer a DFA grouped source is to the sediment source, the higher its contribution. Equations used to predict the source contribution using the DFA method include:

$$D_m = \sum_{i=1}^{n} \frac{\rho_i}{100} |F_i(source_m) - F_i(sediment)| \quad (77)$$

$$W_m = \frac{1}{D_m} \quad (78)$$

$$W = \sum_{i=1}^{m} \frac{1}{D_m} \quad (79)$$

$$P_m = \frac{W_m}{W} * 100\% \quad (80)$$

where D_m was the distance for source m, ρ_i was the percent function i correctly classified the groups, W_m was the weighting for source m, W was the total weighting, P_m was the contribution from source m (%), m was the number of sources, n was the number of functions used to group the sources (obtained from DFA output), $F_i(source_m)$ was the center of the source m from

Function i (obtained from DFA output), and F_i (sediment) was the center of the sediment from Function i (obtained from DFA output).

3.7 Model Efficiency

Soil erosion and deposition rates were estimated based on three methods. The first was the fingerprint method, which estimated source contributions by land cover category at the watershed scale. Second, the Cs-137 method was used to estimate the spatial distribution of soil erosion and deposition along transects. The third was using the WEPP model. When evaluating the Fingerprint method, the Cs-137 method was assumed the true erosion and deposition rates since measured soil loss data were not available. The method defined by Nearing (2000) was used, which calculates differences between categories and then identifies the fraction of acceptable predictions for the whole watershed. The technique had five components:

i. Relative difference (R_{diff}) for each paired data, defined as:

$$R_{diff} = \frac{(A_{model,i} - A_{Cs-137,i})}{(A_{model,i} + A_{Cs-137,i})} \quad (81)$$

ii. The 95 confidence interval (CI) for each data pair, calculated using:

$$CI = m \log_{10} M + b \quad (82)$$

where M was the soil erosion rate from the Cs-137 method.

iii. Lower and upper bounds (LB and UB), which were calculated using:

$$m = 0.236 \quad and \quad b = -0.641 \qquad \text{(lower bound)} \quad (83)$$

$$m = -0.179 \quad and \quad b = 0.416 \qquad \text{(upper bound)} \quad (84)$$

iv. Relative mean error (RME), which was calculated using:

$$RME = \frac{1}{n} \sum_{i=1}^{n} \left(\frac{|C_i - C_i'|}{C_i}\right)^2 \quad (85)$$

where C_i was the measured chemical property for sediment source i, C'_i was the predicted chemical property for sediment source i using the results from the fingerprinting method, and n was the number of the sediment sources.

When evaluating WEPP predictions, the Cs-137 method was also assumed the true erosion and deposition rates since measured soil loss data were not available. First, the Coefficient of Determination (R^2) was used to compare the WEPP model predictions to the Cs-137 estimates, defined as:

$$R^2 = 1 - \frac{\sum_{i=1}^{n}(A_{Cs-137,i} - A_{model,i})^2}{\sum_{i=1}^{n}(A_{Cs-137,i} - \overline{A_{Cs-137,i}})^2} \quad (86)$$

where $A_{Cs\text{-}137,i}$ was the Cs-137 estimate for the i category, $A_{model,i}$ was the model for the i category, $\overline{A_{Cs-137,i}}$ was the mean Cs-137 estimate. Next, the Nash and Sutcliffe efficiency (NSE) was used to compare the WEPP model predictions to the Cs-137 estimates (Nash and Sutcliffe, 1970, Risse et al., 1993). Finally, graphical techniques were also utilized.

3.8 Statistical Tests

Collins et al. (1997a) developed a two-stage statistical test procedure to identify chemical properties that identified differences among sediment sources. Next, these properties were used in the Mixing model to estimate the contribution by source. The first step used the Kruskal-Wallis H-test to identify chemical properties that were significantly different among the sediment sources. The second stage used the stepwise Discriminant Function Analysis (DFA) to identify the minimum number of properties, which passed the Kruskal-Wallis H-test, which can most discriminate the sources.

3.8.1 Kruskal-Wallis H-test

The Kruskal-Wallis H-test was a nonparametric procedure used to compare more than two populations in a completely randomized design. The test was applied by ranking all data from 1 to n for all k groups, and then calculating the rank sum for each of the i^{th} sample, T_i. Next, the H test statistic was calculated using (Yockey, 2011):

$$H = \frac{12}{n\,(n+1)} \sum_{i=1}^{k} \frac{T_i^2}{n_i} - 3(n+1) \tag{87}$$

where n_i (i = 1, 2, ..., k) was the sample size for the i^{th} group. The hypothesis tests were:

H_0: k groups were not significantly different

H_a: at least one group was different.

The Kruskal-Wallis H-test was performed using the SPSS software Version 20.0 (IBM, Inc.) using a p-value of 0.05. The sediment sources were categorized into two groups; Source 1 included upland and gully, and Source 2 included cultivated land, rangeland and gully.

3.8.2 Discriminant Function Analysis (DFA)

DFA was a statistical analysis used to combine similar observations into groups using independent variables (Yockey, 2011), i.e. the method evaluates if a set of independent variables can assign membership of observations to different categorical groups. DFA can be used when groups are known a priori and the sample size of the smallest group is greater than the number of the independent variables. For this study, the independent variables were chemical properties, and the groups were the sediment sources. The Wilks' lambda method (Collins et al., 2010) was used for the DFA using p-values of 0.05 and 0.1 for the property included and removed, respectively. The DFA was performed using the SPSS software Version 20.0 (IBM, Inc.).

CHAPTER IV

RESULTS AND DISCUSSION

4.1 Cs-137 method

4.1.1 *Soil erosion rates predicted by Cs-137 method*

4.1.1.1 Reference Site Evaluation and Comparison

Eighteen reference samples were collected at the Town of Colony and Fort Cobb Reservoir sites (Table 7). Using the large soil rings, the Cs-137 activities were 150 and 1930 Bq m^{-2} from the Town of Colony and the Fort Cobb Reservoir reference sites, respectively. Based on Agudo (1998) estimate of global Cs-137 deposition by latitude (Figure 33), the Cs-137 activity measured at the Town of Colony was from a disturbed site and thus did not represent the total Cs-137 inventory of the Bull Creek watershed. Using the 15 five-centimeter diameter soil-probe data, the average Cs-137 activity at the Fort Cobb site was estimated to be 1340 Bq m^{-2}, which was less than the large-diameter soil ring estimate. Therefore, based on the global Cs-137 input estimate of 2600 Bq m^{-2}, the samples collected using the large soil rings at the State Park near the Fort Cobb Reservoir were chosen to present reference conditions. Figure 34 shows the vertical distribution of the Cs-137 at the Ft Cobb Reservoir reference site showing an exponential reduction in Cs-137 with depth. The peak Cs-137 activity was a few centimeters below the surface resulting from the downward diffusion and migration of the Cs-137 over time. These

characteristics were also reported by other researchers for undisturbed soils (Huh and Su, 2004, Shand et al., 2013)

Table 7 Cs-137 inventory for the reference sites in the Fort Cobb Reservoir watershed based on 30 cm deep soil samples.

Sites ID	Cs-137 ($Bq\ m^{-2}$)	Location	Sampling Method	Sample Diameter (cm)
R1	1880	Fort Cobb	Large Soil Ring	86
R2	1980	Fort Cobb	Large soil ring	86
R3	151	Town of Colony	Large soil ring	86
R4	1170	Fort Cobb	Soil Probe	5
R5	1620	Fort Cobb	Soil probe	5
R6	1331	Fort Cobb	Soil probe	5
R7	1015	Fort Cobb	Soil probe	5
R8	1140	Fort Cobb	Soil probe	5
R9	1277	Fort Cobb	Soil probe	5
R10	1356	Fort Cobb	Soil probe	5
R11	1698	Fort Cobb	Soil probe	5
R12	1413	Fort Cobb	Soil probe	5
R13	1532	Fort Cobb	Soil probe	5
R14	1394	Fort Cobb	Soil probe	5
R15	900	Fort Cobb	Soil probe	5
R16	1543	Fort Cobb	Soil probe	5
R17	1389	Fort Cobb	Soil probe	5
R18	1352	Fort Cobb	Soil probe	5

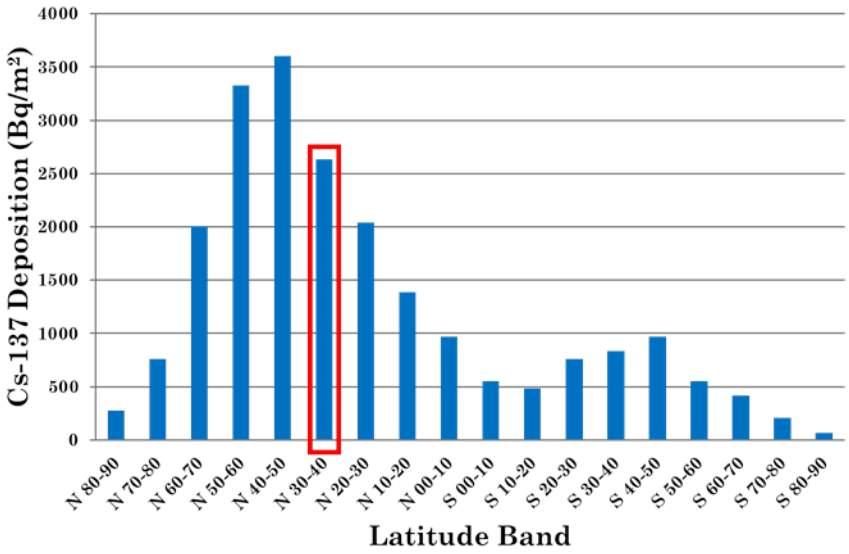

Figure 33 Global Cs-137 deposition in the soil by latitude band for the year 2012 (original data from Agudo, 1998). Highlighted bar in red was for the Bull Creek watershed.

The Cs-137 vertical distribution for rangeland in the Bull Creek watershed also indicated downward diffusion and migration (Figure 35). Therefore, the Diffusion and Migration model was chosen to calculate the soil loss for the rangeland. Comparing the Cs-137 reference and rangeland vertical distributions, it was indicated that the Cs-137 in the rangeland area migrated deeper compared to the reference site. The slower migration at the reference site may be a result of the forest landcover, which contained a substantial litter layer containing primarily fallen leaves on the soil surface. The litter can intercept Cs-137 and thus would only migrate into the soil by diffusion into rainfall or decay of the leaves (Rafferty et al., 2000). In addition, organic matter increased the adsorption of the Cs-137, which resulted in a higher concentration in the surface soil layer, as illustrated in Figure 35.

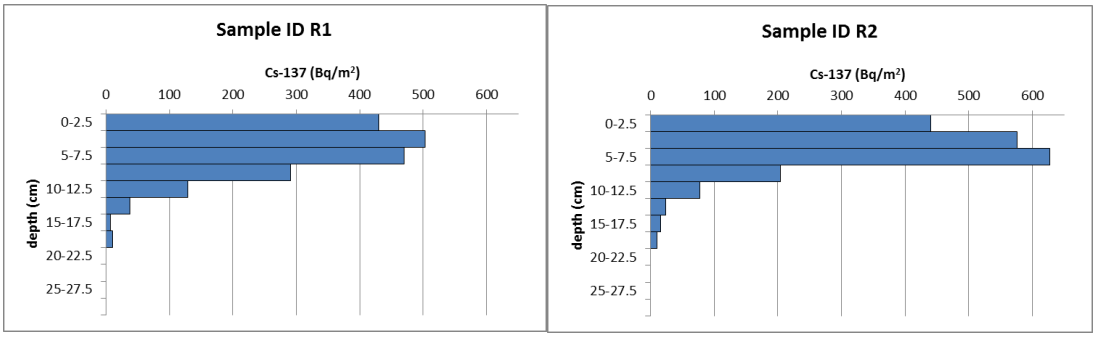

Figure 34 Cs-137 vertical distribution at the Fort Cobb Reservoir reference site for two samples, R1 and R2.

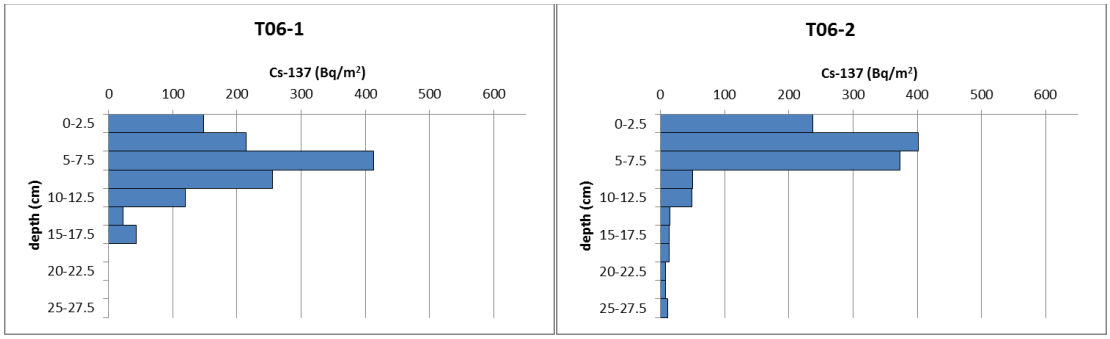

(a) Top (b) Middle-top

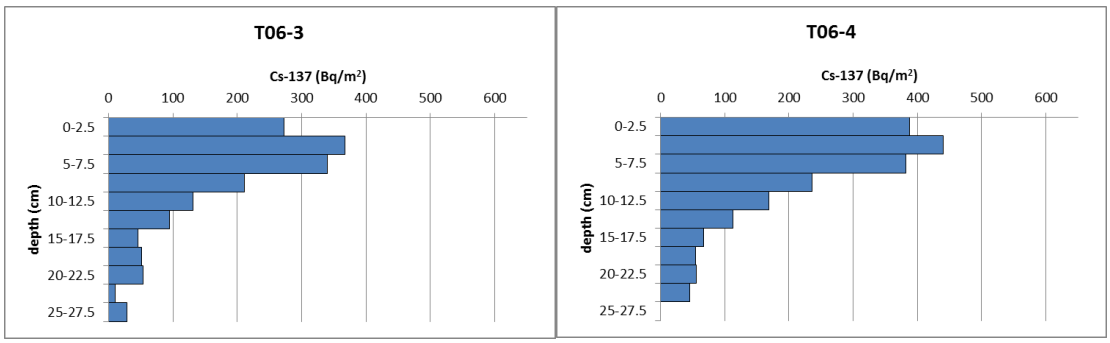

(c) Middle-bottom (d) Bottom

Figure 35 Cs-137 vertical distribution for the transect 06 in the Bull Creek watershed from the top (a) to the bottom (d) of the hillslope.

The Cs-137 vertical distribution in cultivated soils was reported to be evenly distribution through the plow layer (Zhang et al., 1990). The plow layer in the Bull Creek watershed was approximately 20 cm. The Cs-137 migrated below the plow layer and the vertical distribution did not appear to be evenly distributed for cultivated Transect 11 (Figure 36), with peak Cs-137 levels between 5 and 20 cm. Terrace building and/or maintenance may have contributed to this. Although it may not have contributed, it should be noted that the cultivated land also had scheduled grazing periods every year.

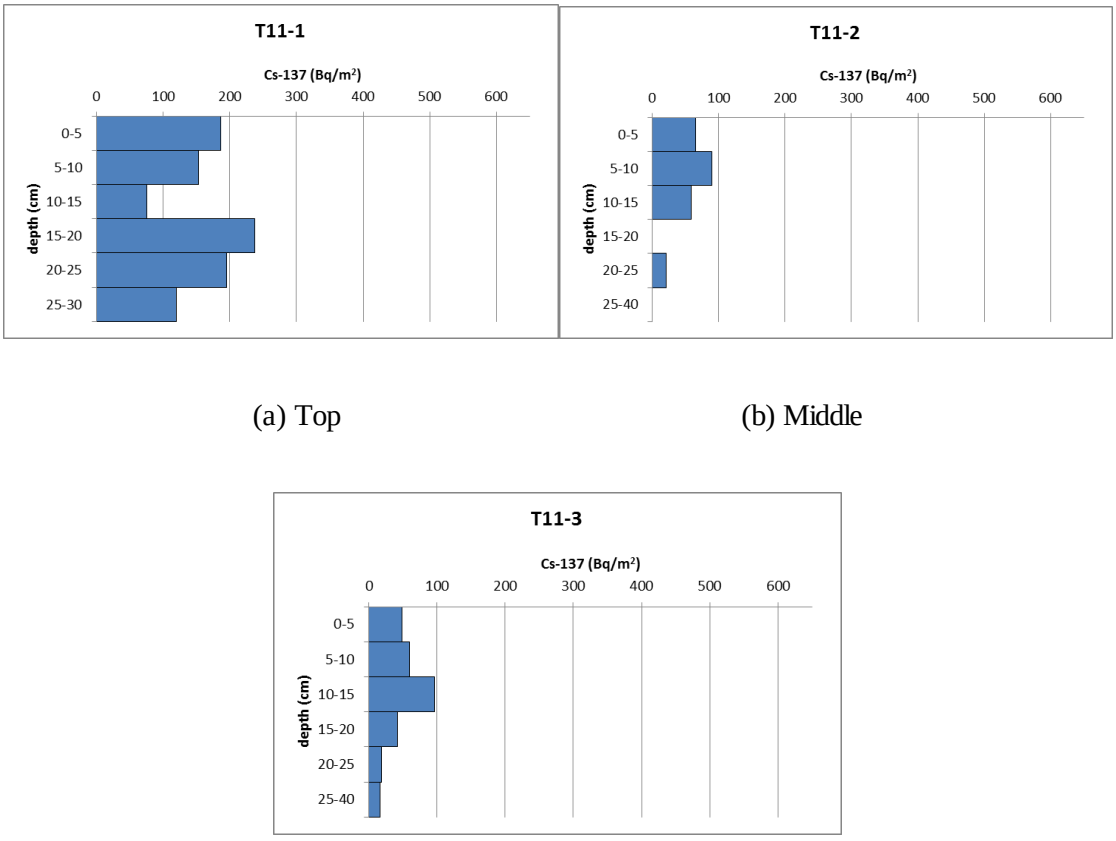

(a) Top

(b) Middle

(c) Bottom

Figure 36 Cs-137 vertical distribution for the cultivated soil in the Bull Creek watershed from the top (a) to the bottom (c) of the hillslope.

4.1.1.2 Soil erosion and deposition rates for transects

4.1.1.2.1 Soil erosion rates predicted with and without particle size correction factors

The soil erosion and deposition rates for the rangeland transects were calculated using the Migration and Diffusion model. For the cultivated land, all the four conversion models were used. Note that only transect 11 was cultivated land and the other transects were rangeland. Transect 01, the 01 sample from transect 03 and transect 09 were missing.

Table 8 provides the soil erosion and deposition rates predicted by the Migration and Diffusion Model for rangeland transects, and Figure 37, Figure 38, and Figure 39 illustrate the 95 percent confidence intervals for the rangeland with and without the particle size correction factor Z, and the cultivated land, respectively. The Z for cultivated land and rangeland were 1.2 and 2.9, respectively. Table 9 shows the SSAs used to calculate the Z and the Z values for rangeland and cultivated land with erosion and deposition points. Table 9 shows that the rangeland soil had lower SSA compared to the cultivated soil, and sediment had the highest SSA. This corroborates the sediment enrichment process via selective deposition of larger particles.

Table 8 Soil erosion and deposition rates predicted by the Migration and Diffusion Model for rangeland transects in the Bull Creek watershed.

Transect ID – Sample Number	Cs-137 inventory	Erosion Rate* - Using Z**	Erosion Rate - Without Z**	Position on Hillslope	Distance to Top of Hillslope	Elevation	Slope Steepness
	Bq m^{-2}	kg ha^{-1} yr^{-1}	kg ha^{-1} yr^{-1}		m	m	%
T02-01	1577	-0.5	-1.2	top	15	493	1
T02-02	1771	-0.2	-0.6	middle-top	51	492	2
T02-03	1132	-1.0	-2.5	middle-bottom	99	491	3
T02-04	1180	-0.9	-2.4	bottom	162	490	5
T03-02	1330	-0.7	-1.9	top	65	496	3
T03-03	1750	-0.2	-0.7	middle	94	495	4
T03-04	1362	-0.7	-1.8	bottom	125	493	8
T04-04	1577	-0.5	-1.2	top	65	496	3
T04-03	1714	-0.3	-0.8	middle-top	113	495	3
T04-02	1401	-0.6	-1.7	middle-bottom	183	492	5
T04-01	1332	-0.7	-1.9	bottom	240	490	4
T05-04	1733	-0.3	-0.7	top	42	487	12
T05-03	482	-1.9	-4.7	middle-top	71	484	10
T05-02	466	-1.9	-4.8	middle-bottom	106	481	9
T05-01	1077	-1.1	-2.7	bottom	143	478	8
T06-01	1217	-0.9	-2.3	top	45	487	10
T06-02	1181	-0.9	-2.4	middle-top	100	485	7
T06-03	1606	-0.4	-1.1	middle-bottom	153	481	8
T06-04	1951	0.2	0.1	bottom	204	477	6

Transect ID – Sample Number	Cs-137 inventory	Erosion Rate* - Using Z**	Erosion Rate - Without Z**	Position on Hillslope	Distance to Top of Hillslope	Elevation	Slope Steepness
T07-01	1372	-0.7	-1.8	top	22	488	5
T07-02	1222	-0.9	-2.3	middle	63	485	11
T07-03	540	-1.8	-4.5	bottom	138	477	10
T08-01	1372	-0.7	-1.8	top	22	488	5
T08-02	1130	-1.0	-2.5	middle	73	484	8
T08-03	384	-2.0	-5.1	bottom	138	479	11
T10-03	336	-2.1	-5.2	top	386	492	2
T10-02	377	-2.0	-5.1	middle	464	487	10
T10-01	358	-2.1	-5.3	bottom	512	483	6

*Negative number indicates erosion and a positive number indicates deposition.
**Particle size correction factor.

Table 9 Specific surface area and particle size correction factor for cultivated land and rangeland with erosion and deposition places

Landuse	Specific Surface Area (m^2 g^{-1})		Z*	
	Sample 1	Sample 2	Erosion	Deposition
Rangeland	3.3	3.8	2.9	0.34
Cultivated Land	11.4	11.7	1.2	0.85
Sediment	14.9		N/A	

* particle size correction factor

With the exception of the bottom downslope location on Transect 6, all erosion/deposition rates were negative implying erosion. However, the 95 percent confidence intervals were very wide, and thus statistically the sampling locations may have been deposition areas for the rangeland sites. When Z was included in the Migration and Diffusion model, the CIs were smaller compared to without using Z since the Cs-137 concentration was lower (see Equation 79; Nearing, 2000). The Nearing (2000) CI equation 79 accounts for the selective deposition of larger particles, which results in a higher concentration of fine particles in the sediment; thus resulting in a higher Cs-137 concentration per unit weight of sediment. Since the conversion models do not account for the fine particle enrichment, they overestimate soil erosion rates and underestimate deposition rates. He and Walling (1996) reported that Cs-137 was preferentially associated with fine particles, and thus including Z reduces the erosion predictions. However, the particle size correction factor may not be uniform for all soil types (Parsons and Foster, 2011). Figure 40 illustrates the increase in predicted erosion rates when using Z based on the Migration and Diffusion model. Figure 40 also shows that rangeland had a steeper slope compared to the cultivated land, indicating that the selective deposition was influenced more in rangeland compared to cultivated land. A shortcoming of Z was it did not account for rainfall intensity, plant coverage, topography and other factors that affect the selective deposition process.

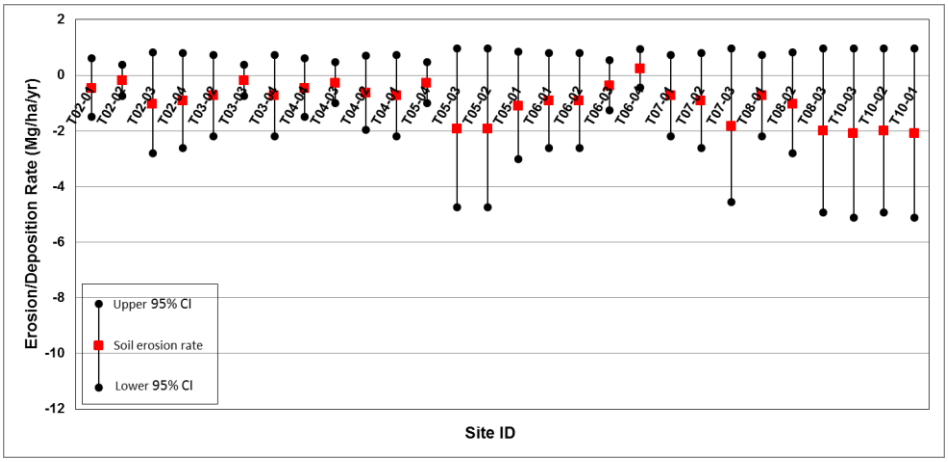

Figure 37 Erosion/deposition rate means with 95 percent confidence intervals for rangeland soil samples using the soil particle correction factor (Z), using the Migration and Diffusion model.

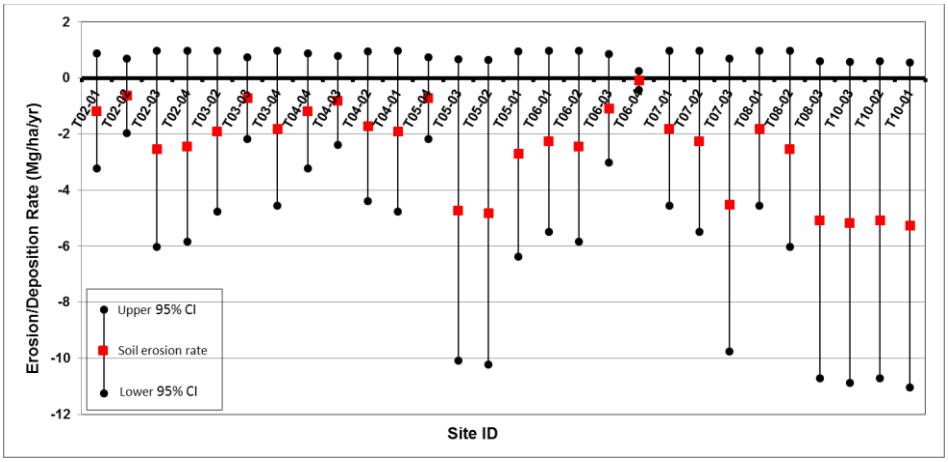

Figure 38 Erosion/deposition rate means with 95 percent confidence intervals for rangeland soil samples without using the soil particle correction factor (Z), using the Migration and Diffusion model.

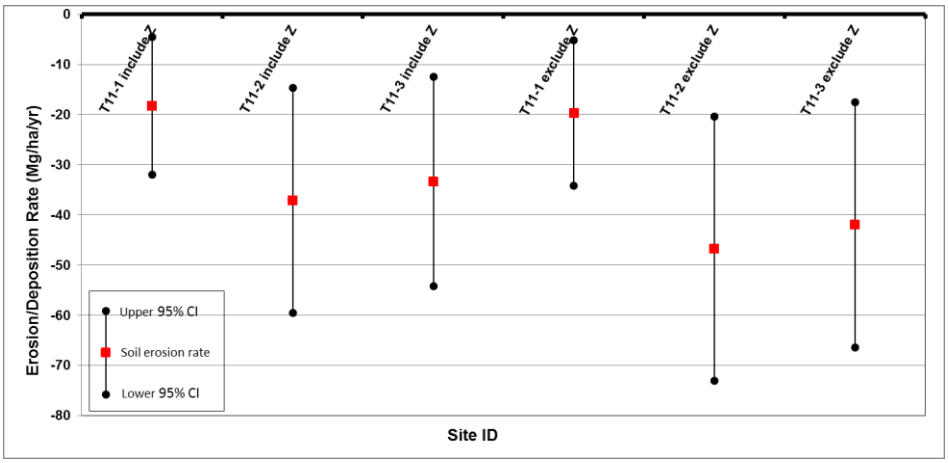

Figure 39 Erosion/deposition rate means with 95 percent confidence intervals for cultivated land soil samples with and without using the soil particle correction factor, Z, using the Mass Balance III model.

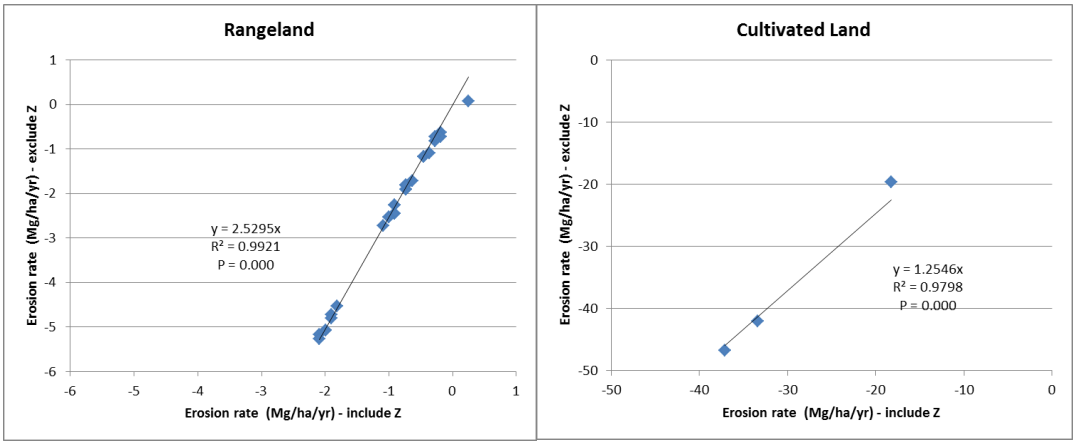

Figure 40 Comparison between predicted erosion/deposition rate using the Migration and Diffusion model for rangeland and Mass Balance III for cultivated land - with and without using the soil particle correction factor (Z).

4.1.1.2.2 Cs-137 method for rangeland

Figure 40 shows the relationship between the erosion rates and the slope steepness change. For rangeland, the erosion rates were negatively correlated with slope steepness at an α=0.05, while the erosion rates were not significantly correlated to slope steepness for the cultivated land. This may have been due in part by the low sample size and/or the terraces in the cultivated land.

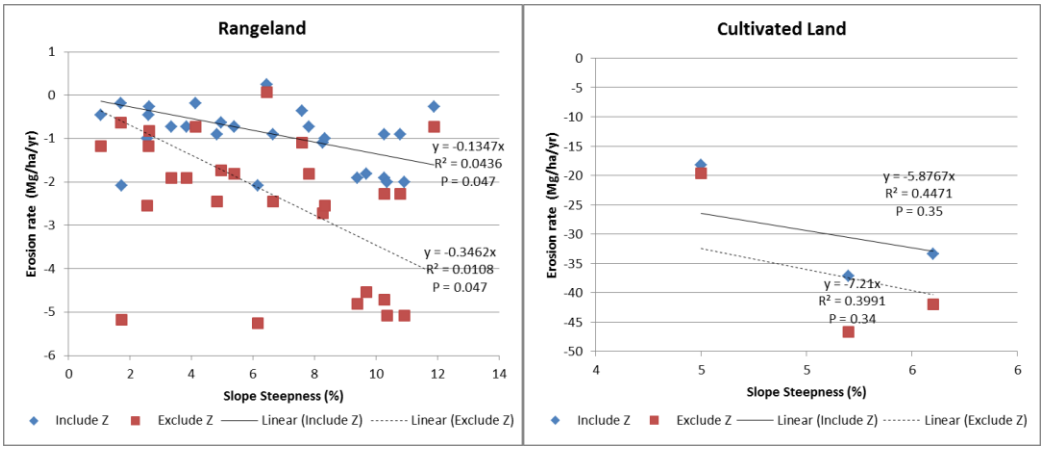

Figure 41 Erosion rates change with the slope steepness for rangeland and cultivated land.

Based on proximity (Figure 24) and observations in the field, transect 02, 03 and 04 were described together as one group. These three transects had similar landform, the slope steepness increased from the top to the bottom, and had an average slope steepness 3.6%. Transect 03 was out of the watershed; however, it was adjacent to watershed and had the same soil type and land use as the rangeland in the subwatershed. Transect 05 and 06 were a second group, which had an average slope steepness of 8.8%, and the slope steepness decreased from the top to the bottom of the slope. Transects 07 and 08 were a third group, which had the same landform as the first group, however they had larger average slope steepness of 8.4%. Transect 10 and 11 were discussed individually. The slope steepness first increased and then decreased for transect 10, and had an

average slope steepness was 6.1%. Transect 11 was the only cultivated hillslope and the slope steepness for the middle of the terrace was 5.1%.

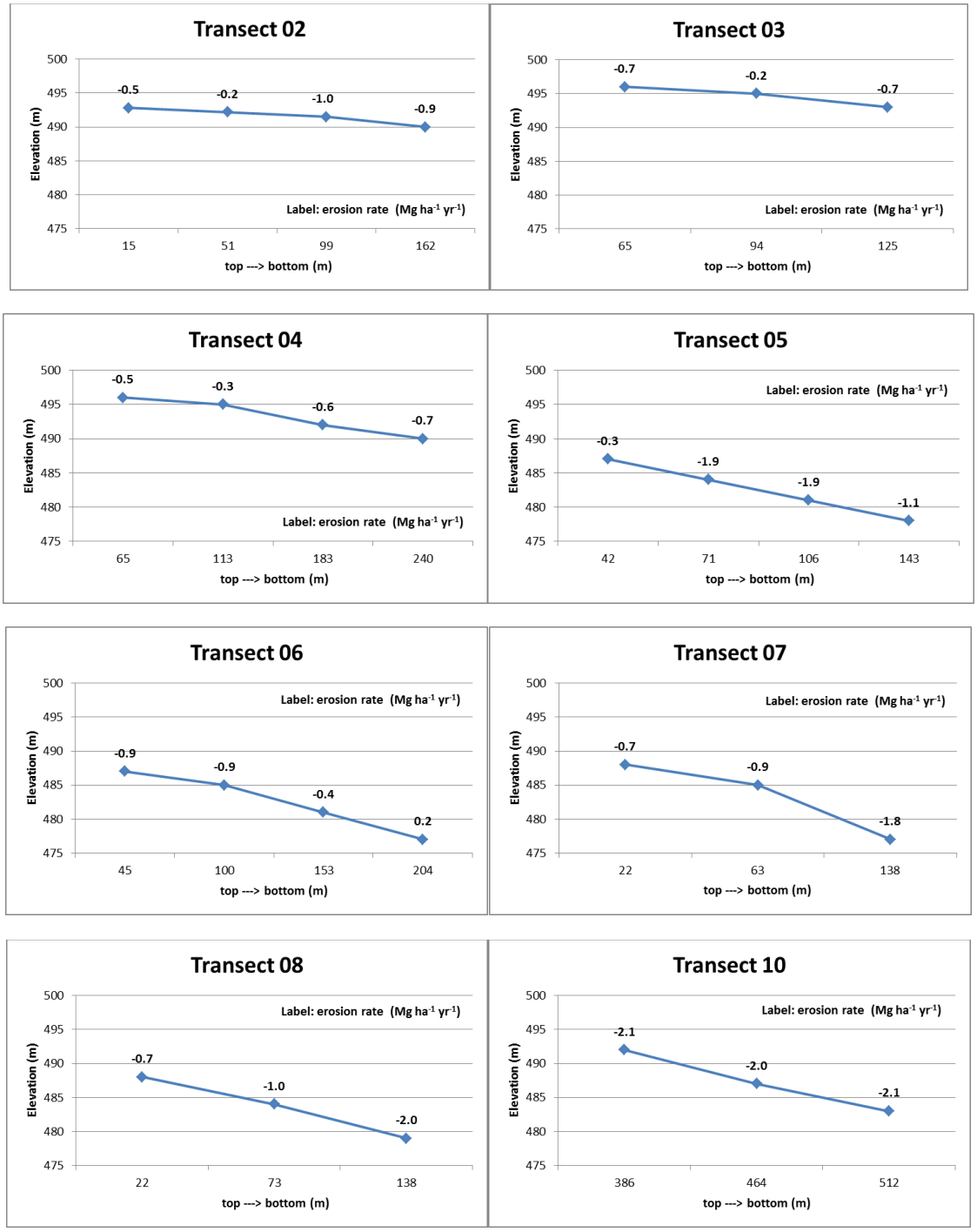

Figure 42 Transect profiles and soil erosion rates predicted by the Cs-137 method for the rangeland (using the Diffusion and Migration model).

(a) Top (b) Middle

(c) Bottom

Figure 43 Vegetative cover change from the top to the bottom of the hillslope for Transect 03 in the Bull Creek watershed.

The soil erosion rates using Cs-137 method predicted included Z for all transects are given in Figure 42 (the Diffusion and Migration model was used for the rangeland and Mass Balance Model III was used for the cultivated land). Transect 02, 03 and 04 soil erosion rates decreased from the top to the middle-top of the hillslope then increased from the middle-top to the bottom of the hillslope. For all the transects, there was a change of the dominant plant type from the top

to the middle-top locations. As shown in Figure 43 for transect 03, the top of the hillslope vegetative cover was lower than the bottom, and there was a clear change at the middle of the hillslope. The vegetative cover increased at the middle of the transect, which reduced the soil loss. From the middle-top to the bottom of the hillslope, the dominant plant types and vegetative cover were similar.

Transect 05 and 06 were located on a small hill with the upslope samples taken on a rocky outcrop; the slope steepness decreased from the top to the bottom of the hillslope. As can be seen from the Figure 42 (d), the soil erosion rates first increased and then decreased for the transect 05; and the soil erosion rates decreased from the top to the bottom for the transect 06 with a deposition point at the end of the transect. At the top of these two transects, the slope steepness were larger than the middle-top. In addition, the top of the transect had less vegetative coverage than the middle-top. This may explain why the top of the transect 06 had almost equally erosion rates as the middle-top. Although it was not sampled, there was a large proportion of the rock outcrop at the top of the transect 05 (Figure 44), which may reduce the soil loss (Poesen et al., 1994).

Figure 44 Top of transect 05 in the Bull Creek watershed.

Transects 07 and 08 started at the same top of a hill and both ended before they reached gullies, and the slope steepness increased from the top to the bottom (Figure 45). The predicted soil erosion rates increased from the top to the bottom of the transect, and the erosion rates increased faster from the middle to the bottom compared to the top to the middle. This coincided with the landform, which convex profiles. And it was most steepness at the end of the bottom.

The slop steepness for transect 10 increased significantly and then decreased from the top to the bottom and had a concave profile. The vegetative cover did not appear to change from the top to the bottom of the transect. However, the soil erosion rates were similar for the three sampling points. Based on the flow direction map (Figure 46), the sampling positions did not follow the flow direction for the transect 10, which means the three samples for the transect 10 cannot represent the top, middle and bottom of one hillslope. Based on the photo for the transect 10 (Figure 47), the hillslope was difficult to visually identify, and thus transect 10 was not discussed or compared to WEPP predictions.

Figure 45 Transect 08 in the Bull Creek watershed.

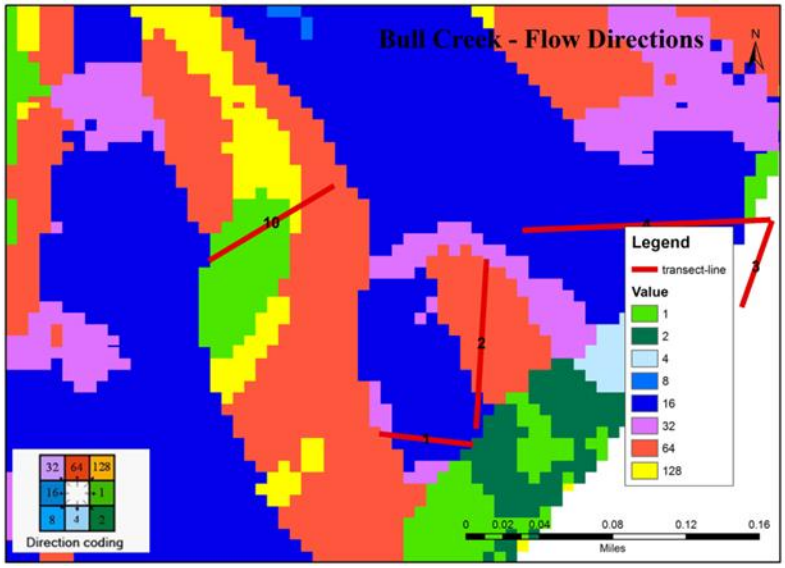

Figure 46 Flow directions for transect 10 in the Bull Creek watershed.

Figure 47 Transect 10 in the Bull Creek watershed.

4.1.1.2.3 Cs-137 method for cultivated land

Transect 11 was the only transect in the cultivated land. There were three terraces in the sampled area. Samples were taken using the same method as for the rangeland transets (dashed blue lines,

Figure 48). To analyze the effects of terraces on the Cs-137 method to predict soil erosion, soil core samples were taken at the upslope terrace bank (red dot, Figure 48) and the downslope terrace bank (blue dot, Figure 48). Table 10 and Table 11 present predicted soil erosion rates using the Cs-137 method. Four conversion models (Proportional Model, Mass Balance Model I, II, and III) were evaluated with and without the particle size correction factor Z. The Mass Balance model I predicted the highest soil erosion rates, and the results from the other three models were similar. The soil erosion rates predicted by the Mass Balance model III with the Z are given in Figure 49. The Mass Balance model III assumed that the erosion at the top of the hillslope was caused only by tillage. However, the model predicted zero soil loss caused by tillage for the middle and upslope terrace bank. The results from all the four models had similar trends (Figure 50), with the lowest soil erosion rate at the top of the transect, increased at the middle segment, and reduced slightly at the upslope terrace bank.

Figure 48 Arial Photograph of Transect 11 (Google Earth, 2012). Red dots were the upslope terrace bank; blue dots were the downslope terrace bank; blue dash lines were where soil samples were collected; red line shows the estimated flow direction.

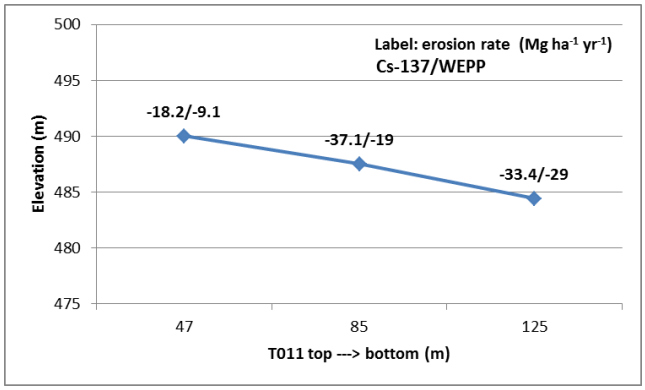

Figure 49 Transect profiles and soil erosion rates predicted by the Cs-137 method for the cultivated land (using the Mass Balance Model III).

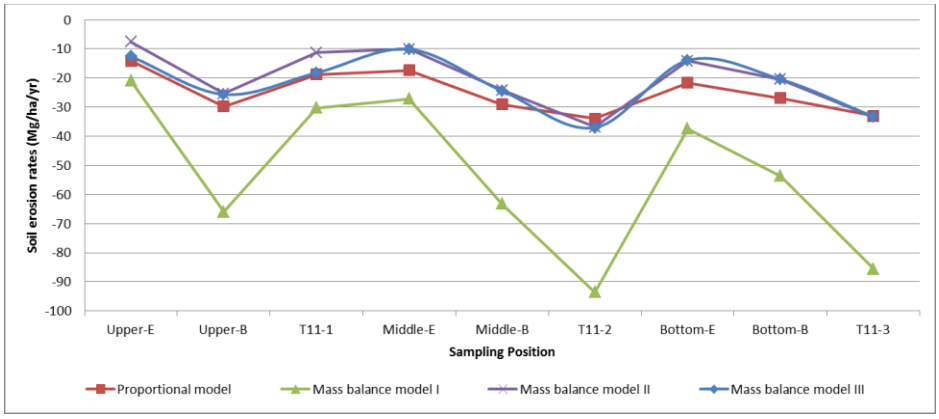

Figure 50 Soil erosion rates predicted by the Cs-137 Mass Balance Model III for the cultivated land in the Bull Creek watershed (Upper-E, middle-E and bottom-E were samples from the upslope terrace bank - red dot from Figure 48 from left to right; Upper-B, middle-B and bottom-B were samples from the downslope terrace bank - blue dot from Figure 48 from left to right).

Table 10 Soil erosion and deposition rates predicted by the Migration and Diffusion Model – cultivated land, excluding the soil particle size correction factor (Z), in the Bull Creek watershed.

Transect ID – Sample Number	Cs-137 activity (Bq m^{-2})	Soil Erosion Rate (Mg ha^{-1} yr^{-1})			
		Proportional Model	Mass Balance Model I	Mass Balance Model II	Mass Balance Model III
T11-1	968	23.8	39.0	14.8	19.7
T11-2	235	40.8	115	46.2	46.9
T11-3	281	39.9	105	42.1	41.9

Table 11 Soil erosion and deposition rates predicted by the Migration and Diffusion Model – cultivated land, included the soil particle size correction factor (Z), in the Bull Creek watershed.

Transect ID – Sample Number	Cs-137 activity (Bq/m^2)	Soil Erosion Rates ($Mg\ ha^{-1}\ yr^{-1}$)			
		Proportional Model	Mass balance Model I	Mass balance Model II	Mass balance Model III
T11-1	968	18.8	30.3	11.2	18.2
T11-2	235	33.9	93.5	36.8	37.0
T11-3	281	33.0	85.6	33.4	33.2

There were two primary reasons why the Mass Balance model II and III had dissimilar results from the Proportional model. The first was tillage typically occurred following harvest (late May to early June) and before planting for the next crop (late August to early September). High rainfall periods were typically in the spring and fall, and thus freshly deposited Cs-137 was mixed by tillage in the plow layer prior to the high rainfall periods. Therefore, the Mass Balance model II and III can be simplified to the Proportional model after Cs-137 was well mixed in the plow layer. The second possible reason why there were similar predictions between the Proportional model, Mass Balance model II and III results was the Mass Balance II and III assumed that soil below the tillage layer had little Cs-137. However, in the study area, the cultivated soil below the tillage layer contained Cs-137 (Figure 36).

The Mass Balance models predicted the largest soil erosion rates, in part, due to the assumption that all the Cs-137 fallout occurred in 1963. Although Cs-137 fallout had a peak in 1963, Cs-137 deposition was 48, 20 and 32 percent for the periods before 1963, in the year 1963 and after 1963, respectively, based on the average Cs-137 fallout for the north hemisphere (Zapata, 2002). Assuming all Cs-137 was deposited in 1963 neglects Cs-137 decay prior to 1963. Although the Cs-137 deposited after 1963 decayed longer, the Cs-137 deposited after 1963 was less than the Cs-137 deposited before 1963. So, Cs-137 inventory needed to be removed faster than it should be to have the same sampled Cs-137 activity. As a result, this assumption overestimated soil loss.

To analyze the effect of the terraces on the soil erosion and the Cs-137 method, erosion rates for the terrace samples were calculated using the four conversion models for cultivated land. From the soil erosion rates in Table 12 and Table 13, it can be seen that downslope terrace bank had larger erosion rates than the upslope terrace bank; and the upslope terrace bank had an average lower erosion rate than the middle part. The downslope terrace bank had steep slope steepness (normally largest for one terrace). The upslope terrace bank had the same slope steepness or may a little higher elevation than the middle, and would reduce or trap the runoff. From the field observation, there were normally small water pools at the upslope terrace bank after rainfall. Similar results were also reported by other researcher (Lu and Higgitt, 2000). The Cs-137 inventory decreased with increasing slope steepness along different types of terraces. This was due to the increasing soil erosion with the increasing slope steepness.

Table 12 Soil erosion rates, excluding the soil particle size correction factor (Z), for the terraces using the Proportional Model, Mass Balance Model I, II and III in the Bull Creek watershed.

Sample ID*	Cs-137 ($Bq\ m^{-2}$)	Soil Erosion Rate ($Mg\ ha^{-1}\ yr^{-1}$)			
		Proportional Model	Mass Balance Model I	Mass Balance Model II	Mass Balance Model III
Upper-E	1190	17.0	24.9	9.2	12.6
Upper-B	439	35.6	78.7	30.7	31.2
Middle-E	1040	20.9	32.3	12.1	12.1
Middle-B	465	35.0	75.6	29.4	29.6
Bottom-E	825	26.0	44.8	17.0	16.8
Bottom-B	577	32.1	64.1	24.7	24.7

*Upper-E, middle-E and bottom-E were samples from the upslope terrace bank (red dot from Figure 48 from left to right); Upper-B, middle-B and bottom-B were samples from the downslope terrace bank (blue dot from Figure 48 from left to right).

Table 13 Soil erosion rates, including the soil particle size correction factor (Z), for the terraces using the Proportional Model, Mass Balance Model I, II and III in the Bull Creek watershed.

Sample ID*	Cs-137 (Bq m^{-2})	Soil Erosion Rate (Mg ha^{-1} yr^{-1})			
		Proportional Model	Mass Balance Model I	Mass Balance Model II	Mass Balance Model III
Upper-E	1190	14.1	20.9	7.6	12.6
Upper-B	439	29.8	65.9	25.3	25.6
Middle-E	1040	17.3	27.1	10.1	10.1
Middle-B	465	29.1	63.2	24.2	24.4
Bottom-E	825	21.7	37.4	14.1	13.9
Bottom-B	577	26.9	53.6	20.4	20.4

*Upper-E, middle-E and bottom-E are the samples from the upslope terrace bank (red dot from Figure 48 from left to right); Upper-B, middle-B and bottom-B are the samples from the downslope terrace bank (blue dot from Figure 48 from left to right).

4.1.2 Cs-137 method evaluation

4.1.2.1 Reference site variability

Table 14 shows the measured Cs-137 inventory for all the reference samples. The Cs-137 from the forest reference sample near Bull Creek was only 151 Bq m^{-2}, which indicated it was heavily disturbed. The remaining reference samples were collected in a forested area near Fort Cobb reservoir. The samples collected using the large soil ring had the highest Cs-137 inventory, with a mean Cs-137 inventory of 1929 ± 96 (standard error of the mean) Bq m^{-2}, a standard deviation of 69.5 Bq m^{-2}, and a coefficient of variation (CV) of 3.6%. The samples collected using the soil probe had a mean of 1340 ± 111 Bq m^{-2}, a standard deviation of 219 Bq m^{-2} and a CV of 16%. Although the larger sampling equipment area may not result in more reliable results (Sutherland, 1991), the samples taken using the large soil ring had smaller CV and were closer to the average Cs-137 deposition for the study area reported by Agudo (1998). UNSCEAR (1993) also reported the deposition of Cs-137 in the United State (Figure 51), with more than 3000 Bq m^{-2} in 1993 for

the study area, which was converted to the year 2012; this was more than 1937 Bq m^{-2} Cs-137 in the year of 2012. This confirmed using the Fort Cobb Reservoir site using the large soil rings as the reference CS-137 levels.

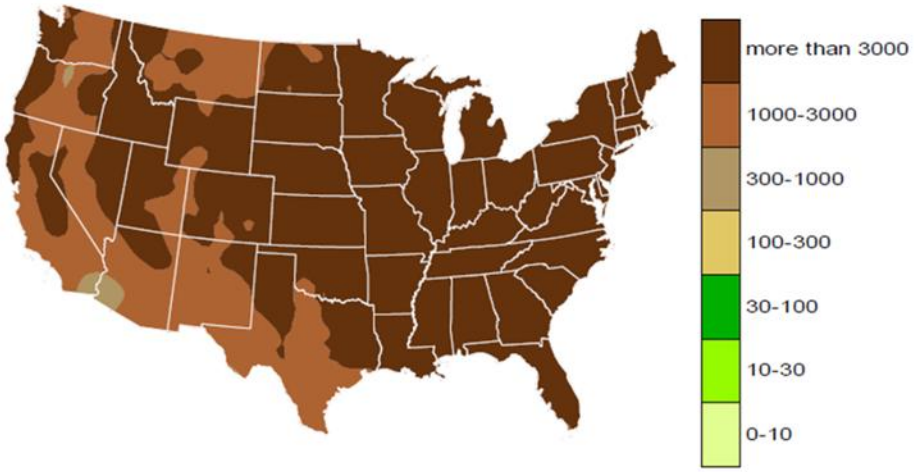

Figure 51 Cs-137 deposition density (Bq m^2) due to the Nevada Test Site and global fallout in the USA (UNSCEAR, 1993).

Table 14 Reference site Cs-137 soil sample concentrations.

Sample No.	Cs-137 Activity (Bq m^{-2})	Sampling Equipment Surface Area (cm^2)	Sampling Equipment	Location
FCR 1	1165	18	Soil probe	Fort Cobb
FCR 2	1621	18	Soil probe	Fort Cobb
FCR 3	1331	18	Soil probe	Fort Cobb
FCR 4	1015	18	Soil probe	Fort Cobb
FCR 5	1140	18	Soil probe	Fort Cobb
FCR 6	1277	18	Soil probe	Fort Cobb
FCR 7	1355	18	Soil probe	Fort Cobb
FCR 8	1698	18	Soil probe	Fort Cobb
FCR 9	1413	18	Soil probe	Fort Cobb
FCR 10	1532	18	Soil probe	Fort Cobb
FCR 11	1394	18	Soil probe	Fort Cobb
FCR 12	900	18	Soil probe	Fort Cobb
FCR 13	1542	18	Soil probe	Fort Cobb
FCR 14	1389	18	Soil probe	Fort Cobb

Sample No.	Cs-137 Activity (Bq m^{-2})	Sampling Equipment Surface Area (cm^2)	Sampling Equipment	Location
FCR 15	1352	18	Soil probe	Fort Cobb
R1	1880	6296	Large soil ring	Fort Cobb
R2	1978	6296	Large soil ring	Fort Cobb
BC-R	151	6296	Large soil ring	Colony

The Cs-137 inventory in the reference site was essential to calculating the soil loss. Since all erosion/deposition rates were calculated by comparing the Cs-137 to the reference site, the change of the reference inventory affected all predicted soil erosion/deposition rates. What is more, the magnitude of the reference Cs-137 inventory defined a sampling site as an erosion or deposition point. Figure 52 shows the relationship between the reference Cs-137 inventory and the predicted soil loss rates using the Diffusion and Migration model (example of transect 6 bottom sample, T06-4, Table 8). The reference inventories used in Figure 52 were the sampled reference inventory in Table 14 (excluding sample BC-R). When the reference inventory was smaller than the sampled point, the sampled point was defined as a deposition point. When the reference inventory was larger than the sampled inventory, the sampled point was defined as an erosion point.

Although different sampling methods have been evaluated to collect reference samples, large variance in Cs-137 reference site samples have still been reported (Zapata, 2002). Sutherland (1996) article review reported a median CV of 19% with a range of 1.5 to 86%. Owens and Walling (1996) studied cause the Cs-137 variance in reference sites, and found that the main reasons was the random spatial distribution of Cs-137, even in small undisturbed area. The soil properties, plant coverage, micro-topography and other factors which affect the spatial distribution of rainfall, also cause the random spatial distribution of Cs-137. Sampling and testing errors also contribute to the Cs-137 variance. However, the errors caused by the sampling and testing were complicated. Sutherland's (1991) showed that an increase in the sampling number

might not necessarily reduce the CV. Neither fewer samples but using sampling equipment with large area would reduce the CV (Sutherland, 1991).

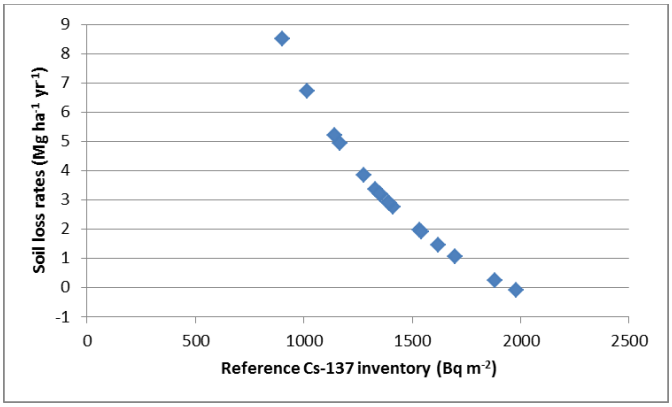

Figure 52 Relationship between reference Cs-137 inventory and the soil erosion rates predicted by using the Diffusion and Migration model (T06-4 in Table 8; positive soil loss rates are deposition and negative rates are erosion).

In conclusion, the random spatial distribution of Cs-137 in reference sites can affect the predicted soil loss significantly. Therefore, selection of a reference site, the sampling method, and the number of samples must be treated with caution. Note that these same issues may also affect the field soil samples, especially in uncultivated areas.

4.1.2.2 Measurement error

The Cs-137 signal in soil samples decrease with time. As the signal decreases, the measurement error of Gama Spectrometry increases (Wei, 2007). Figure 53 gives the relationship between the measurement error and Cs-137 activity for this study. The average measuring error was 16% with the minimum and maximum of 0 and 115%, respectively, and the standard deviation was 20%. Figure 54 shows the histogram of the measurement error. When the Cs-137 activity was less than 190 Bq m^{-2}, the measurement average error was larger than 10%. Xie et al. (2010) reported that when the measurement error was larger than 10%, 13% of the samples had Cs-137 activities

lower than the reported minimum detectable activity, which was 1.0 Bq kg^{-1} (Kannan et al., 2002). Therefore, samples with low Cs-137 activity cannot be measured accurately even there was detectable Cs-137 in the soil.

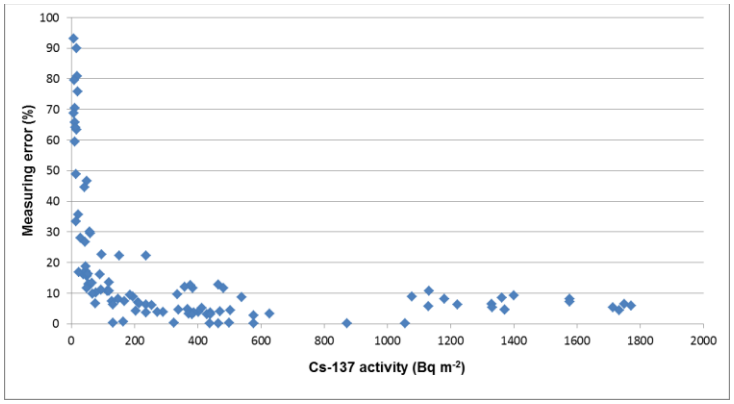

Figure 53 Relationship between measurement error and Cs-137 activity.

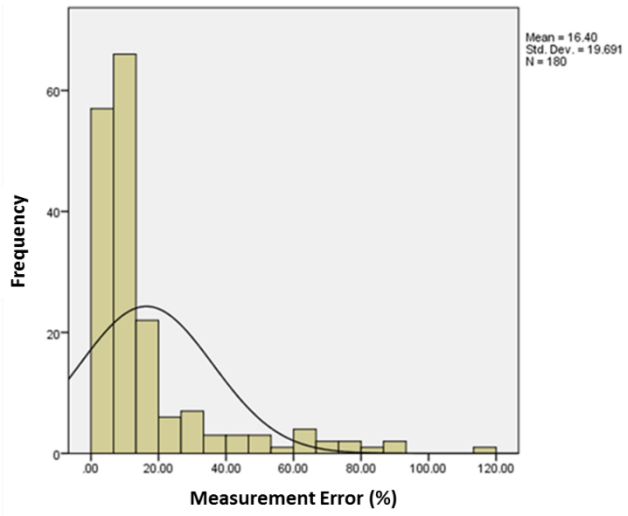

Figure 54 Distribution of Cs-137 measurement error.

The testing time for the Gama Spectrometry was initially set to 2880 seconds (8 hours). However, due to different Cs-137 signal strength in each sample, the testing time was adjusted and ranged from 11690 to 83770 seconds, with an average of 37120 seconds. And14% was less than 2880

seconds. Although there was not a clear relationship between the testing times and the Cs-137 activity (Figure 55), the counting time could affect the Cs-137 measurement. When Cs-137 decays it emits gamma photons, the gamma photons hit the detector, and the corresponding number of gamma photons is recorded, which was defined as the Cs-137 activity. Since Cs-137 decay randomly, the lower the testing time the fewer random signals were counted. Another source of error was related to the Cs-137 measurement was the tested sample weight varied from 250 to 400 g, with an average of 328 g. Yet another source of error was the sample weight, because the sample weight not only decided the Cs-137 amount, but also the distance from the sample surface to the detector. Radu et al. (2009) showed that the distance from the sample to the detector could significantly affect the count rates.

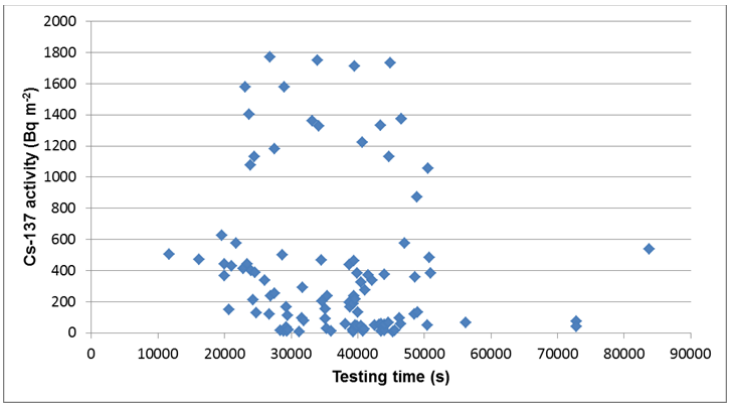

Figure 55 Relationship between the testing time and Cs-137 activity.

4.1.2.3 Fine particles and surface area

Since research has shown that Cs-137 was positively correlated to fine particle fraction, the particle size correction factor was widely used in the conversion models to reflect the selective deposition process with erosion and sedimentation (Walling et al., 2006). Figure 56 shows the relationships between Cs-137 activity and silt and clay particles for this study. The Cs-137 activity did not have a strong positive relationship with the fine particles.

He and Walling (1996) found that as the fraction of sand particles increased, there was also an increase in Cs-137 absorption onto the sand particles. Cs-137 absorption to clay varies for different clay mineralogy and the other soil properties (Eberl, 1980). For example, Cs-137 was exchangeable by potassium (K) and the organic matter, which could reduce the absorption of Cs-137 onto clay (Rafferty et al., 1997, Wendling et al., 2005). Oscarson et al. (1994) tested the Cs-137 absorption on condensed and loose clay and found that condensed clay decreased Cs-137 by up to 50% compared to loose clay. Since most Cs-137 was tested on loose soil, Cs-137 in undisturbed natural soils may not have as strong relationship with clay as reported.

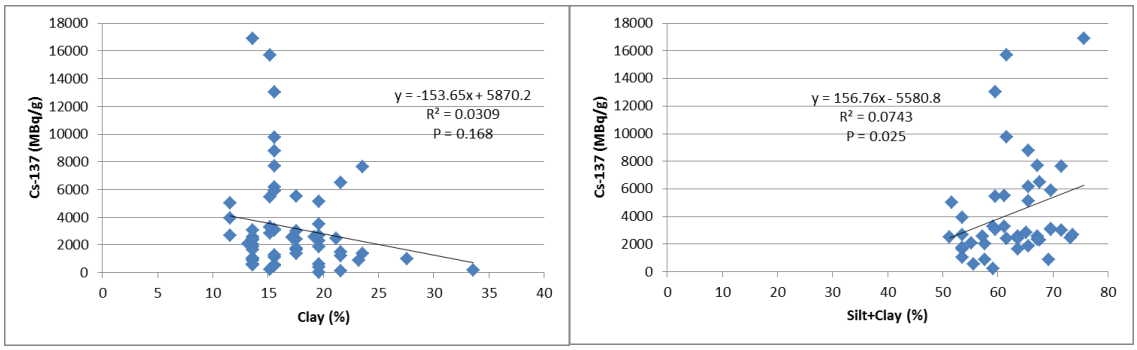

(a) (b)

Figure 56 Relationship between Cs-137 activity and percent silt and clay particles.

4.1.2.4 Cs-137 fallout rates

Yang et al. (1998) studied the effect of annual Cs-137 fallout input on prediction uncertainty in the conversion model. Most studies have used the annual input fraction of Cs-137 for north hemisphere from data published by Owens et al. (1996), which were based on global Sr-90 data. Figure 57 illustrates the effect of annual Cs-137 input on soil loss prediction using the Mass Balance II. The line 1, 2 and 3 represented the soil loss predicted using different annual Cs-137 input. When assuming all Cs-137 input was in 1963, it would overestimate the soil loss. This study utilized these data published by Owens et al. (1996). However, the Cs-137 inputs in the

study area were different from the average for north hemisphere. Since no observed data for the study area were found, it was difficult to quantify how the Cs-137 annual inputs affected the predicted soil loss.

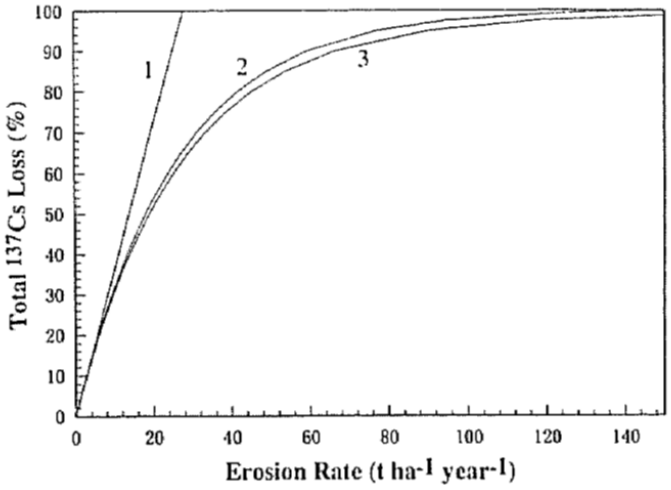

Figure 57 Relationship between Cs-137 annual inputs and the soil loss prediction (Yang et al., 1998). Line 1 assumed all Cs-137 input was in year 1963; line 2 used the inputs calculated by equations by same reference as above (Yang et al., 1998); line 3 used the annual Cs-137 inputs published by Owens et al. (1996).

4.2 Fingerprinting method

4.2.1 Sub-watershed sediment source contributions

The fingerprinting method had two main steps to predict sediment source contributions. The first step used statistical methods to identify significant chemical properties for the mixing model. The second step was to use the mixing model to predict sediment source contributions. Six sediment traps were selected and used in the mixing model based on the original mixing model, Collins' method and the DFA method and are shown in Figure 58. For each subwatershed, the sediment sources contribution were identified as one of two sources; Source Group 1 was upland and gully,

and Source Group 2 was cultivated land, rangeland and gully. Note the upland areas were defined as the sum of the cultivated land and rangeland. Source Groups 1 and 2 were both analyzed separately to determine how defining sources would influent the fingerprinting method. The results from the original mixing model are given in Table 15. Based on the statistical tests, seven of the 15 subwatersheds had elements that were significantly different between the sources. Some of the elements had higher concentrations in the sediment than the source soil, while some elements had lower concentration in the sediment than in the sources. Since all the samples were wet sieved using the 63μm mesh, the ones out of range were eliminated from the analysis. The reasons for the this phenomenon may differ for each element, and further research should be done to study the properties of each element during the erosion processes.

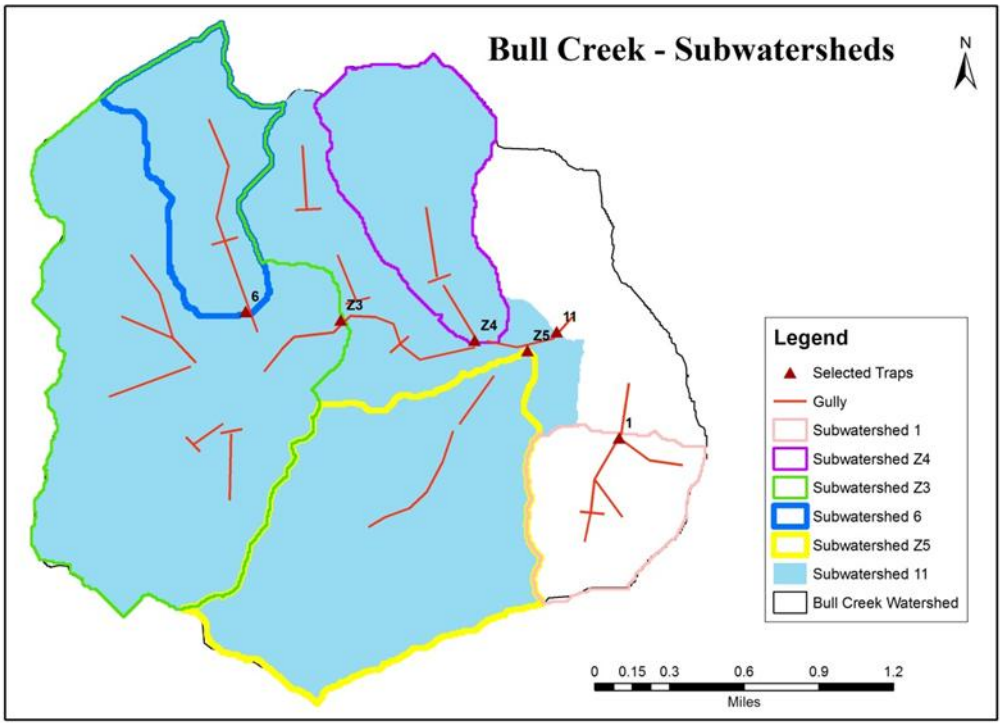

Figure 58 Subwatersheds for the six selected sediment traps for the fingerprinting method in the Bull Creek watershed.

Table 15 Results from the fingerprinting method for the sub-watersheds in the Bull Creek watershed.

Sub-watershed No.	Area (ha)	Element	Source Group 1 (%)		Source Group 2 (%)			Root Mean Error (%)	Area (%)	
			[1]U	[2]G	[3]C	[4]R	G		C	R
1	100	Br	6.7	93				<0.1	24	76
		Br			0.0	10	90	<0.1		
6	110	Zr	64	36				<0.1	56	44
		Hf1	77	23				<0.1		
		Combined[5]	72	28				0.2		
		As			6	89	5	<0.1		
		As,H			0	88	12	1.3		
Z3	510	Zr	94	6				<0.1	63	37
		Ca	82	18				<0.1		
		Co	82	18				<0.1		
		Mn	87	13				<0.1		
		Combined	84	16				<0.1		
		Mg,Ca			36	50	14	<0.1		
		Zr,Cs-137			8	0	92	1.1		
		Combined			33	52	15	1.3		
Z4	140	Ba	62	38				3.4	73	27
		Cs	2	98				83		
		Combined	3	97				87		
		Zr,Hf			0	86	14	0.3		
		Hf,C			0	49	51	22		
		C, Cs-137			0	1	99	7.1		
		Combined			0	2	98	23		
Z5	300	S	77	23				<0.1	60	40
		Ca	84	16				<0.1		
		Mn	17	83				<0.1		
		Combined	78	22				4.1		
		Ca,Zr			39	48	13	<0.1		
		Mo,Zr			82	18	0	<0.1		
		Zr,Br			24	55	21	<0.1		
		Br,Cs-137			37	2	61	<0.1		
		Combined			72	0	28	19		

[1] upland (Rangeland plus Cultivated land);
[2] gully;
[3] cultivated land;
[4] rangeland;
[5] all chemical properties

To evaluate the fingerprinting method, all significant properties that qualified for the mixing model were used individually or in a set of two elements, and then combined. Figure 60 and Figure 61 compared the results for Source Group 1 and Source Group 2, respectively. For Source Group 1, the results calculated using different chemicals were quite different for subwatersheds Z4 and Z5; Source Group 2 also showed different results. When comparing the upland and gully contributions predicted from Source Groups 1 and 2 (Figure 62), similar conclusions were drawn. For Z3, only the Source Group 2 using Zr and Cs-137 had lower erosion from upland and higher erosion from gully sources.

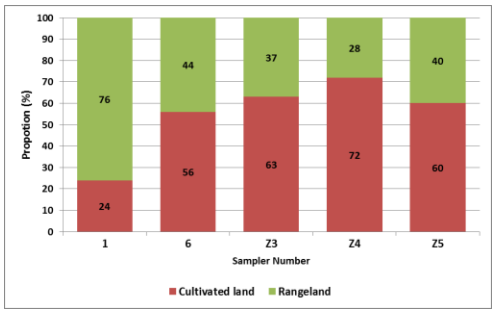

Figure 59 Cultivated land and rangeland area proportion for each subwatershed.

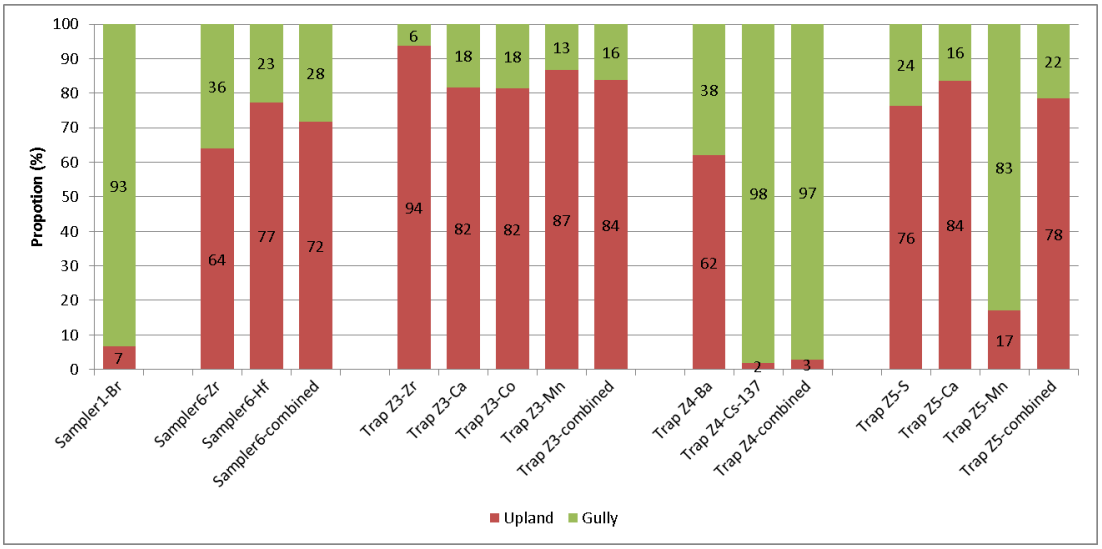

Figure 60 Source Group 1 upland and gully contributions by sub-watershed in the Bull Creek watershed using the fingerprinting method.

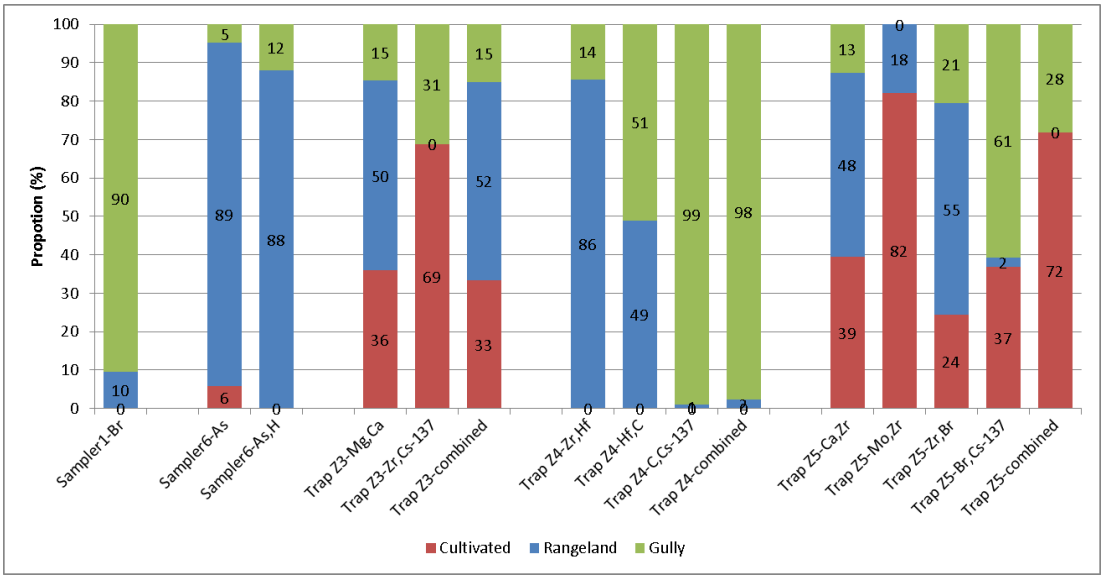

Figure 61 Source Group 2 cultivated land, rangeland and gully contributions by sub-watershed in the Bull Creek watershed using the fingerprinting method.

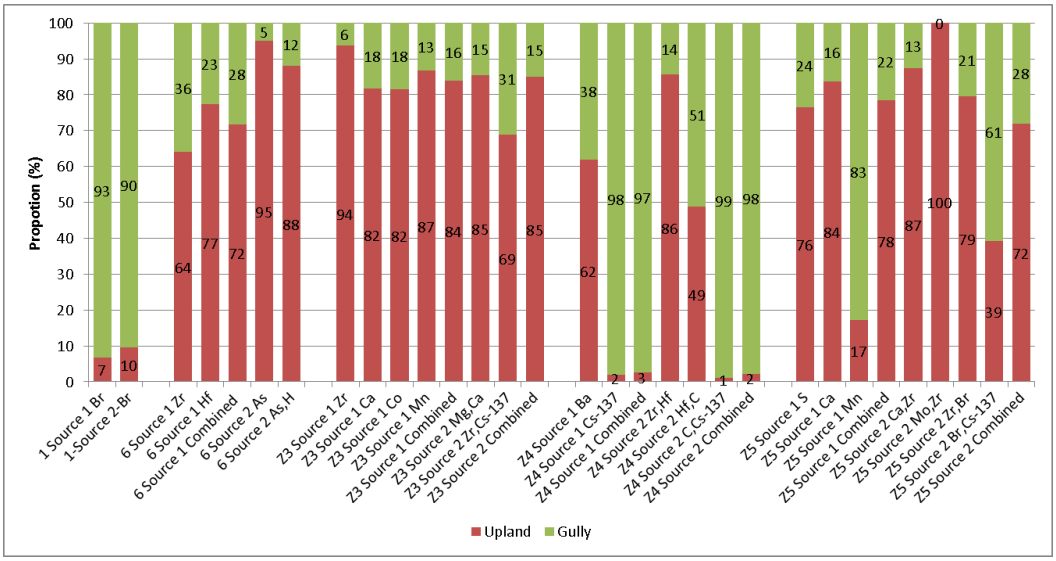

Figure 62 Source contribution comparison between Source Group 1 and 2 using the fingerprinting method.

Subwatershed 1 had well developed gullies, especially at the head cut (Figure 63). The landcover at the head cut and along the gully banks was rangeland and was not wooded like other channels

in the watershed. In this subwatershed, cultivated land was only 24% and runoff from the cultivated land traveled through grassland before reaching the gully.

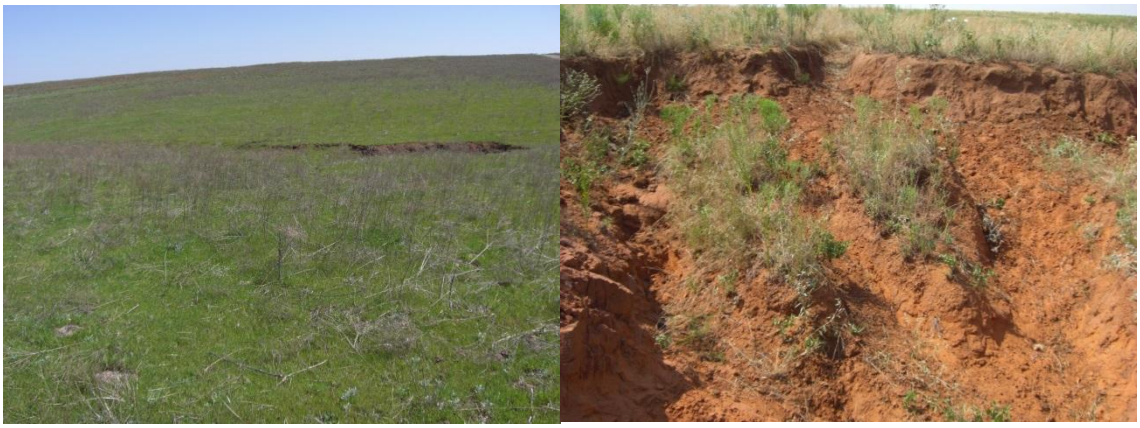

Figure 63 Gully head cut in subwatershed 1 in the Bull Creek watershed.

For subwatershed 6, the upland contributed less sediment from Source Group 1 compared to Source Group 2, and Source Group 2 showed that almost all sediment from upland was from rangeland. The Kruskal-Wallis T-test at the 0.05 level showed that the As concentrations were significantly different between cultivated land and rangeland, but there was no significantly difference between rangeland and channel samples. Note that the gullies in subwatershed 6 were surrounded by forest and rangeland separated the cultivated land from the gullies. One possibility for the high contribution from rangeland would be that rangeland acted as vegetation buffer and trapped most of all the sediment from the cultivated land and the gully contribution was also low. Another possibility would be that if the element was not significantly different between rangeland and gully; the mixing model may not predict the contribution from rangeland and gully accurately. In another word, the mixing model cannot identify which sediment was from rangeland and which was from the gully.

Subwatershed 6 was contained within subwatershed Z3 and the entire subwatershed was similar. However, the source contributions for the fingerprinting method using the Zr and Cs-137 were

quite different from each other. Possible reasons included the high Cs-137 data variance and the fingerprinting method was based on the average contribution from five storm events. However, only one storm event had enough sediment to measure Cs-137. Source Group 2 was recalculated for the one storm event and the fingerprinting method using Mg and Ca showed that the sediment had 1% from cultivated land, 91% from rangeland and 8% from gullies; results using Zr and Cs-137 showed 100% was from cultivated land. Note that the results from Mg and Ca had a RME of <0.1% and the Zr and Cs-137 had an error of 225,000%. The latter had larger error because Zr had different concentration distribution in the sources from Cs-137. For the Zr, the concentration was lowest in the cultivated soil samples, then rangeland, and highest in the gully. The Zr concentration in the sediment was the closest to the rangeland samples. For Cs-137, the concentration was lowest in the gully samples, then cultivated land, and highest in the rangeland. The Cs-137 in sediment was closest to cultivated land. This means if use Zr only, mixing model would predict highest contribution from rangeland but if use Cs-137 only, the mixing model would predict highest contribution from the cultivate land. The different element distribution in the sources decided the fail or large error of the mixing model. Mg and Ca concentrations had the same distribution in the sources (sediment samples were both closest to cultivated land). This means that use either Mg or Ca, mixing model would predict the similar results.

The results for Z4 and Z5 both varied a lot when using different chemical properties. For the Z5, the channels were well covered by trees and grass, but the average predicted contribution from gully was higher than the other subwatersheds, except subwatershed 1 where channels were not well covered and had active head cuts. It was likely that the pond in the middle end of the subwatershed (Figure 64) had an effect on the sediment transport. Although there was spillway on the pond, there would be water flow out of the pond for large rainfall events. The element concentration distributions in the sources were also examined for the Z4 and Z5 subwatersheds. When the two elements used in the mixing model had different distributions (element

concentration in the sediment closest to the element concentration in certain source), the mixing model tend to predict higher error. Note that the same element may contribute may contribute different amounts in the mixing model for different subwatersheds. All the element concentrations in surface samples were listed in Appendices.

Elements listed in Table 15 for each subwatershed were in the order that the DFA selected them for the mixing model. The higher on the list, the more the element(s) can separate sources correctly and had lower errors. This supported the use of the DFA in properly selecting elements.

Figure 64 Pond location in subwatershed Z5 in the Bull Creek watershed. The watershed boundary is the white line.

Table 16 Source contribution predicted by the Collins' method.

Subwatershed	Source Group 1 (%)		Source Group 2 (%)		
ID	Upland	Gully	Cultivated	Rangeland	Gully
1	100	0	100	0	0
6	100	0	0	100	0
Z3	100	0	0	0	100
Z4	100	0	0	100	0
Z5	0	100	0	100	0

The Collins' method was applied to the study area with the results given in Table 16. The Collins' method only identified one source for each subwatershed, which was expected due to the high variance of the source data. When the SV_{si} (weighting representing the within-source variability of fingerprint property *i* in source category *s*) was small, the element concentration from the source was reduced significantly, and the remaining source would dominate. Therefore, the Collins's method was not suitable for this study.

The DFA has been used to classify groups for a wide range of disciplines (Armitage, 1950, Cornfield, 1962, Bhatia, 1983, Ramos and Rickard Liow, 2013). Although DFA has been used to selected properties for the fingerprinting method, it has not been used to predict the source contribution directly (Walling et al., 1999). However, the DFA can be used to predict the source contribution and thus overcome some of the disadvantage of the mixing model. Results from DFA method are listed in Table 17 and Table 18, and Figure 65 and Figure 66, and were compared to those from the mixing model. Only highly significant elements that distinguished the sources were used in the comparison. For the subwatersheds Z3, Z4 and Z5, the DFA method used more elements than the mixing model to achieve the maximum classification accuracy. For the comparison, the corresponding mixing model was changed to use the same elements to predict the source contributions.

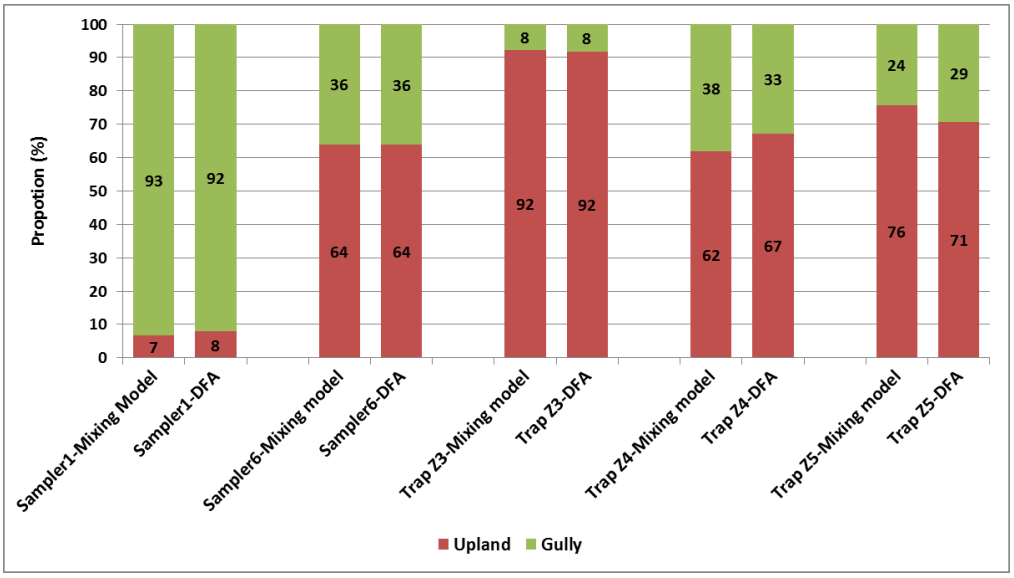

Figure 65 Comparison of results for the Mixing model and the DFA method for Source 1, upland and gullies.

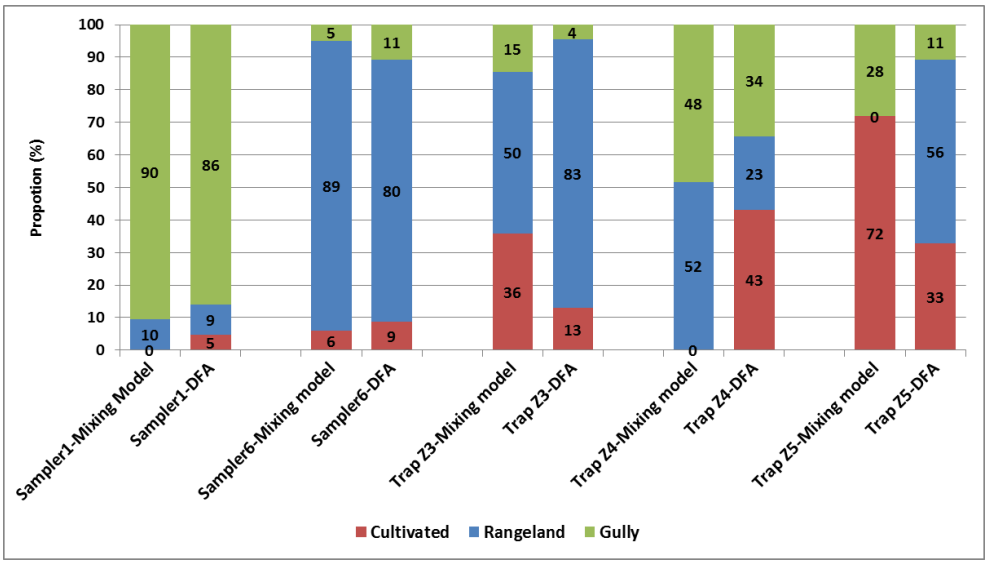

Figure 66 Comparison of results for the Mixing model and the DFA method for Source 2, cultivated land, rangeland and gullies.

Table 17 Fingerprinting method results from mixing model and the Discriminant Function Analysis method (DFA) method for Source Group 1, upland and gully.

Subwatershed ID	Element	Method	Source Contribution (%)		Root Mean Error (%)	Correct Classification (%) *
			Upland	Gully		
1	Br	Mixing Model	7	93	<0.1	100
		DFA	8	92	<0.1	
6	Zr	Mixing Model	64	36	<0.1	100
		DFA	64	36	<0.1	
Z3	Mn, Zr	Mixing Model	92	8	<0.1	95
		DFA	92	8	<0.1	
Z4	Ba	Mixing Model	62	38	3.4	87
		DFA	67	33	3.3	
Z5	Mn, S	Mixing Model	76	24	2.1	100
		DFA	71	29	3.5	

* % of original grouped cases correctly classified

Table 18 Fingerprinting method results from mixing model and the Discriminant Function Analysis method (DFA) method for Source Group 2, cultivated land, rangeland and gullies.

Subwatershed ID	Element	Method	Cultivated	Rangeland	Gully	Root Mean Error (%)	Correct Classification (%) *
			Source Contribution (%)				
1	Br	Mixing Model	0	10	90	<0.1	89
		DFA	5	9	86	0.7	
6	As	Mixing Model	6	89	5	<0.1	67
		DFA	9	80	11	<0.1	
Z3	Mg, Ca	Mixing Model	36	50	14	<0.1	79
		DFA	13	83	4	1.7	
Z4	Zr, Hf, C	Mixing Model	0	52	48	7.7	87
		DFA	43	23	34	14	
Z5	Ca, Zr	Mixing Model	72	0	28	<0.1	84
		DFA	33	56	11	<0.1	

* % of original grouped cases correctly classified

The Wilcoxon Signed Ranks Test, a nonparametric paired test, at a significance level of 0.05 was performed to compare the source contributions and the model error between the mixing model and DFA method, with the results shown in Table 19. When predicting two source contributions using the same properties, the mixing model and DFA method did not have significant difference. The DFA method did not have statistically higher model error than the fingerprinting method. When predicting three sources, although there were no significant differences among the source contributions, the DFA method had significant higher model error than the mixing model. When comparing Source 1 and Source 2, Source 2 on average had larger model error and the percentage

of original grouped cases correctly classified decreased from 96% to 81% for Sources 1 and 2, respectively. Moreover, when predicting three sources, the mixing model more likely predicted zero contribution for some source. Predicting zero contribution with three source types has also been reported by other researchers (Small et al., 2002, Carter et al., 2003). Lees (1997) found that the fingerprinting method fail percentage increased with increasing number of sources.

Table 19 Wilcoxon Signed Ranks test results comparing the Mixing model and the Discriminant Function Analysis method (DFA) method.

Paired Test	Source Group	Z-value for Wilcoxon Signed Ranks Test	p-value
Model Error	1[1]	-0.94	0.35
Model Error	2[2]	-2.02	0.04
Upland Contribution	1	-0.14	0.89
Gully Contribution	1	-0.14	0.89
Cultivated Land Contribution	2	-0.14	0.89
Rangeland Contribution	2	-0.41	0.69
Gully Contribution	2	-1.48	0.14

[1]upland and gullies
[2]cultivated land, rangeland and gullies

The mixing model, Collins' method and DFA method were also performed for the whole Bull Creek watershed, with the results given in Table 20 and Table 21. For the Source 1 the Mixing model and the DFA predicted similar results. However, for Source 2 the two methods predicted different contribution for the cultivated land and rangeland. The Mixing model predicted higher soil loss for the cultivated land and lower soil loss from rangeland compared to the DFA method. Typically, cultivated land will have higher soil erosion rates compared to rangeland. However, in this study area, the sediment from the cultivated land was transported through the rangeland before reaching the channel. The rangeland acted as a natural buffer strip, which can trap

sediment from the cultivated land (Zhang et al., 2010). Therefore, even if the cultivated land had higher erosion rates, it likely had a lower sediment delivery ratio at the watershed outlet. More information was needed to evaluate the results with three sources.

Wilson et al. (2008) used the fingerprinting method to study the source contribution for the Fort Cobb Reservoir watershed. Their results showed that the upland contribution to the deposited sediment was 52±7% and the gully contributed 48±7%. When predicting two sources, both the Mixing model and the DFA method predicted reasonable results. However, when predicting three sources, both methods predicted higher contributions from upland sources (cultivated land plus rangeland) and lower gully contribution. Source 2 had smaller model error than Source 1; nevertheless, the more sources included, the lower the correct classification rates. Small et al. (2002) reported that as the number of sources increased, possibility of spurious numerical solutions increased.

Table 20 Comparison of fingerprinting methods source contributions for the Bull Creek watershed for Source Group 1, upland and gully.

Method	Upland	Gully	Root Mean Error (%)	% of original grouped cases correctly classified
	Contribution (%)			
Collins'	100	0	3.3E+7	87
Mixing Model	50	50	3.8	
DFA*	57	43	4.1	

* Discriminant Function Analysis

Table 21 Comparison of fingerprinting methods source contributions for the Bull Creek watershed for Source Group 2, cultivated land, rangeland and gullies.

Method	Cultivated Land	Rangeland	Gully	Root Mean Error (%)	% of original grouped cases correctly classified
	Contribution (%)				
Collins'	0	100	0	1.6E+5	79
Mixing Model	43	17	40	1.0	
DFA*	21	42	37	1.4	

* Discriminant Function Analysis

To investigate the occurrence of a zero contribution and determine if it was related to the number of sources, the mixing model was used for the whole Bull Creek watershed. Sediment collected from the outlets of the subwatersheds using trap samples was considered as spatial sources for the outlet of the whole watershed (see Collins et al., 1996). Sampler 11 was the trap that collected sediment at the outlet of the whole watershed, less subwatershed 1. To avoid overlap of the subwatersheds, traps 4, 5, 6, 9, Z2, and Z5 were selected as the sources for the whole watershed, with the results given in Table 22.When the source number increased, the percentage of original grouped cases correctly classified decreased. The Collins' method still predicted sediment contribution only from one source and had largest model error. Although the mixing model predicted the lowest model error, it predicted zero contribution from three subwatersheds. The DFA did not predict any source contribution as zero. This indicated that the DFA method might avoid the potential spurious numerical solutions of the mixing model.

Table 22 Fingerprinting method source contributions by subwatershed for the Bull Creek watershed.

Method	Subwatershed						Root Mean Error (%)	% of original grouped cases correctly classified
	4	5	6	9	Z2	Z3		
	Contribution (%)							
Collins'	0	0	100	0	0	0	3000	70
Mixing Model	0	47	0	0	2	51	0.5	
DFA*	23	17	14	19	13	14	7.7	

* Discriminant Function Analysis

4.2.2 Fingerprinting method evaluation

4.2.2.1 Element concentrations greater than source concentrations

Elements that passed the Kruskal-Wallis H-test but had sediment concentrations that outside the range of their sources are listed in Table 23. Koiter et al. (2013) reviewed the chemical transformations during the water erosion processes, and found that the elements can enrich in the sediment (e.g., selective erosion and atmospheric deposition) or be lost during the transportation (e.g., leaching, dissolved elements infiltrated and absorbed to soil, biological inputs). Among the elements given in Table 23, H, Sr, Zr and Hf were both enriched and reduced in the sediment. Sampling and measurement errors were the likely causes of element concentrations greater than the surface source. Only ten samples had two replicates with differences between replicates ranging from 8 - 30%. However, only 1.0 g was used for the ICP-MS analysis, which introduces uncertainty associated with the representativeness of the soil samples. Another possible reason for excessive concentrations was the mean concentrations were used. Some elements were in the range of the observed minimum and maximum concentrations. However, the model can only use the mean concentrations.

Table 23 Element sediment concentrations greater than and less than surface samples (source) for the fingerprinting method.

Sediment Concentration	
Greater than Surface Samples	Less than Surface Samples
Na, H, Li, Mn, Co, Cu, As, Sr, Ba, Ge, Zr, Hf, C	Br, N, Cs-137, Si, Ti, H, Ge, B, Mg, Sr, Nb, Hf, Mo, Zr

4.2.2.2 Number of sources and chemical properties

The mixing model fail chance increased with the increasing number of sources. Martinez-Carreras et al. (2008) also found that the number of elements used in the mixing model could affect the uncertainty of the source contribution prediction. They reported that with an increase of the number of properties, the uncertainty range of the source concentrations decreased, the uncertainty was independent of the property type.

4.2.2.3 Particle size correction factor

Elements were found to have a strong relationship with the particle size and organic matter due to the SSA (Walling et al., 2000). The particle size correction factor, Z, was the same as the one used in the Cs-137 method. However, research showed that particle size correction factors varied for different elements and that relationships between the SSAs were not uniform (Russell et al., 2000). The selective deposition process had varying effects on different elements. The effect was greater (Na) than others (Mn, Fe, Zn, etc.). Moreover, sediment was transported in the form of both aggregates and primary particles, and detachment, transport and deposition change along the flow path (Schiettecatte et al., 2008). As the transport capacity increases, the selective deposition process becomes less significant. Motha et al. (2002) corrected the particle size and organic matter by comparing the field collected source runoff and the suspended sediment, and then compared the chemical concentrations in the original sediment and the concentrations calculated

using the particle size correction. Their results showed significant differences for geochemical and magnetic properties, but no significant differences for isotopes (Cs-137 and Pb-210). Therefore, due to the lack of clear relationships between the element properties and particle size, the existing particle size correction factor was not utilized.

For this study, the element concentration change with the clay content is given in Figure 67. All the elements used in the mixing model were included in Figure 67. There were no clear relationships between the element concentrations and clay content. Similar results were found by Stone and Walling (1997). The possibility for this phenomenon would be that the different absorption of the element on fine particles and the different parent materials for sampling soils.

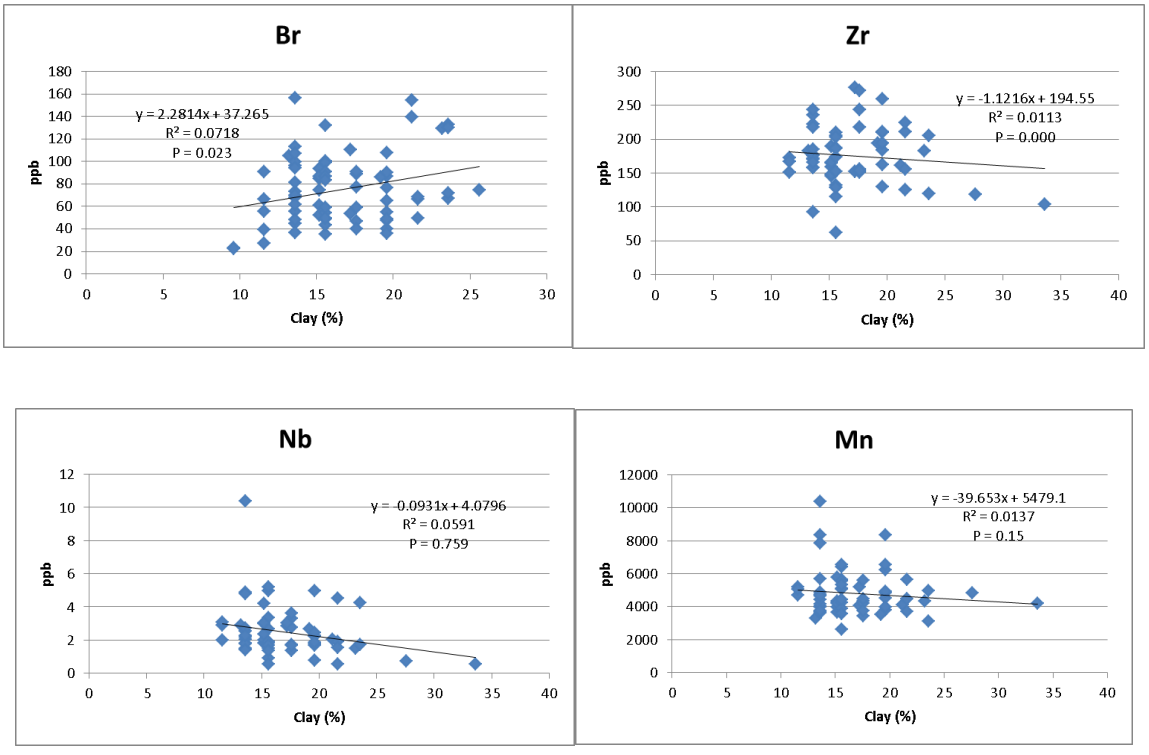

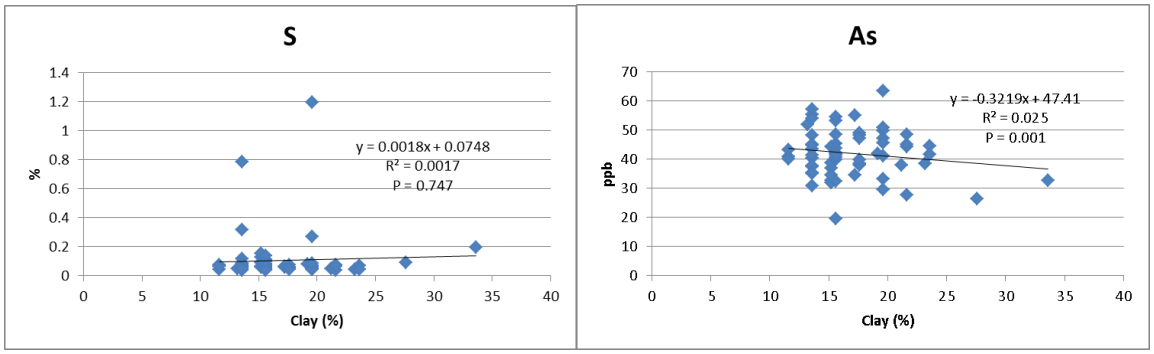

(e) (f)

Figure 67 Relationship between element concentration and percent clay.

Phillips et al. (2000) reported that when using the sediment trap for the fingerprinting method, a representative sediment sample could be collected when the grain size was smaller than 63 µm. Application of the sediment trap assumed that the selective deposition processes had limited influence when the grain size was less than 63µm (Walling et al. 2000). Some researcher limited the grain size to 10µm (Wilkinson et al., 2009).

4.3 WEPP soil loss predictions and source comparison

4.3.1 Cs-137 and WEPP hillslope soil loss prediction comparison

Different WEPP hillslope models were developed for each of the eight of the 11 transects. Transects 1 and 9 had missing Cs-137 samples and transect 10 likely had sampling errors and thus were not included in the WEPP simulations. Soil loss predictions from WEPP and the Cs-137 method are given in Figure 68. Note that the Cs-137 predictions included the particle size correction factor (Z). For transect 11, the Cs-137 results were from the Mass Balance Model III with Z. The negative value in the Figure 68 means an erosion rate and a positive value means a deposition rate. The WEPP hillslope model for the rangeland had all the same inputs parameters except the hillslope steepness, slope length and the soil type for the top parts of the transect 5 and

6. The top parts of the transect 5 and 6 had the Quinlan-rock outcrop complex soil while the other parts had the same Quinlan-Woodward complex soil as the other transects. The positions where the plant coverage changed for each transect. Samples for the Cs-137 method were taken at the points where coverage changed or slope steepness changed.

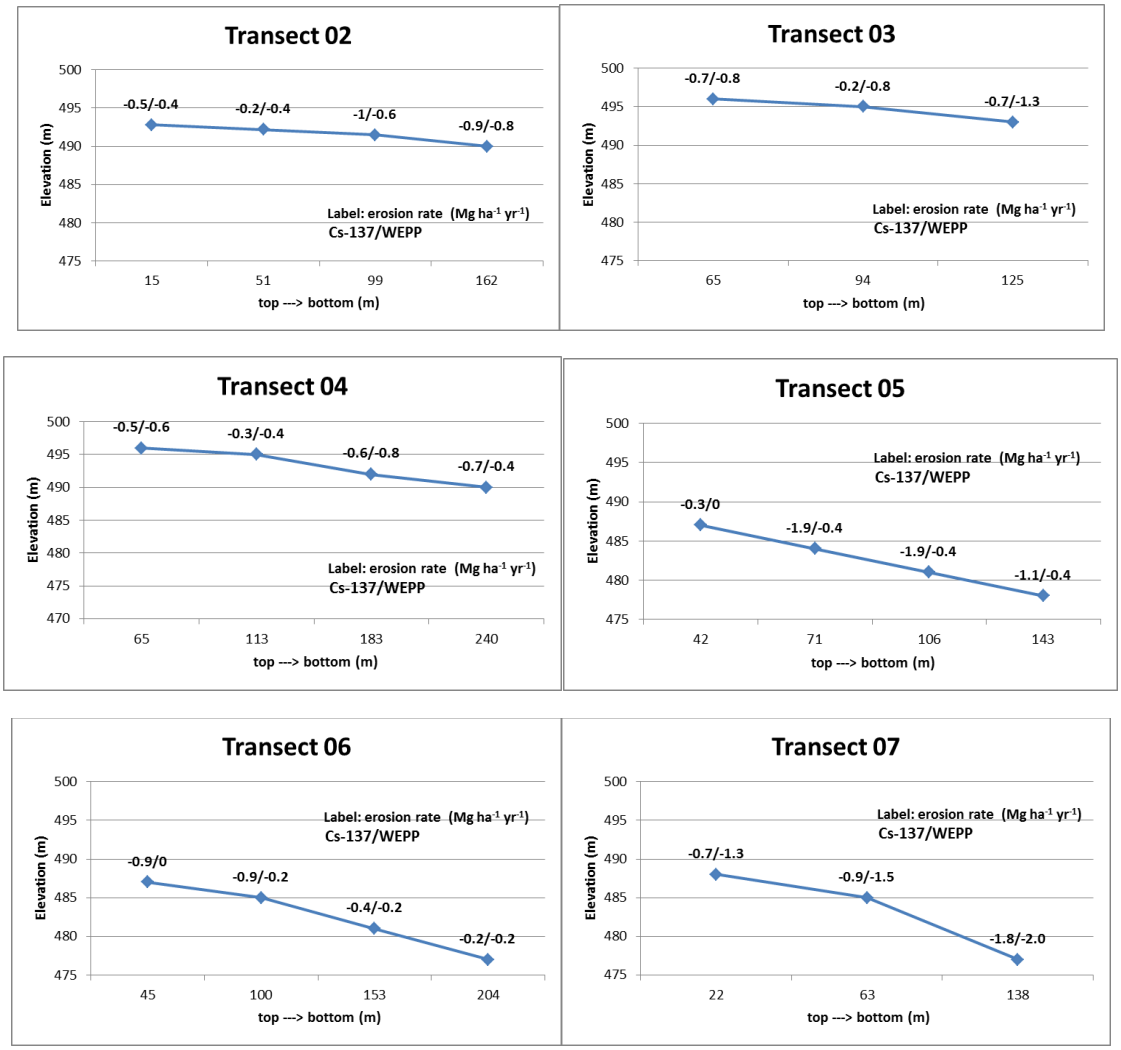

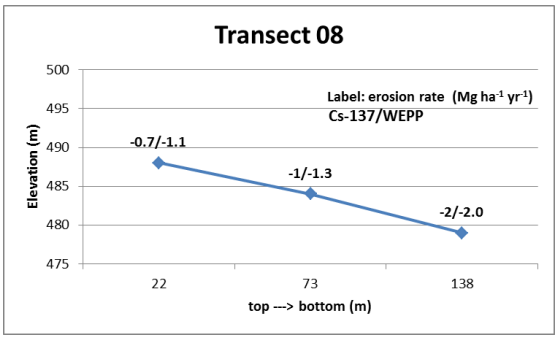

Figure 68 Rangeland soil loss predicted using the Cs-137 method with the particle correction factor, Z, and WEPP.

The soil loss predicted by WEPP increased from the slope top to the bottom. The second sampling point (top-middle of the transect) had almost the same soil loss as the first sampling point (top of the transect) reflected the influence of the plant coverage change. The soil erosion rates were highly related to the slope steepness. Figure 69 shows the relationship between soil erosion and slope steepness, and shows that the soil erosion rates increased with the increasing slope steepness. However, transect 5 and 6 were two exceptions; they had the highest average slope steepness with the lowest average soil erosion rates. This was because the tops of transect 5 and 6 had a large amount of rocks which resulted in very low erosion (Ellison, 1948).

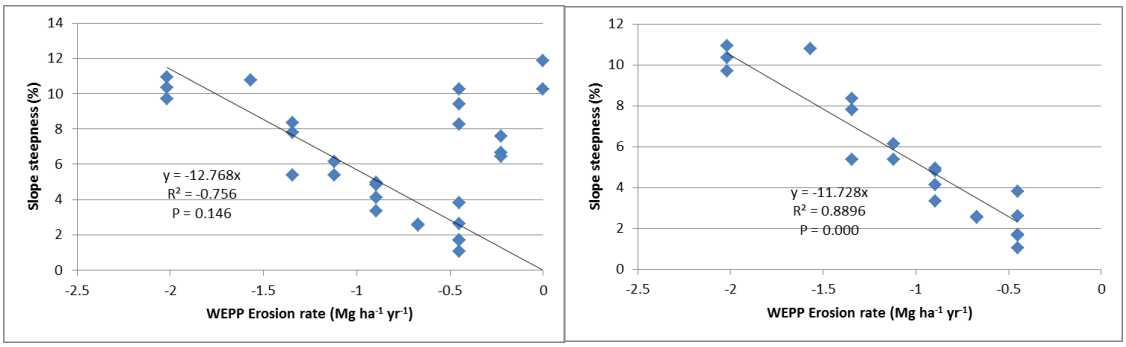

(a) (b)

Figure 69 Relationship between WEPP predicted soil erosion rates and slope steepness for rangeland: (a) samples from all the rangeland transects (b) all the rangeland transects except transect 5 and 6.

For the cultivated land, the effects of the terrace were incorporated into the WEPP model by adjusting the slope length and steepness. Comparison between cultivated land soil erosion predicted by WEPP and the Cs-137 method are given in Figure 70 and Table 24. The WEPP predicted significantly low soil erosion rates compared to the Cs-137 method. However, at the downslope terrace bank, WEPP predicted higher soil erosion rates compared to the Cs-137 method, which was due to the high steep slope steepness of the downslope terrace bank. The soil erosion rates changed from the top to the bottom on the cultivated transect and had the same trend for both the Cs-137 method and WEPP (Figure 71). Due to the lack of detailed field measured steepness data, the three terraces were set to the same steepness and length in the WEPP hillslope model. Terrance maintenance and cattle grazing data were not available and thus not included in the WEP model.

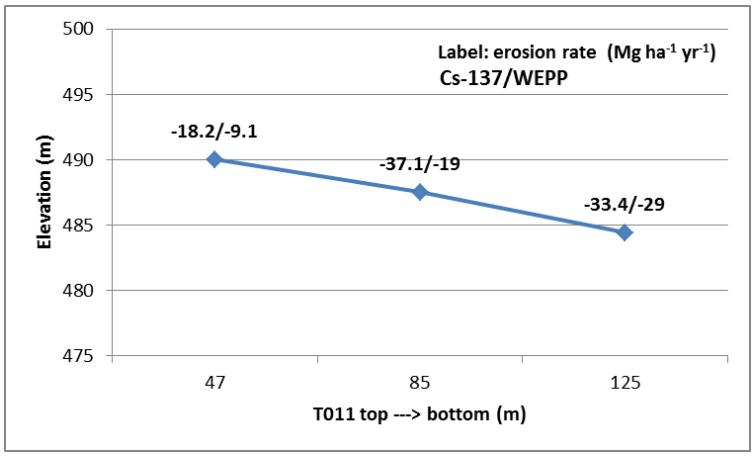

Figure 70 Comparison between soil loss predicted from the Cs-137 method and WEPP for cultivated land in the Bull Creek watershed.

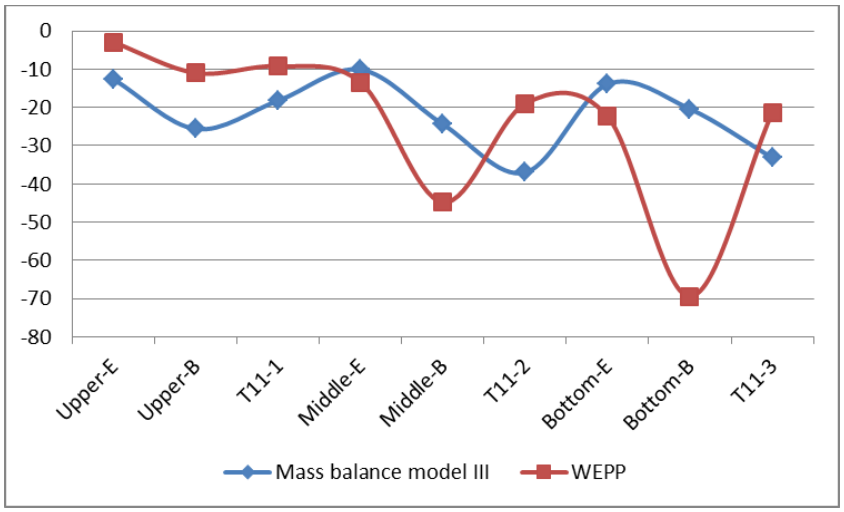

Figure 71 Comparison between soil erosion rates change between the Cs-137 method and WEPP from the top to the bottom of the hillslope for the cultivated transect for.

Table 24 Predicted soil loss comparison between the Cs-137 method and WEPP for terraces.

Sample Number	Cs-137 (Bq/m^2)	Soil Loss ($Mg\ ha^{-1}\ yr^{-1}$)				
		Proportional Model	Mass Balance Model I	Mass Balance Model II	Mass Balance Model III	WEPP
Upper-E*	1190	-14	-21	-8	-13	-3
Upper-B**	439	-30	-66	-25	-26	-11
Upper Middle	968	-19	-30	-11	-18	-9
Middle-E	1040	-17	-27	-10	-10	-13
Middle-B	465	-29	-63	-24	-24	-45
Middle	234	-34	-94	-37	-37	-19
Bottom-E	825	-22	-37	-14	-14	-22
Bottom-B	577	-27	-54	-20	-20	-69
Bottom Middle	281	-33	-86	-33	-33	-21

*Upper-E, middle-E and bottom-E are the samples from the end of the terrace (red dot from Figure 48 from left to right); ** Upper-B, middle-B and bottom-B are the samples from the downslope terrace bank (blue dot from Figure 48 from left to right).

Figure 72 shows the relationship between the WEPP model and the Cs-137 method. From the figure, it may difficult to see a clear relationship. However, the results from these two methods were significantly correlated at the 0.01 level (based on Bivariate correlation test), and there was no significant difference between the medians (Nonparametric paired sample Wilcoxon test). WEPP predicted significantly lower soil erosion rates compared to the Cs-137 method (paired t-test, 0.05 level). The Nash–Sutcliffe model efficiency (NSE) coefficient was used to compare the WEPP model predictions with the Cs-137 method. Using the Cs-137 method results as the observed data (independent variable), the NSE efficiencies were high for the rangeland (0.95), cultivated land (0.78), and the combined data (0.78).

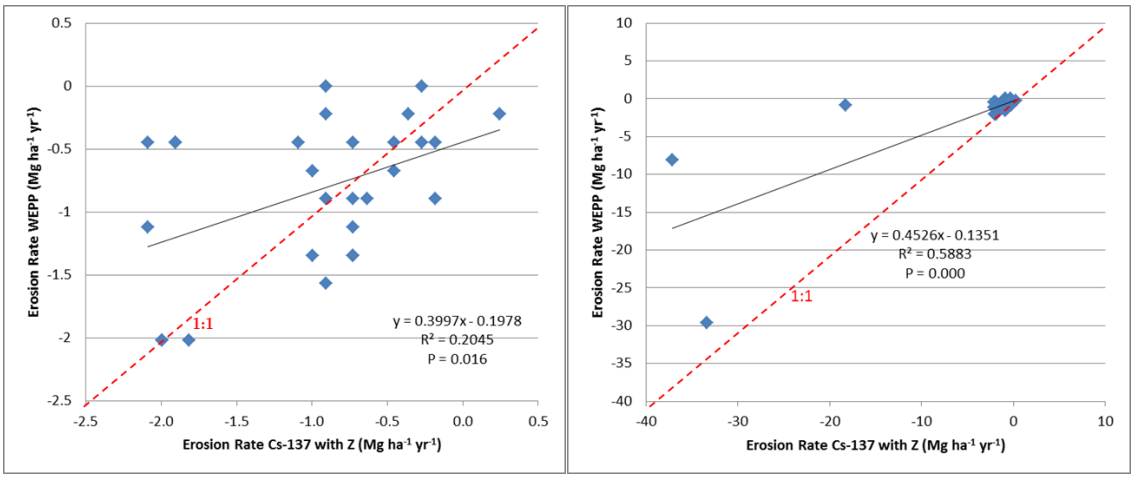

(a) (b)

Figure 72 Comparison between WEPP and Cs-137 method predictions: (a) rangeland, (b) upland (rangeland and cultivated land).

4.3.2 Source contribution comparison between fingerprinting method and WEPP watershed model

Sediment yield predicted by the WEPP watershed model for each subwatershed are given in Table 25 and Table 26. The sediment contributions were calculated based on the sediment yield from each landuse in the watershed. The results were compared to the fingerprinting method in Figure 73 and Figure 74. The WEPP watershed model predicted a lower sediment yield from the rangeland compared to which from the fingerprinting method. For the subwatershed 6 and Z4, the cultivated land had higher sediment yield than the channel and for the other subwatersheds; the cultivated land had lower sediment yield than the channel. For subwatershed Z5 and 11, the upland contributed less than the channel, and for the other subwatershed, the upland contributed more than the channel. All the rangeland contributed lest than 10% of the total sediment. The cultivated land had a higher percentage in the total sediment for the subwatersheds 6 and Z4, and less for the rest subwatersheds.

Table 25 Source contributions predicted by the WEPP watershed model for the Bull Creek watershed.

Subwatershed ID	Contribution (%)			
	Upland			Channel
	Cultivated land	Rangeland	Total	
1	41	9.6	51	49
6	65	7.9	73	27
Z3	45	8.4	53	47
Z4	63	2.0	65	35
Z5	33	3.4	36	64
11	18	2.6	20	80

Table 26 Sediment yield predicted by the WEPP watershed model for the Bull Creek watershed.

Subwatershed ID	Sediment Yield (t/ha/yr)				Area (ha)	Delivery Ratio
	Upland			Channel		
	Cultivated Land	Rangeland	Total			
1	1.7	0.4	2.1	2.0	34	0.40
6	2.9	0.4	3.2	1.2	108	0.43
Z3	2.5	0.5	2.9	2.6	480	0.39
Z4	5.7	0.2	5.9	3.2	130	0.50
Z5	2.8	0.3	3.1	5.4	300	0.52
11	3.0	0.4	3.5	13.7	1080	0.14

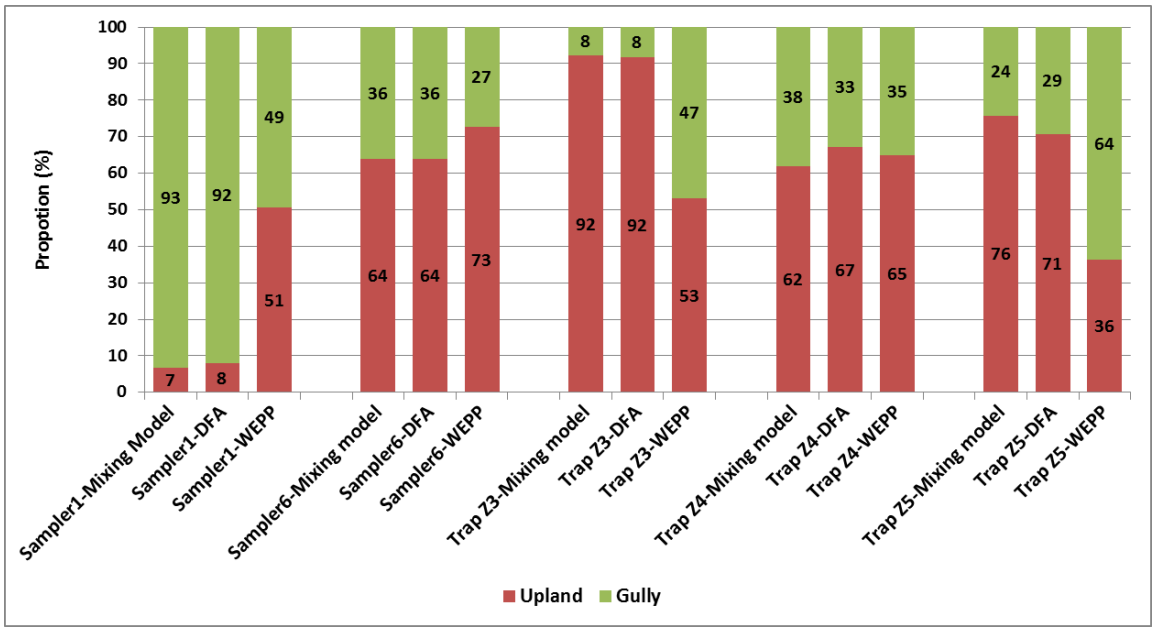

Figure 73 Comparing the source contribution predicted by fingerprinting method and WEPP watershed model (upland and gully).

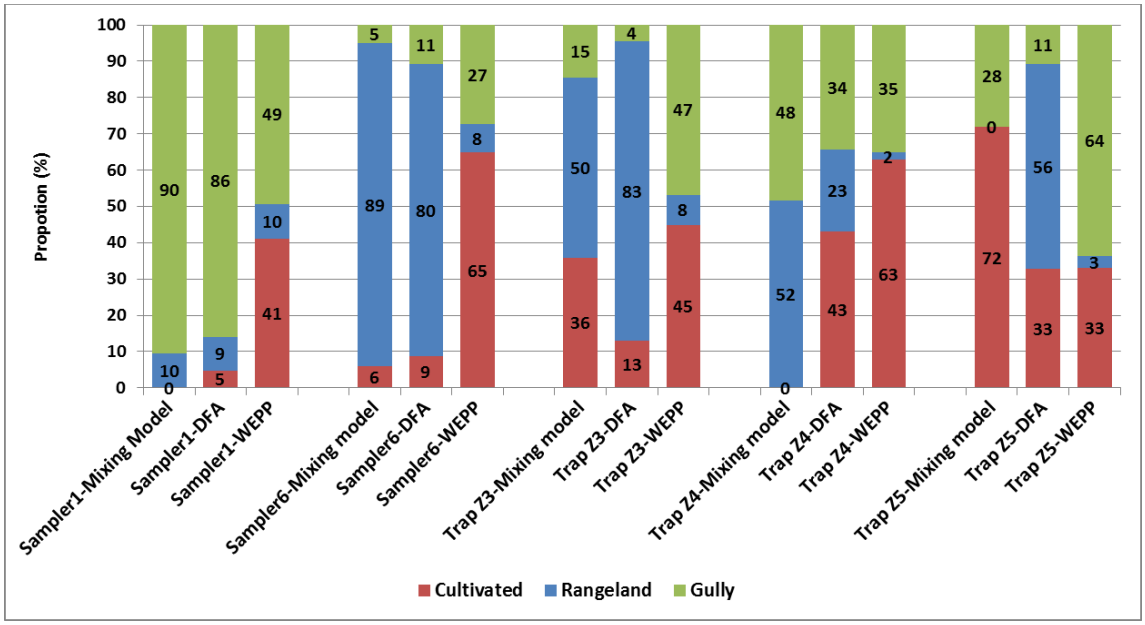

Figure 74 Comparing the source contribution predicted by fingerprinting method and WEPP watershed model (cultivated land, rangeland and gully).

When comparing to the results from the fingerprinting method, WEPP predicted less erosion from the gullies in subwatershed 1. Although WEPP can simulate the channel erosion, it did not include the classical gully erosion. Gullies developing in this area would limit the predictions from WEPP. For the subwatersheds 6 and Z4, which had similar landforms, all three models had similar results when there were two source types (up land and gully). WEPP predicted higher sediment yield from the cultivated land, while the fingerprinting method predicted more sediment contribution from the rangeland. WEPP predicted higher sediment yield from channel and lower sediment yield from the upland for subwatersheds Z3 and Z5. In these two subwatersheds, there were small ponds and some channels were connected using pipes, these were not considered in the WEPP watershed model. The overall mean and median contributions from these three sources predicted by fingerprinting method and WEPP were not significantly different at the 95% confidence level, except for the cultivated land contributions predicted by DFA and WEPP.

CHAPTER V

SUMMARY AND CONCLUSIONS

The Cs-137 and fingerprinting methods have become popular techniques to predict soil loss in recently years. These two methods were used to predict hillslope soil loss and source contribution in the Bull Creek watershed. Results were compared to the process-based soil erosion model WEPP. The advantages and limitations of the Cs-137 and fingerprinting methods were discussed.

The Cs-137 method predicted reasonable long-time average soil erosion and deposition rates with less information and a one-time soil sampling compared to the WEPP hillslope model. The Cs-137 method also predicted the spatial erosion/deposition distribution along a hillslope that integrated soil erosion factors like soil properties, landcover, land management, and other over time. However, analyzing the effect of a single soil erosion factor using the Cs-137 method was difficult. Sampling methods for the Cs-137 method are critical. Precise reference site measurements were crucial to predict soil loss and sediment deposition accurately. The reference site Cs-137 inventory had a large variance due in part to the random micro-scale effects. Field samples had similar problems, and thus replicate samples were recommended. High measuring errors were also recognized for the Gama spectrometer for low signal samples, and the instrument operator adds uncertainty in the measurements.

For the Cs-137 method, the conversion model was recommended based on the vertical distribution of the Cs-137 and current and historical land management. The Diffusion and

Migration model was used for rangeland and all of the conversion models, except the Mass Balance Model I, appropriately predicted erosion for the cultivated land. The use of the particle size correction factor, Z, with the conversion models requires additional research. For example, using both particle size and organic matter correction factors over corrects. In addition, for this study Cs-137 levels did not have a clear relationship with clay particles as reported in the literature. Future improvements in the Cs-137 method to estimate soil and erosion and deposition in areas similar to Bull Creek watershed include: 1) improving the sampling method to account for micro-scale factors that affect the Cs-137 distribution, 2) develop a more accurate method to reflect the influence of the selective deposition processes, and 3) additional research to characterize the soil erosion and deposition process for the terrace system.

The fingerprinting method provided useful information on watershed-scale source contributions. This method predicted source contributions more accurately for two sources; as the number of sources increased, the accuracy decreased. Three methods were used to identify sediment sources: the mixing model, the Collins' improved model, and the Discriminant Function Analysis (DFA). Due to the large sample variance, the Collins' improved model was not used for this study. Results from DFA method had slightly larger model errors compared to the mixing model, but predictions were not significantly different. The DFA method was recommended since the mixing model predicted zero contribution for some sources when the source number was greater than two. Additional research is needed to evaluate the DFA method for identifying source contributions since it has the potential to provide results that are more reasonable and avoid the spurious numerical solutions of the mixing model.

An obstacle encountered for the fingerprinting method was accurately accounting for the fine particle enrichment during the sediment transport process. Element selection should be based on the statistical methods and the properties of elements to adsorb to fine particles. For this study area, the elements used in the fingerprinting method did not have clear relationships with the fine

particles, which added uncertainty in the predictions. Each element may have a unique particle size correction factor, and thus using a single particle correction factor contributed to uncertainty. Therefore, the particle size correction factor was not used in the fingerprinting method. Effects of the selective deposition process were minimized by sieving all samples using a 63 μm mesh prior to testing.

When there were two source types, the fingerprinting method and WEPP watershed model predicted similar source contributions. However, with three source types their predictions diverged. In addition, WEPP predicted significantly less sediment yield from the rangeland compared to the fingerprinting method, and thus the fingerprinting method predicted rangeland contributed a large proportion of the total sediment yield. It is important to clarify the difference between soil erosion predictions and inferences drawn from the fingerprinting method, which only estimates the relative source contributions. Combining erosion models with the fingerprinting method provides a more detailed evaluation of erosion predictions, which may result in improved land management recommendations and decisions.

RECOMMENDATIONS FOR FUTURE RESEARCH

Recommended future research includes improving the accuracy of the reference site information for the Cs-137 method by increasing the sample number and collecting samples using the large soil ring by depth along with increasing the number of reference locations. Next, developing an improved particle size correction factor is critical. Additional studies may include developing relationships between the soil properties (isotopes and elements) and particle size, accounting for changes in element enrichment and loss during the transport process, and evaluating both the organic and particle size correction factors. Laboratory or plot scale erosion studies should be conducted using special tracers to study particle size and element changes during transport.

Finally, improvements in the DFA method should be evaluated using an indoor rainfall simulator to develop a series of controlled experiments to investigate mixtures of different source materials.

REFERENCES

Agudo, E. G. 1998. Global distribution of ^{137}Cs inputs for soil erosion and sedimentation studies. Pages 117-121 Use of ^{137}Cs in the study of soil erosion and sedimentation: proceedings of a consltants meeting. FAO/IAEA Division of Nuclear Techniques in Food and Agriculture, Vienna.

Alldredge, A. W. and F. W. Whicker. 1972. A method for measuring soil erosion and deposition with Beta Particle Attenuation. Journal of Range Management **25**:393-398.

Anderson, E. C. 1958. Radioactivity of people and milk: 1957. Science **128**:882-886.

Armitage, P. 1950. Sequential analysis with more than two alternative hypotheses, and its relation to discriminant function analysis. Journal of the Royal Statistical Society. Series B (Methodological) **12**:137-144.

Bacchi, O. O. S., K. Reichardt, and G. Sparovek. 2003. Sediment spatial distribution evaluated by three methods and its relation to some soil properties. Soil and Tillage Research **69**:117-125.

Basher, L. R. 2000. Surface erosion assessment using ^{137}Cs: examples from New Zealand. Acta geológica hispánica **35**:219-228.

Beasley, D. B., L. F. Huggins, and E. J. Monke. 1980. ANSWERS: A model for watershed planning. Transactions of the Asae **23**:938-944.

Beck, H. L. 1966. Environmental gamma radiation from deposited fission products, 1960-1964. Health Physics **12**:313-322.

Belyaev, V. R., P. J. Wallbrink, V. N. Golosov, A. S. Murray, and A. Y. Sidorchuk. 2005. A comparison of methods for evaluating soil redistribution in the severely eroded Stavropol region, southern European Russia. Geomorphology **65**:173-193.

Bhatia, M. R. 1983. Plate tectonics and geochemical composition of sandstones. The Journal of Geology:611-627.

Bhuyan, S. J., P. K. Kalita, K. A. Janssen, and P. L. Barnes. 2002. Soil loss predictions with three erosion simulation models. Environmental Modelling & Software **17**:135-144.

Bondár, I., X. Yang, R. G. North, and C. Romney. 2001. Location calibration data for CTBT monitoring at the Prototype International Data Center. pure and applied geophysics **158**:19-34.

Brown, R. B., N. H. Cutshall, and G. F. Kling. 1981a. Agricultural erosion indicated by ^{137}Cs redistribution: I. levels and distribution of ^{137}Cs activity in soils. Soil Science Society of America Journal **45**:1184-1190.

Brown, R. B., G. F. Kling, and N. H. Cutshall. 1981b. Agricultural erosion indicated by ^{137}Cs redistribution: II. estimates of erosion rates. Soil Science Society of America Journal **45**:1191-1197.

Bunzl, K., W. Schimmack, K. Kreutzer, and R. Schierl. 1989. Interception and retention of chernobyl-derived ^{134}Cs, ^{137}Cs and ^{106}Ru in a spruce stand. Science of the Total Environment **78**:77-87.

Busacca, A., C. Cook, and D. Mulla. 1993. Comparing landscape-scale estimation of soil erosion in the Palouse using Cs-137 and RUSLE. Journal of Soil and Water Conservation **48**:361-367.

Cambray, R. S., K. Playford, G. Lewis, and R. Carpenter. 1989. Radioactive fallout in air and rain: results to the end of 1988. Environmental and Medical Sciences Division, United Kingdom Atomic Energy Authority.

Cambray, R. S., K. Playford, and G. N. J. Lewis. 1985. Radioactive fallout in air and rain: results to the end of 1984. U.K. Atomic Energy Authority Report, Harwell, UK.

Campbell, B. L. 1983. Application of environmental Caesium-137 for the determination of sedimentation rates in reservoirs and lakes and related catchment studies in developing countries. Radioisotopes in Sediment Studies, Technology Document **298**:7-30.

Campbell, B. L., R. J. Loughran, and G. L. Elliott. 1982. Caesium-137 as an indicator of geomorphic processes in a drainage basin system. Australian Geographical Studies **20**:49-64.

Carter, J., P. N. Owens, D. E. Walling, and G. J. L. Leeks. 2003. Fingerprinting suspended sediment sources in a large urban river system. Science of the Total Environment **314–316**:513-534.

Cochrane, T. A. and D. C. Flanagan. 1999. Assessing water erosion in small watersheds using WEPP with GIS and digital elevation models. Journal of Soil and Water Conservation **54**:678-685.

Collins, D. E. Walling, and G. J. L. Leeks. 1996. Composite fingerprinting of the spatial source of fluvial suspended sediment: a case study of the Exe and Severn River basins, United Kingdom. Géomorphologie: relief, processus, environnement **2**:41-53.

Collins, A. L. and D. E. Walling. 2002. Selecting fingerprint properties for discriminating potential suspended sediment sources in river basins. Journal of Hydrology **261**:218-244.

Collins, A. L. and D. E. Walling. 2004. Documenting catchment suspended sediment sources: problems, approaches and prospects. Progress in Physical Geography **28**:159-196.

Collins, A. L., D. E. Walling, and G. J. L. Leeks. 1997a. Source type ascription for fluvial suspended sediment based on a quantitative composite fingerprinting technique. Catena **29**:1-27.

Collins, A. L., D. E. Walling, and G. J. L. Leeks. 1997b. Use of the geochemical record preserved in floodplain deposits to reconstruct recent changes in river basin sediment sources. Geomorphology **19**:151-167.

Collins, A. L., D. E. Walling, L. Webb, and P. King. 2010. Apportioning catchment scale sediment sources using a modified composite fingerprinting technique incorporating property weightings and prior information. Geoderma **155**:249-261.

Cornfield, J. 1962. Joint dependence of risk of coronary heart disease on serum cholesterol and systolic blood pressure: a discriminant function analysis. Page 58 *in* Federation Proceedings.

Davis, J. J. 1963. Cesium and its relationship to potassium in ecology. Reinhold, New York.

Davis, J. J. and R. F. Foster. 1958. Bioaccumulation of radioisotopes through aquatic food chains. Ecology **39**:530-535.

de Jong, S. M., M. L. Paracchini, F. Bertolo, S. Folving, J. Megier, and A. P. J. de Roo. 1999. Regional assessment of soil erosion using the distributed model SEMMED and remotely sensed data. Catena **37**:291-308.

de Miguel, E., S. Charlesworth, A. Ordóñez, and E. Seijas. 2005. Geochemical fingerprints and controls in the sediments of an urban river: River Manzanares, Madrid (Spain). Science of the Total Environment **340**:137-148.

Dearing, J. A., K. Alström, A. Bergman, J. Regnell, and P. Sandgreen. 1990. Recent and long-term records of soil erosion from southern Sweden. Pages 173-191 *in* J. Boardman, I. D. L. Foster, and J. A. Dearing, editors. Soil erosion on agricultural land. British Geomorphological Research Group, Coventry, UK.

Dietz, L. A. and C. F. Pachucki. 1973. ^{137}Cs and ^{134}Cs half-lives determined by mass spectrometry. Journal of Inorganic and Nuclear Chemistry **35**:1769-1776.

Eberl, D. D. 1980. Alkali cation selectivity and fixation by clay minerals. Clays Clay Miner. **28**:161.

Elliott, G. L., B. L. Campbell, and R. J. Loughran. 1990. Correlation of erosion measurements and soil Caesium-137 content. International Journal of Radiation Applications and Instrumentation. Part A. Applied Radiation and Isotopes **41**:713-717.

Evans, E. J. and A. J. Dekker. 1966a. Fixation and release of Cs-137 in soils and soil separates. Canadian Journal of Soil Science **46**:217-222.

Evans, E. J. and A. J. Dekker. 1966b. Plant uptake of Cs-137 from nine Canadian soils. Canadian Journal of Soil Science **46**:167-176.

Flanagan, D. C., J. R. Frankenberger, and B. A. Engel. 2004. Web-based GIS application of the WEPP model. ASAE Paper.

Flanagan, D. C. and J. M. Laflen. 1997. The USDA water erosion prediction project (WEPP). Eurasian soil science **30**:524-530.

Foster, G. R. and L. J. Lane. 1987. User requirements: USDA-Water Erosion Prediction Project (WEPP). National Soil Erosion Research Laboratory, USDA, Agricultural Research Service, W. Lafayette, Ind. (USA).

Foster, G. R. and M. A. Nearing. 1995. Hill slope erosion component,ch11. USDA.

Fredriksson, L., B. Eriksson, and et al. 1959. Studies of soil-plant-animal interrelationships with respect to fission products, peaceful uses of atomic energy. Pages 449-470 Proceedings 2nd international conference, United Nations, Geneva, Switzerland.

Frissel, M. J. and R. Pennders. 1983. Models for the accumulation and migration of ^{90}Sr, ^{137}Cs, $^{239+240}Pu$ and ^{241}Am in the upper layer of soils. Pages 63-72 *in* P.J. Coughtrey, J.N.B. Bell, and T. M. Roberts, editors. Ecological aspects of radionuclide release, Blackwell, Oxford.

Froehlich, W. and D. E. Walling. 2005. Using environmental radionuclides to elucidate sediment sources within a small drainage basin in the Polish Flysch Carpathians. Sediment Budgets **1**:102-112.

Fuhrmann, M., M. Lasat, S. Ebbs, J. Cornish, and L. Kochian. 2003. Uptake and release of cesium-137 by five plant species as influenced by soil amendments in field experiments. Journal of Environmental Quality **32**:2272-2279.

Gaspar, L., A. Navas, D. E. Walling, J. Machín, and J. Gómez Arozamena. 2013. Using ^{137}Cs and ^{210}Pbex to assess soil redistribution on slopes at different temporal scales. Catena **102**:46-54.

Hanson, W. C. 1980. Worldwide fallout. DOE/TIC-22800 edition. Department of Energy, Washington, DC.

He, Q. and D. Walling. 2003. Testing distributed soil erosion and sediment delivery models using ^{137}Cs measurements. Hydrological Processes **17**:901-916.

He, Q. and D. E. Walling. 1996. Interpreting particle size effects in the adsorption of ^{137}Cs and unsupported ^{210}Pb by mineral soils and sediments. Journal of Environmental Radioactivity **30**:117-137.

He, Q. and D. E. Walling. 1997. The distribution of fallout ^{137}Cs and ^{210}Pb in undisturbed and cultivated soils. Applied Radiation and Isotopes **48**:677-690.

Hrachowitz, M., F. Maringer, C. Steineder, and M. H. Gerzabek. 2005. Soil redistribution model for undisturbed and cultivated sites based on chernobyl-derived Cesium-137 fallout. Journal of Environmental Quality **34**:1302-1310.

Hudson, N. 1995. Soil conservation. Iowa State University Press, Ames.

Huh, C. A. and C. C. Su. 2004. Distribution of fallout radionuclides (^{7}Be, ^{137}Cs, ^{210}Pb and ^{239,240}Pu) in soils of Taiwan. Journal of Environmental Radioactivity **77**:87-100.

Jetten, V., A. de Roo, and D. Favis-Mortlock. 1999. Evaluation of field-scale and catchment-scale soil erosion models. Catena **37**:521-541.

Jetten, V., G. Govers, and R. Hessel. 2003. Erosion models: quality of spatial predictions. Hydrological Processes **17**:887-900.

Jong, E. D., J. R. Bettany, and H. Villar. 1982. Preliminary investigations on the use of ^{137}Cs to estimate erosion in Saskatchewan. Canadian Journal of Soil Science **62**:673-683.

Juracek, K. and A. Ziegler. 2009. Estimation of sediment sources using selected chemical tracers in the Perry lake basin, Kansas, USA. International Journal of Sediment Research **24**:108-125.

Kachanoski, R. G. 1987. Comparison of measured soil 137-Cesium losses and erosion rates. Canadian Journal of Soil Science **67**:199-203.

Kachanoski, R. G. and E. de Jong. 1984. Predicting the temporal relationship between soil Cesium-137 and erosion rate. Journal of Environmental Quality **13**:301-304.

Kannan, V., M. P. Rajan, M. A. R. Iyengar, and R. Ramesh. 2002. Distribution of natural and anthropogenic radionuclides in soil and beach sand samples of Kalpakkam (India) using hyper pure germanium (HPGe) gamma ray spectrometry. Applied Radiation and Isotopes **57**:109-119.

Kim, J. M. and G. D. Stucky. 2000. Synthesis of highly ordered mesoporous silica materials using sodium silicate and amphiphilic block copolymers. Chemical Communications:1159-1160.

Kirkby, M. J., R. Abrahart, M. D. McMahon, J. Shao, and J. B. Thornes. 1998. MEDALUS soil erosion models for global change. Geomorphology **24**:35-49.

Knisel, W. G. 1980. CREAMS: A field-scale model for chemicals, runoff and erosion from agricultural management systems.

Koiter, A. J., P. N. Owens, E. L. Petticrew, and D. A. Lobb. 2013. The behavioural characteristics of sediment properties and their implications for sediment fingerprinting as an approach for identifying sediment sources in river basins. Earth-Science Reviews **125**:24-42.

Laflen, J. M., D. C. Flanagan, and B. A. Engel. 2004. Soil erosion and sediment yield prediction accuracy using WEPP. JAWRA Journal of the American Water Resources Association **40**:289-297.

Laflen, J. M., L. J. Lane, and G. R. Foster. 1991. WEPP: A new generation of erosion prediction technology. Journal of Soil and Water Conservation **46**:34-38.

Lees, J. A. 1997. Mineral magnetic properties of mixtures of environmental and synthetic materials: linear additivity and interaction effects. Geophysical Journal International **131**:335-346.

Li, S., D. A. Lobb, M. J. Lindstrom, and A. Farenhorst. 2007. Tillage and water erosion on different landscapes in the northern North American Great Plains evaluated using 137Cs technique and soil erosion models. Catena **70**:493-505.

Li, S., D. A. Lobb, and M. J. Linstrom. 2006. Measuring and modeling tillage erosion in cereal-based production in the Canadian Prairies. Advances in in GeoEcology **28**:281-289.

Livens, F. R. and D. L. Rimmer. 1988. Physico-chemical controls on artificial radionuclides in soil. Soil Use and Management **4**:63-69.

Long, Y., X. Zhang, A. Wen, and X. He. 2012. ^{137}Cs fingerprinting technique for erosion and sedimentation studies. Journal of Mountain Science **9**:34-40.

Longmore, M. E. 1982. The Caesium-137 dating technique and associated applications in Australia - a review.*in* W. Ambrose and P. Duerden, editors. Archaeometry: an Australasian perspective. Australian National University Press, Canberra, Australia.

López-Vicente, M., A. Navas, and J. Machín. 2008. Identifying erosive periods by using RUSLE factors in mountain fields of the Central Spanish Pyrenees. Hydrology and Earth System Sciences **12**:523-535.

Loughran, R. J. and B. L. Campbell. 1995. The identification of catchment sediment sources. Pages 189-205 *in* I.D.L. Foster, A.M. Gurnell, and B. W. Webb, editors. Sediment and Water Quality in River Catchments, Wiley, Chichester, UK.

Lowrance, R., S. McIntyre, and C. Lance. 1988. Erosion and deposition in a field/forest system estimated using Cesium-137 activity. Journal of Soil and Water Conservation **43**:195-199.

Lu, X. X. and D. L. Higgitt. 2000. Estimating erosion rates on sloping agricultural land in the Yangtze Three Gorges, China, from caesium-137 measurements. Catena **39**:33-51.

Mabit, L., M. Benmansour, and D. E. Walling. 2008. Comparative advantages and limitations of the fallout radionuclides ^{137}Cs, ^{210}Pbex and ^{7}Be for assessing soil erosion and sedimentation. Journal of Environmental Radioactivity **99**:1799-1807.

Mabit, L. and E. Fulajtar. 2007. The use of ^{137}Cs to assess soil erosion and sedimentation processes: advantages and limitations. Pages 338-339 Book of the extended Synopses of the International Conference on Environmental Radioactivity: From measurements and assessments to regulation. IAEA Publication.

Martinez-Carreras, N., F. Gallart, J. F. Iffly, L. Pfister, D. E. Walling, and A. Krein. 2008. Uncertainty assessment in suspended sediment fingerprinting based on tracer mixing models: a case study from Luxembourg. Pages 94-105 *in* J. Schmidt, T. Cochrane, C. Phillips, S. Elliott, T. Davies, and L. Basher, editors. Sediment dynamics in changing environments. IAHS Press, Witney, UK.

Martinez, C., G. R. Hancock, and J. D. Kalma. 2009. Comparison of fallout radionuclide (caesium-137) and modelling approaches for the assessment of soil erosion rates for an uncultivated site in south-eastern Australia. Geoderma **151**:128-140.

Martz, L. W. and E. de Jong. 1987. Using Cesium-137 to assess the variability of net soil erosion and its association with topography in a Canadian Prairie landscape. Catena **14**:439-451.

Matisoff, G., E. C. Bonniwell, and P. J. Whiting. 2002. Soil erosion and sediment sources in an Ohio Watershed using Beryllium-7, Cesium-137, and Lead-210. J. Environ. Qual. **31**:54-61.

Matisoff, G. and P. J. Whiting. 2011. Measuring soil erosion rates using natural (^{7}Be, ^{210}Pb) and anthropogenic (^{137}Cs, ^{239,240}Pu) radionuclides - Handbook of environmental isotope geochemistry. Pages 487-519 *in* M. Baskaran, editor. Springer Berlin Heidelberg.

McHenry, J. R. and J. C. Ritchie. 1977. Physical and chemical parameters affecting transport of ^{137}Cs in arid watersheds. Water Resour. Res. **13**:923-927.

Menzel, R. G. 1960. Transport of Strontium-90 in runoff. Science **131**:499-500.

Meyer, L. D. and W. H. Wischmeier. 1969. Mathematical simulation of the process of soil erosion by water. Transactions of the Asae **12**:754-758

Misra, R. K. and C. W. Rose. 1996. Application and sensitivity analysis of process-based erosion model GUEST. European Journal of Soil Science **47**:593-604.

Mizugaki, S., Y. Onda, T. Fukuyama, S. Koga, H. Asai, and S. Hiramatsu. 2008. Estimation of suspended sediment sources using ^{137}Cs and ^{210}Pbex in unmanaged Japanese cypress plantation watersheds in southern Japan. Hydrological Processes **22**:4519-4531.

Mizugaki, S., Y. Onda, T. Fukuyama, S. Koga, and S. Hiramatsu. 2006. A method of fingerprinting the sources of fluvial sediment using environmental radionuclides—a case study of Tsuzura River watershed. Proceedings of the Seventh Workshop on Environmental Radioactivity:159–167.

Moore, I. D., P. E. Gessler, G. A. Nielsen, and G. A. Peterson. 1993. Soil attribute prediction using terrain analysis. Soil Sci. Soc. Am. J. **57**:443-452.

Morgan, R. P. C., J. N. Quinton, R. E. Smith, G. Govers, J. W. A. Poesen, K. Auerswald, G. Chisci, D. Torri, and M. E. Styczen. 1998. The European Soil Erosion Model (EUROSEM): a dynamic approach for predicting sediment transport from fields and small catchments. Earth Surface Processes and Landforms **23**:527-544.

Motha, J. A., P. J. Wallbrink, P. B. Hairsine, and R. B. Grayson. 2002. Tracer properties of eroded sediment and source material. Hydrological Processes **16**:1983-2000.

Motha, J. A., P. J. Wallbrink, P. B. Hairsine, and R. B. Grayson. 2003. Determining the sources of suspended sediment in a forested catchment in southeastern Australia. Water Resour. Res. **39**:1056.

Motha, J. A., P. J. Wallbrink, P. B. Hairsine, and R. B. Grayson. 2004. Unsealed roads as suspended sediment sources in an agricultural catchment in south-eastern Australia. Journal of Hydrology **286**:1-18.

Mukundan, R., D. Radcliffe, J. Ritchie, L. Risse, and R. McKinley. 2010. Sediment fingerprinting to determine the source of suspended sediment in a southern piedmont stream. Journal of Environmental Quality **39**:1328-1337.

Nash, J. E. and J. V. Sutcliffe. 1970. River flow forecasting through conceptual models part I - A discussion of principles. Journal of Hydrology **10**:282-290.

Nearing, M. A. 2000. Evaluating soil erosion models using measured plot data: accounting for variability in the data. Earth Surface Processes and Landforms **25**:1035-1043.

Nishita, H., A.J. Steen, and K. H. Larson. 1958. Release of Sr^{90} and Cs^{137} from Vina Loam upon prolonged cropping. Soil Science **86**:195 - 201.

Nishita, H., B.W. Kowalewsky, A.J. Steen, and K. H. Larson. 1956. Fixation and extractibility of fission products contaminating various soils and clays: I. ^{90}Sr, ^{91}Y, ^{106}Ru, ^{137}Cs, and ^{144}Ce. Soil Science **81**:317- 326.

Noboru, Y., M. Shunji, and C. Morito. 1969. Radioecology of Cesium-137 and Strontium-90 in a forest. Journal of Radiation Research (Tokyo) **10**:107-112.

Onori, F., P. De Bonis, S. Grauso, I. N. A. f. N. T. E. Enea, E. P. the Environment, and D. Technologies. 2006. Soil erosion prediction at the basin scale using the revised universal soil loss equation (RUSLE) in a catchment of Sicily (southern Italy). Environmental Geology **50**:1129-1140.

ORTEC. 2003. Review of the physics of semiconductor detectors. ORTEC, Oak Ridge, TN.

Oscarson, D. W., H. B. Hume, and F. King. 1994. Sorption of cesium on compacted bentonite. Clays and clay minerals **42**:731-736.

Owens, P. N. and D. E. Walling. 1996. Spatial variability of caesium-137 inventories at reference sites: an example from two contrasting sites in England and Zimbabwe. Applied Radiation and Isotopes **47**:699-707.

Owens, P. N., D. E. Walling, and Q. He. 1996. The behaviour of bomb-derived Caesium-137 fallout in catchment soils. Journal of Environmental Radioactivity **32**:169-191.

Owens, P. N., D. E. Walling, Q. He, J. O. Shanahan, and I. D. L. Foster. 1997. The use of Caesium-137 measurements to establish a sediment budget for the Start catchment, Devon, UK. Hydrological Sciences Journal **42**:405-423.

Parsons, A. J. and L. D. L. Foster. 2011. What can we learn about soil erosion from the use of ^{137}Cs?. Earth-Science Reviews **108**:101-113.

Pasternack, B. S. and N. H. Harley. 1971. Detection limits for radionuclides in the analysis of multi-component gamma ray spectrometer data. Nuclear Instruments and Methods **91**:533-540.

Peart, M. R. and D. E. Walling. 1986. Fingerprinting sediment source the example of a drainage basin in Devon, UK. International Association of Hydrological Sciences Publication **159**:41-55.

Peirson, D. H. and L. Salmon. 1959. Gamma radiation from deposited fallout. Nature **184**:1678 - 1679.

Pennington, W., T. G. Tutin, R. S. Cambray, and E. M. Fisher. 1973. Observations on lake sediments using fallout ^{137}Cs as a tracer. Nature **242**:324-326.

Pennock, D. J., B. Zebarth, and E. De Jong. 1987. Landform classification and soil distribution in hummocky terrain, Saskatchewan, Canada. Geoderma **40**:297-315.

Phillips, J. M., M. A. Russell, and D. E. Walling. 2000. Time-integrated sampling of fluvial suspended sediment: a simple methodology for small catchments. Hydrological Processes **14**:2589-2602.

Pieri, L., M. Bittelli, J. Q. Wu, S. Dun, D. C. Flanagan, P. R. Pisa, F. Ventura, and F. Salvatorelli. 2007. Using the Water Erosion Prediction Project (WEPP) model to simulate field-observed runoff and erosion in the Apennines mountain range, Italy. Journal of Hydrology **336**:84-97.

Poesen, J. W., D. Torri, and K. Bunte. 1994. Effects of rock fragments on soil erosion by water at different spatial scales: a review. Catena **23**:141-166.

Prokhorov, V. M. 1975. Forecasting Cs-137 migration in soils. Pochvovedeniye **11**:60-67.

Quine, T. A. 1995. Estimation of erosion rates from Caesium-137 data: the calibration question. Pages 307-329 Sediment and water quality in river catchments, Chichester, Wiley.

Quine, T. A. 1999. Use of caesium-137 data for validation of spatially distributed erosion models: the implications of tillage erosion. Catena **37**:415-430.

Radu, D., D. Stanga, and O. Sima. 2009. ETNA software used for efficiency transfer from a point source to other geometries. Applied Radiation and Isotopes **67**:1686-1690.

Rafferty, B., M. Brennan, D. Dawson, and D. Dowding. 2000. Mechanisms of ^{137}Cs migration in coniferous forest soils. Journal of Environmental Radioactivity **48**:131-143.

Rafferty, B., D. Dawson, and A. Kliashtorin. 1997. Decomposition in two pine forests: The mobilisation of ^{137}Cs and K from forest litter. Soil Biology and Biochemistry **29**:1673-1681.

Ramos, S. D. S. and S. J. Rickard Liow. 2013. Discriminant Function Analysis. The Encyclopedia of Applied Linguistics.

Renard, K. G., G. R. Foster, and G. A. Weesies. 1997. Predicting soil erosion by walter: A guide to conservation planning with the Revised Universal Soil Loss Equation (RUSLE). *in* U. A. H. No.703, editor.

Renschler, C. S., D. C. Flanagan, B. A. Engel, and J. R. Frankenberger. 2002. GeoWEPP-The Geo-spatial interface for the Water Erosion Prediction Project. *in* ASAE meeting paper.

Risse, L. M., M. A. Nearing, A. D. Nicks, and J. M. Laflen. 1993. Error assessment in the Universal Soil Loss Equation. Soil Science Society of America Journal **57**:825-833.

Ritchie, J. C., P. H. Hawks, and J. R. McHenry. 1975. Deposition rates in valleys determined using fallout Cesium-137. Geological Society of America Bulletin **86**:1128-1130.

Ritchie, J. C., J.A. Spraberry, and J. R. McHenry. 1974. Estimating soil erosion from the redistribution of fallout Cs-137. Soil Science Society of America Proceedings **38**:137-139.

Ritchie, J. C. and J. R. McHenry. 1973. Vertical distribution of fallout Cesium-137 in cultivated soils. Journal Name: Radiat. Data Rep., v. 14, no. 12, pp. 727-728; Other Information: Orig. Receipt Date: 30-JUN-74:Medium: X.

Ritchie, J. C. and J. R. McHenry. 1975. Fallout Cs-137: a tool in conservation research. Journal of Soil and Water Conservation **30**:283-286.

Ritchie, J. C., J. R. McHenry, A. C. Gill, and P. H. Hawks. 1972. Fallout Cs-137 in reservoir sediments. Health Physics **22**:97-98.

Ritchie, J. C. and C. A. Ritchie. 2008. Bibliography of publications of Cs-173 studies related to soil erosion and sediment depostion. USDA-ARS Hydrology and Remote Sensing Laboratory, http://hydrolab.arsusda.gov/cesium137bib.htm.

Robbins, J. A. and D. N. Edgington. 1976. Depositional processes and the determination of recent sedimentation rates in Lake Michigan. Pages 378-390 Proceedings second federal conference on the Great Lakes, Ann Arbor, MI.

Robbins, J. A., D. N. Edgington, and A. L. W. Kemp. 1978. Comparative ^{210}Pb, ^{137}Cs, and pollen geochronologies of sediments from Lakes Ontario and Erie. Quaternary Research **10**:256-278.

Robinson, C. A., M. Ghaffarzadeh, and R. M. Cruse. 1996. Vegetative filter strip effects on sediment concentration in cropland runoff. Journal of Soil and Water Conservation **51**:227-230.

Rogowski, A. S. and T. Tamura. 1965. Movement of ^{137}Cs by runoff, erosion and infiltration on the Alluvial Captina Silt Loam. Health Physics **11**:1333-1340.

Rogowski, A. S. and T. Tamura. 1970a. Environmental mobility of Cesium-137. Radiation Botany **10**:35-45.

Rogowski, A. S. and T. Tamura. 1970b. Erosional behavior of Cesium-137. Health Physics **18**:467-477.

Roy, J. C., J. E. Côté, A. Mahfoud, S. Villeneuve, and J. Turcotte. 1988. On the transport of chernobyl radioactivity to eastern Canada. Journal of Environmental Radioactivity **6**:121-130.

Russell, M. A., D. E. Walling, and R. A. Hodgkinson. 2000. Appraisal of a simple sampling device for collecting time-integrated fluvial suspended sediment samples. IAHS Publication(International Association of Hydrological Sciences):119-127.

Schiettecatte, W., D. Gabriëls, W. Cornelis, and G. Hofman. 2008. Enrichment of organic carbon in sediment transport by interrill and rill erosion processes. Soil Science Society of America Journal **72**:50-55.

Schulz, R. K., R. Overstreet, and I. Barshad. 1960. On the soil chemistry of Cesium-137. Soil Science **89**:16-27.

Shand, C. A., K. Rosén, K. Thored, R. Wendler, and S. Hillier. 2013. Downward migration of radiocaesium in organic soils across a transect in Scotland. Journal of Environmental Radioactivity **115**:124-133.

Shinonaga, T., W. Schimmack, and M. H. Gerzabek. 2005. Vertical migration of ^{60}Co, ^{137}Cs and ^{226}Ra in agricultural soils as observed in lysimeters under crop rotation. Journal of Environmental Radioactivity **79**:93-106.

Sidorchuk, A. and V. Golosov. 1996. Calibration of soil-erosion models based on study of radioactive fallout. Eurasian soil science **28**:383-395.

Simon, D., S. Helliwell, and K. Robards. 1997. Pesticide toxicity endpoints in aquatic ecosystems. Journal of Aquatic Ecosystem Stress and Recovery **6**:159-177.

Small, I. F., J. S. Rowan, and S. W. Franks. 2002. Quantitative sediment fingerprinting using a Bayesian uncertainty estimation framework. International Association of Hydrological Sciences, Publication **276**:443-450.

Smith, D. D. 1941. Interpretation of soil conservation data for field use. Agricultural Engineering **22**:173 - 175.

Smith, H. G. and D. Dragovich. 2008. Improving precision in sediment source and erosion process distinction in an upland catchment, south-eastern Australia. Catena **72**:191-203.

Sparovek, G., O. Bacchi, E. Schnug, S. Ranieri, and I. D. Maria. 2000. Comparison of three water erosion prediction methods (^{137}Cs, WEPP, USLE) in south-east Brazilian sugarcane production. Tropenlandwirt **101**:107-118.

Spitsyn, V. I., V. D. Balukova, A. F. Naumova, V. V. Gromov, F. M. Spinidomov, E. M. Vetrov, and G. I. Grafov. 1958. A study of the migration of radioelements in the soil. Pages 439-448 2nd International Conference on Peaceful Uses of Atomic Energy, United Nations, Geneva

Squire, H. M. and L. J. Middleton. 1966. Behaviour of Cs-137 in soils and pastures a long term experiment. Radiation Botany **6**:413-423.

Stefano, C., V. Ferro, P. Porto, and S. Rizzo. 2005. Testing a spatially distributed sediment delivery model (SEDD) in a forested basin by cesium-137 technique. Journal of Soil and Water Conservation **60**:148-157.

Stolpe, N. B. 2005. A comparison of the RUSLE, EPIC and WEPP erosion models as calibrated to climate and soil of south-central Chile. Acta Agriculturae Scandinavica, Section B-Soil & Plant Science **55**:2-8.

Stone, P. M. and D. E. Walling. 1997. Particle size selectivity considerations in suspended sediment budget investigations. Pages 63-70 The Interactions Between Sediments and Water. Springer.

Sutherland, R. A. 1991. Examination of caesium-137 areal activities in control (uneroded) locations. Soil Technology **4**:33-50.

Sutherland, R. A. 1996. Caesium-137 soil sampling and inventory variability in reference samples; literature survey. Hydrological Processes **10**:34-54.

Thakur, P., S. Ballard, and R. Nelson. 2012. Radioactive fallout in the United States due to the Fukushima nuclear plant accident. Journal of Environmental Monitoring **14**:1285-1492.

Theocharopoulos, S. P., H. Florou, D. E. Walling, H. Kalantzakos, M. Christou, P. Tountas, and T. Nikolaou. 2003. Soil erosion and deposition rates in a cultivated catchment area in central Greece, estimated using the 137Cs technique. Soil and Tillage Research **69**:153-162.

Tiessen, K. H. D., S. Li, D. A. Lobb, G. R. Mehuys, H. W. Rees, and T. L. Chow. 2009. Using repeated measurements of ^{137}Cs and modelling to identify spatial patterns of tillage and water erosion within potato production in Atlantic Canada. Geoderma **153**:104-118.

Tiwari, A. K., L. M. Risse, and M. A. Nearing. 2000. Evaluation of WEPP and its comparison with USLE and RUSLE. Transactions of the Asae **43**:1129-1135.

Toy, T. J., G. R. Foster, and K. G. Renard. 2002. Soil erosion: processes, prediction, measurement, and control. John Wiley & Sons, New York.

Turnage, K. M., S. Y. Lee, J. E. Foss, K. H. Kim, and I. L. Larsen. 1997. Comparison of soil erosion and deposition rates using radiocesium, RUSLE, and buried soils in dolines in East Tennessee. Environmental Geology **29**:1-10.

U.S. Department of Agriculture, A. R. S., National Sediment Laboratory. 2003. Revised Universal Soil Loss Equation Version 2 (RUSLE2).*in* A. R. S. U.S. Department of Agriculture, editor., Washington, D.C.

U.S. Department of Agriculture Natural Resources Conservation Service. 1997. A geography of hope. U.S. Government Printing Office, Washington, DC.

UNSCEAR. 1993. Sources and effects of Ionizing radiation - report to the General Assembly, with scientific annexes. United Nations, New York.

USDA. 1995. Water Erosion Prediction Project.*in* USDA, editor. USDA–ARS National Soil Erosion Research Laboratory, USDA ARS National Soil Erosion Research Laboratory, West Lafayette, IN.

USDA. 2012. WEPP.*in* N. S. E. R. Lab, editor. Water Erosion Prediction Project.

Wallbrink, P. J., B. P. Roddy, and J. M. Olley. 1997. Quantifying the redistribution of soils and sediments within a post-harvested forest coupe near Bombala. New South Wales, Australia. CSIRO Land and Water Report **7**:97.

Walling, D., Q. He, and P. Whelan. 2003. Using ^{137}Cs measurements to validate the application of the AGNPS and ANSWERS erosion and sediment yield models in two small Devon catchments. Soil and Tillage Research **69**:27-43.

Walling, D., Y. Zhang, and Q. He. 2006. Models for Converting Measurements of Environmental Radionuclide Inventories (^{137}Cs, Excess ^{210}Pb, and ^{7}Be) to Estimates of Soil Erosion and Deposition Rates (Including Software for Model Implementation). Department of Geography, University of Exeter, Exeter, UK. Available from the senior author at: DE Walling@ Exeter. ac. uk.

Walling, D. E., S. B. Bradley, and C. J. Wilkinson. 1986a. A Caesium-137 budget approach to the investigation of sediment delivery from a small agricultural drainage basin in Devon, UK. International Association of Hydrological Sciences Publication No. **159**:423-435.

Walling, D. E., A. L. Collins, and R. W. Stroud. 2008. Tracing suspended sediment and particulate phosphorus sources in catchments. Journal of Hydrology **350**:274-289.

Walling, D. E. and Q. He. 1999. Improved models for estimating soil erosion rates from Cesium-137 measurements. Journal of Environmental Quality **28**:611-622.

Walling, D. E., P. N. Owens, B. D. Waterfall, G. J. Leeks, and P. D. Wass. 2000. The particle size characteristics of fluvial suspended sediment in the Humber and Tweed catchments, UK. Science of the Total Environment **251**:205-222.

Walling, D. E. and T. A. Quine. 1990. Use of Caesium-137 to investigate patterns and rates of soil erosion on arable fields. Pages 33-53 *in* J. Broadman, I.D.I. Foster, and J. A. Dearing, editors. Soil erosion on agricultural land, Wiley, London.

Walling, D. E. and T. A. Quine. 1992. The use of Caesium-137 measurements in soil erosion surveys. International Association of Hydrological Sciences Publication **210**:143-152.

Walling, D. E., S.B. Bradley, and C.J. Lambert. 1986b. Conveyance losses of suspended sediment within a flood plain system. International Association of Hydrological Sciences Publication No. **159**:119-131.

Wei, X. 2007. 东北黑土区小流域土壤侵蚀空间分异规律研究. Doctoral dissertation. Beijing Normal University, Beijing,China.

Wendling, L. A., J. B. Harsh, T. E. Ward, C. D. Palmer, M. A. Hamilton, J. S. Boyle, and M. Flury. 2005. Cesium desorption from illite as affected by exudates from rhizosphere bacteria. Environmental Science & Technology **39**:4505-4512.

Wetherbee, G. A., D. A. Gay, T. M. Debey, C. M. B. Lehmann, and M. A. Nilles. 2012. Wet deposition of fission-product isotopes to North America from the Fukushima Dai-ichi Incident, March 2011. Environmental Science & Technology **46**:2574-2582.

Wilkinson, S. N., P. J. Wallbrink, G. J. Hancock, W. H. Blake, R. A. Shakesby, and S. H. Doerr. 2009. Fallout radionuclide tracers identify a switch in sediment sources and transport-limited sediment yield following wildfire in a eucalypt forest. Geomorphology **110**:140-151.

Williams, J. R. 1990. The Erosion-Productivity Impact Calculator (EPIC) model: a case history. Philosophical Transactions: Biological Sciences **329**:421-428.

Williams, J. R., S. L. Neitsch, and J. G. Arnold. 1999. Soil and Water Assessment Tool user's manual. Texas: Texas Blackland Research Center： Texas Agricultural Experiment Station.

Wilson, R. A. Kuhnle, D. D. Bosch, J. L. Steiner, P. J. Starks, M. D. Tomer, and G. V. Wilson. 2008. Quantifying relative contributions from sediment sources in Conservation Effects Assessment Project watersheds. Journal of Soil and Water Conservation **63**:523-532.

Wilson, B. N., B. J. Barfield, A. D. Ward, and I. D. Moore. 1984. A hydrology and sedimentology watershed model. Part I: operational format and hydrologic component Transactions of American Society of the Agricultural Engineers **27**:1370-1377.

Wischmeier, W. H. 1959. A rainfall erosion index for a Universal Soil-loss Equation. Soil Sci. Soc. Am. J. **23**:246-249.

Wischmeier, W. H. and D. D. Smith. 1978. Predictiong rainfall erosion losses: A guide to conservation planning. USDA Agriculture Handbook. No. 537.

Xie, L., Z. Zhang, N. Cong, X. Wang, and Y. Li. 2010. Grain-size records of tidal flat sediments near Yuantuojiao point, estuary of the north branch of the Changjiang River and grain-size responses to environment changes. Uaternary Science **30**:984-993.

Yang, H., Q. Chang, M. Du, K. Minami, and T. Hatta. 1998. Quantitative model of soil erosion rates using ^{137}Cs for uncultivated soil. Soil Science **163**:248-257.

Yockey, R. D. 2011. SPSS demystified: a step-by-step guide to successful data analysis : for SPSS version 18.0. Prentice Hall/Pearson, Upper Saddle River, NJ.

Yutaka, N. and S. Masamichi. 1967. Accumulation of radionuclides in coastal sediment of Japan (I) Fallout radionuclides in some coastal sediments in 1964-1965. Journal of radiation research **8**:37-43.

Zapata, F. 2002. Handbook for the assessment of soil erosion and sedimentation using environmental radionuclides. Kluwer Academic Publishers, Dordrecht.

Zhang, X., X. Bai, and X. Liu. 2011. Application of a ^{137}Cs fingerprinting technique for interpreting responses of sediment deposition of a karst depression to deforestation in the Guizhou Plateau, China. Science China Earth Sciences **54**:431-437.

Zhang, X., D. L. Higgitt, and D. E. Walling. 1990. A preliminary assessment of the potential for using caesium-137 to estimate rates of soil erosion in the Loess Plateau of China. Hydrological Sciences Journal **35**:243-252.

Zhang, X., X. Liu, M. Zhang, R. A. Dahlgren, and M. Eitzel. 2010. A review of vegetated buffers and a meta-analysis of their mitigation efficacy in reducing nonpoint source pollution. Journal of Environmental Quality **39**:76-84.

Zhang, X., Y. Long, X. He, J. Fu, and Y. Zhang. 2008. A simplified ^{137}Cs transport model for estimating erosion rates in undisturbed soil. Journal of Environmental Radioactivity **99**:1242-1246.

Zhang, X., M. Nearing, L. Risse, and K. McGregor. 1996. Evaluation of WEPP runoff and soil loss predictions using natural runoff plot data. Transactions of the Asae **39**:855-863.

Zhang, X., Z. Wen, M. Feng, Q. Yang, and J. Zheng. 2007. Application of ^{137}Cs fingerprinting technique to interpreting sediment production records from reservoir deposits in a small catchment of the Hilly Loess Plateau, China. Science in China Series D: Earth Sciences **50**:254-260.

Zingg, A. W. 1940. Degree and length of land slope as it affects soil loss in runoff. Agricultural Engineering **21**:59 - 64.

APPENDICES

Table A 1 Central point information of the soil samples for cultivated land and rangeland in Bull Creek watershed

Soil Sample Number	Soil Type*	Land cover	The point take the note in GPS		Remarks
			Latitude(N)	Longitude(W)	
FS01	54&55	Cultivated	35°20′59.9432″	98°43′38.0357″	
FS02	51	Cultivated	35°20′55.9305″	98°43′32.3225″	
FS03	50	Cultivated	35°20′53.7661″	98°43′28.4637″	
FS04	54&55	Cultivated	35°20′49.1150″	98°43′15.7128″	Ignore the small area 54
FS05	47	Cultivated	35°21′7.5206″	98°43′23.8691″	
FS06	39&40	Cultivated	35°21′15.1332″	98°43′33.1334″	
FS07	7&8	Cultivated	35°21′16.7268″	98°43′19.6817″	
FS08	54&55	Cultivated	35°21′10.0719″	98°43′16.9114″	
FS09	50&51	Cultivated	35°21′5.97350″	98°43′42.0017″	
FS10	47	Cultivated	35°20′59.9284″	98°43′13.6938″	Split by road, took samples in the north part
FS11	7&8	Cultivated	35°20′57.3871″	98°42′35.6716″	Not cultivated not rangeland,overseed with weight, for cows.
FS12	54&55	Cultivated	35°21′17.7536″	98°42′13.8694″	
FS13	54&55	Cultivated	35°21′20.2997″	98°43′53.6405″	
FS14	50&51	Cultivated	35°21′19.6080″	98°44′1.40190″	

FS15	7&8	Cultivated	35°21′26.3517″	98°44′3.40583″	
FS16	12	Cultivated	35°22′39.2838″	98°44′3.91389″	Corton in last summer, and weath in fall
FS17	54&55	Cultivated	35°22′35.2349″	98°44′1.09624″	Corton in last summer, and weath in fall
FS18	7&8	Cultivated	35°22′31.1617″	98°43′35.3271″	
FS19	7&8	Cultivated	35°22′34.8940″	98°43′1.95555″	
FS20	39&40	Cultivated	35°22′28.0826″	98°43′4.55796″	
FS21	13	Cultivated	35°22′19.5657″	98°42′56.2049″	Ignore the rock hill in the middle
FS22	50&51	Cultivated	35°22′28.2414″	98°42′51.7280″	
FS23	7&8	Cultivated	35°22′26.0074″	98°42′39.4778″	
FS24	54&55	Cultivated	35°22′25.5289″	98°42′37.2747″	
FS25	39&40	Cultivated	35°22′37.1108″	98°42′34.9726″	Ignore the small grass land
FS26	53	Cultivated	35°22′21.6077″	98°42′45.0913″	A really small area
FS27	39&40	Rangeland	35°22′39.1838″	98°42′53.8591″	
FS28	39&40	Rangeland	35°22′32.3725″	98°43′13.3915″	
FS29	53	Rangeland	35°22′9.76253″	98°42′48.0343″	
FS30	50&51	Rangeland	35°21′57.4817″	98°42′47.7583″	
FS31	39&40	Rangeland	35°22′31.6705″	98°43′40.3052″	
FS32	12	Rangeland	35°22′21.0564″	98°43′57.8504″	
FS33	7&8	Cultivated	35°22′19.9567″	98°44′17.2408″	
FS34	54&55	Rangeland	35°21′59.9250″	98°43′23.2165″	
FS35	39&40	Rangeland	35°22′5.17765″	98°43′5.04169″	
FS36	39&40	Rangeland	35°21′32.9671″	98°43′15.8775″	
FS37	13	Rangeland	35°20′51.7723″	98°42′46.1104″	
FS38	54&55	Rangeland	35°21′38.6624″	98°42′48.3749″	
FS39	7&8	Rangeland	35°21′23.8659″	98°43′12.4914″	
FS40	54&55	Rangeland	35°21′22.5891″	98°42′41.5053″	
FS41	39&40	Rangeland	35°22′12.0685″	98°42′14.8823″	
FS42	38	Rangeland	35°21′40.7695″	98°42′1.60592″	Rock hills,just took one sample for

					all
FS43	39&40	Rangeland	35°21′22.0239″	98°42′3.58496″	
FS44	20	Rangeland	35°21′27.2527″	98°41′41.0093″	
FS45	28	Rangeland	35°22′6.24854″	98°42′8.32134″	
FS46	7&8	Cultivated	35°22′26.5952″	98°42′17.0390″	
FS47	39&40	Cultivated	35°22′16.3442″	98°42′3.80895″	
FS48	39&40	Rangeland	35°21′53.5580″	98°43′51.5260″	
FS49	39&40	Rangeland	35°22′6.9840″	98°43′33.6240″	
FS50	7&8	Rangeland	35°21′58.332″	98°43′42.8740″	

* Soil type refers to the MUKEY in Table 2.

Table A 2 The position and length of gullies in which sediment samples were taken in Bull Creek watershed

Gully Soil Samples' Number	Start		End		Length (m)
	Latitude(N)	Longitude(W)	Latitude(N)	Longitude(W)	
GS01	35°21′14.646″	98°41′55.538″	35°21′14.646″	98°41′2.593″	301.9
GS02	35°21′15.679″	98°42′3.65″	35°21′14.646″	98°41′2.593″	214.9
GS03	35°21′9.46″	98°42′5.223″	35°21′15.679″	98°42′3.65″	198.6
GS04	35°21′14.646″	98°41′2.593″	35°21′42.755″	98°41′53.788″	668.9
GS05	35°21′25.499″	98°41′40.047″	35°21′31.104″	98°41′56.246″	458.2
GS06-North	35°22′9.926″	98°44′1.145″	35°21′47.311″	98°43′44.67″	1192.3
GS06-South	35°21′56.903″	98°44′3.68″			
GS07	35°21′46.524″	98°43′45.894″	35°21′40.144″	98°44′6.914″	565.6
GS08	35°22′38.2″	98°43′41.065″	35°22′12.766″	98°43′37.045″	834.6
GS09	35°22′12.766″	98°43′37.045″	35°21′53.669″	98°43′28.785″	623.1
GS10	35°21′30.137″	98°43′45.304″	35°21′34.507″	98°43′37.613″	244.4
GS11	35°21′32.496″	98°43′35.559″	35°21′18.381″	98°43′35.996″	439.2
GS12	35°21′45.322″	98°43′27.117″	35°21′51.266″	98°42′52.215″	1136.9
GS13	35°22′9.765″	98°43′8.297″	35°22′0.21″	98°43′3.461″	329.8
GS14	35°22′32.808″	98°43′17.095″	35°22′19.581″	98°43′16.163″	415.8
GS15	35°22′19.814″	98°42′45.572″	35°22′5.277″	98°42′42.718″	454.1
GS16	35°21′51.266″	98°42′52.215″	35°21′50.275″	98°42′33.162″	513.7
GS17	35°22′3.47″	98°42′41.203″	35°21′51.409″	98°42′32.405″	434.6
GS18	35°21′51.7″	98°42′30.249″	35°21′56.77″	98°42′8.02″	637.5
GS19	35°21′44.303″	98°42′28.377″	35°21′34.209″	98°42′37.161″	390.3
GS20	35°21′32.854″	98°42′38.734″	35°21′12.774″	98°43′0.549″	883.2

Table A 3 The position information for traps and auto samplers in Bull Creek watershed

Number	Trap or Sampler	Points in the GPS(not very reliable)			Remark
		Latitude	longitude	Altitude (Tietjen et al., 2010)	
0	Trap	35°21′40.03137″	98°41′53.66679″	1433	End of the gully
1	Trap	35°21′31.32180″	98°41′56.24772″	1462	End of the gully
2	Trap	35°21′31.81680″	98°41′55.04586″	1427	End of the gully
3	Auto Sampler	35°21′43.55235″	98°41′53.52342″	1420	End of the gully
4	Trap	35°21′47.77285″	98°43′46.01424″	1521	End of the gully
5	Trap	35°21′46.28619″	98°43′46.20468″	1510	End of the gully
6	Trap	35°21′57.97863″	98°43′31.79496″	1480	End of the gully
7	Trap	35°22′0.33699″	98°43′2.77536″	1485	Main stem,after the gully
8	Trap	35°22′10.73217″	98°42′44.49537″	1480	End of the gully
9	Trap	35°21′50.63931″	98°42′33.07167″	1418	End of the gully
10	Auto Sampler	35°21′50.67468″	98°42′26.46891″	1434	Main stem,after the gully
11	Trap	35°21′53.61183″	98°42′12.16053″	1445	Main stem,before reservoir
12	Trap	35°21′26.78958″	98°43′48.16983″	1551	End of the gully

Number	Trap or Sampler	Points in the GPS(not very reliable)			Remark
		Latitude	longitude	Altitude (Tietjen et al., 2010)	
13	Trap	35°21′27.34200″	98°42′42.26256″	1490	End of the gully

Table A 4 The position information for the 11 transects in Bull Creek watershed

Transect Number	Start Point		Stop Point	
	Latitude	Longitude	Latitude	Longitude
1	35°21′05.09256″	98°41′52.82592″	35°21′04.85073″	98°41′49.60923″
2	35°21′05.24169″	98°41′49.50816″	35°21′10.05705″	98°41′49.09794″
3	35°21′11.19969″	98°41′39.20874″	35°21′08.69166″	98°41′40.23591″
4	35°21′10.90476″	98°41′47.84460″	35°21′11.19969″	98°41′39.20874″
5	35°21′31.92453″	98°42′02.05218″	35°21′33.55551″	98°42′05.53608″
6	35°21′27.92052″	98°42′06.04296″	35°21′33.09039″	98°42′05.68845″
7	35°21′32.43825″	98°41′46.87089″	35°21′35.31384″	98°41′43.85553″
8	35°21′32.34690″	98°41′46.78188″	35°21′29.92266″	98°41′50.42364″
9	35°21′44.25030″	98°41′44.78433″	35°21′42.06870″	98°41′44.79549″
10	35°21′10.01529″	98°41′58.81191″	35°21′12.14649″	98°41′54.45591″
11	35°21′22.57794″	98°42′16.51545″	35°21′23.89239″	98°42′12.1761″

Table A 5 Soil erosion/deposition rates calculated by the Cs-137 method and their lower and upper 95 percent confidence intervals.

Sites	Cs-137 inventory ($Bq\ m^{-2}$)	Erosion/Deposition Rate* Including Z** ($Mg\ ha^{-1}\ yr^{-1}$)	Erosion/Deposition Rate* Excluding Z** ($Mg\ ha^{-1}\ yr^{-1}$)	Confidence Interval include Z**		Confidence Interval exclude Z**		Confidence Interval	
				Lower bound	Upper bound	Lower bound	Upper bound	Include Z	Exclude Z
T02-01	1577	-0.45	-1.19	-1.50	0.60	-3.23	0.87	1.05	2.06
T02-02	1772	-0.18	-0.63	-0.74	0.38	-1.97	0.69	0.56	1.34
T02-03	1132	-1.0	-2.53	-2.82	0.83	-6.03	0.96	1.84	3.49
T02-04	1180	-0.90	-2.44	-2.62	0.81	-5.85	0.96	1.70	3.40
T03-02	1330	-0.72	-1.90	-2.20	0.74	-4.77	0.96	1.46	2.87
T03-03	1750	-0.18	-0.72	-0.74	0.38	-2.20	0.74	0.56	1.46
T03-04	1362	-0.72	-1.81	-2.20	0.74	-4.57	0.96	1.46	2.78
T04-04	1577	-0.45	-1.19	-1.50	0.60	-3.23	0.87	1.05	2.06
T04-03	1714	-0.27	-0.81	-1.01	0.47	-2.40	0.78	0.74	1.59
T04-02	1400	-0.63	-1.72	-1.97	0.69	-4.39	0.94	1.34	2.67

Sites	Cs-137 inventory ($Bq\ m^{-2}$)	Erosion/Deposition Rate* Including Z** ($Mg\ ha^{-1}\ yr^{-1}$)	Erosion/Deposition Rate* Excluding Z** ($Mg\ ha^{-1}\ yr^{-1}$)	Confidence Interval include Z**		Confidence Interval exclude Z**		Confidence Interval	
				Lower bound	Upper bound	Lower bound	Upper bound	Include Z	Exclude Z
T04-01	1330	-0.72	-1.90	-2.20	0.74	-4.77	0.96	1.46	2.87
T05-04	1730	-0.27	-0.72	-1.01	0.47	-2.20	0.74	0.74	1.46
T05-03	482	-1.90	-4.73	-4.77	0.96	-10.1	0.65	2.87	5.38
T05-02	466	-1.90	-4.82	-4.77	0.96	-10.2	0.63	2.87	5.44
T05-01	1080	-1.10	-2.71	-3.02	0.85	-6.38	0.94	1.95	3.67
T06-01	1220	-0.90	-2.26	-2.62	0.81	-5.49	0.96	1.70	3.23
T06-02	1180	-0.90	-2.44	-2.62	0.81	-5.85	0.96	1.70	3.40
T06-03	1610	-0.36	-1.10	-1.28	0.54	-3.02	0.85	0.90	1.95
T06-04	1950	0.25	-0.09	-0.45	0.94	-0.43	0.25	0.69	0.34
T07-01	1370	-0.72	-1.81	-2.20	0.74	-4.57	0.96	1.46	2.78
T07-	1220	-0.90	-2.26	-2.62	0.81	-5.49	0.96	1.70	3.23

Sites	Cs-137 inventory ($Bq\ m^{-2}$)	Erosion/Deposition Rate* Including Z** ($Mg\ ha^{-1}\ yr^{-1}$)	Erosion/Deposition Rate* Excluding Z** ($Mg\ ha^{-1}\ yr^{-1}$)	Confidence Interval include Z**		Confidence Interval exclude Z**		Confidence Interval	
				Lower bound	Upper bound	Lower bound	Upper bound	Include Z	Exclude Z
02									
T07-03	540	-1.81	-4.52	-4.57	0.96	-9.77	0.69	2.78	5.22
T08-01	1370	-0.72	-1.81	-2.20	0.74	-4.57	0.96	1.46	2.78
T08-02	1130	-1.01	-2.53	-2.82	0.83	-6.03	0.96	1.84	3.49
T08-03	384	-1.99	-5.08	-4.95	0.96	-10.7	0.58	2.96	5.64
T10-03	336	-2.08	-5.17	-5.13	0.96	-10.9	0.56	3.05	5.71
T10-02	377	-1.99	-5.08	-4.95	0.96	-10.7	0.58	2.96	5.64
T10-01	358	-2.08	-5.26	-5.13	0.96	-11.0	0.54	3.05	5.80
T11-1	968	-18.2	-19.7	-31.9	-4.5	-34.2	-5.2	13.7	14.5
T11-2	235	-37.1	-46.7	-59.6	-14.6	-73.1	-20.3	22.5	26.4
T11-3	281	-33.4	-42.0	-54.3	-12.5	-66.5	-17.5	20.9	24.5

*Negative is erosion and a position number is deposition;

**Particle size correction factor.

Table A 6 Elements tested by ICP-MS for surface soil and gully samples (Part 1)

Sample No.	Li ppb	B ppb	Na ppb	Mg ppb	Al ppb	P ppb	Ca ppb	V ppb
FS-1	167	73	795	119945	126730	84119	216038	251
FS-2	133	300	567	37652	129116	54116	32012	215
FS-3	263	302	903	82002	180743	52196	28209	260
FS-4	430	380	864	192568	212838	63851	131081	308
FS-5	214	91	737	49292	165094	74371	20755	293
FS-6	200	348	730	97545	151786	86161	195536	231
FS-7	163	705	639	41821	168659	65942	57971	280
FS-8	297	595	1338	131866	212687	66978	261940	350
FS-9	205	324	630	59638	168033	63388	38798	266
FS-10	366	410	808	115737	195896	67351	51119	310
FS-11	272	231	659	70260	187500	56250	177431	275
FS-12	197	391	830	63219	158273	47302	73381	299
FS-13	346	261	886	179484	205163	64946	203125	282
FS-14	249	266	1256	108743	174157	58146	160815	283
FS-15	320	235	716	113605	194017	44798	89595	288
FS-16	257	329	1591	206106	172414	91954	347126	303
FS-17	224	254	1288	169253	173851	74425	270977	292
FS-18	214	259	702	53273	182292	55556	41493	302
FS-19	300	264	1060	110178	221893	50888	116420	289
FS-20	209	162	607	41355	227273	47028	19213	301
FS-21	277	229	788	92738	171779	60583	90644	283
FS-22	366	418	965	111838	259328	59142	63060	414
FS-23	272	532	899	77573	254870	63149	58929	392
FS-24	289	125	707	73909	281716	67724	47015	420
FS-25	256	463	868	88037	267578	70117	69727	416
FS-26	266	280	678	65972	209150	60294	24020	316
FS-27	307	525	1176	137559	213087	69966	138423	340
FS-28	161	329	1046	223620	124026	76948	378571	356
FS-29	340	490	1017	129854	196429	71266	758442	338
FS-30	179	243	791	61502	177052	63806	479851	312
FS-31	262	333	800	108468	219512	82927	90854	319
FS-32	185	394	735	110331	164021	79762	130688	263
FS-33	273	385	730	85319	211957	54484	33152	284
FS-34	228	475	1242	224777	188988	59077	405060	336
FS-35	246	423	1178	155695	183432	61095	231065	328
FS-36	186	335	1014	162011	160140	73324	231564	367
FS-37	207	172	508	51220	170305	67530	41159	261
FS-38	196	296	940	171788	182011	60894	424302	289

Sample No.	Li ppb	B ppb	Na ppb	Mg ppb	Al ppb	P ppb	Ca ppb	V ppb
FS-39	159	107	560	76007	147953	61745	101510	257
FS-40	253	128	519	105189	169497	41667	337736	270
FS-41	229	205	883	77896	153872	44207	69055	241
FS-42	190	369	815	121477	136503	58221	146812	237
FS-43	216	353	833	86869	167788	55556	115909	238
FS-44	212	163	523	58604	167045	45455	90097	234
FS-45	281	241	657	73256	174729	69186	46705	242
FS-46	349	292	696	90359	224183	54085	17304	319
FS-47	301	292	670	79464	192500	51042	52232	271
FS-48	281	178	858	205460	145029	48994	237787	273
FS-49	274	265	707	137043	173293	63415	135671	273
FS-50	231	190	549	79403	139758	57233	62893	211
GS-1	339	177	797	66456	227323	41456	61392	323
GS-2	365	372	1345	199662	210236	77365	346284	368
GS-3	350	283	1267	196284	210899	69595	427365	348
GS-4	287	195	843	112903	187109	60484	150806	282
GS-5	288	250	1430	158146	182236	69382	231742	309
GS-6	308	248	1526	390351	160969	78289	610746	338
GS-7	304	231	2248	281879	150289	64262	334732	305
GS-8	327	185	1271	331933	176647	89706	482143	324
GS-9	316	194	816	192708	193958	65278	245660	311
GS-10	183	73	658	118000	135240	50500	141500	194
GS-11	257	172	1040	204023	192902	73707	273707	295
GS-12	225	164	1224	270522	163310	57276	361194	302
GS-B-12	230	193	1081	257194	143651	56115	351799	299
GS-13	269	281	844	150347	212674	55035	317014	342
GS-14	251	240	623	86201	211591	49026	121266	339
GS-15	330	222	643	75157	235755	43711	45440	314
GS-16	245	385	3157	295455	159621	91919	956061	384
GS-B-16	225	188	4651	146318	141492	58721	190504	291
GS-17	294	329	1584	160096	242644	72596	758654	392
GS-18	273	260	1899	150000	200455	65909	286688	312
GS-19	229	325	1720	149597	149173	68548	529435	274
GS-20	465	575	3582	192164	224888	68657	816418	371
GB 01	128	7589	773	23727	101558	1833	16077	147
GB 02	119	11061	561	28161	72646	2170	224215	117
GB 03	239	56791	2138	182589	127892	5321	203430	272
GB 04	172	-5194	1357	78386	115062	3353	139832	193

Table A 7 Elements tested by ICP-MS for surface soil and gully samples (Part 2)

Sample No.	Mn ppb	Co ppb	Cu ppb	Zn ppb	As ppb	Sr ppb	Cs-133 ppb	Ba ppb
FS-1	4002	61	92	417	31	629	14	841
FS-2	3719	66	98	381	35	285	15	904
FS-3	4266	79	186	427	33	152	17	995
FS-4	4348	75	121	372	32	140	18	1019
FS-5	4726	85	98	396	40	204	16	1175
FS-6	4044	72	103	372	35	350	16	948
FS-7	3303	75	98	351	52	261	17	1065
FS-8	3996	81	147	435	57	299	19	1321
FS-9	4118	73	127	407	38	536	17	1100
FS-10	4676	70	117	407	41	150	18	1252
FS-11	4168	65	107	479	37	286	17	1349
FS-12	4888	76	105	338	43	736	12	1162
FS-13	4903	80	133	461	35	633	19	1042
FS-14	3858	67	123	404	35	487	17	1208
FS-15	4317	78	140	444	38	637	20	1236
FS-16	6415	92	148	530	53	1203	21	1125
FS-17	5629	82	155	447	45	1193	20	1042
FS-18	3602	71	108	363	45	446	18	1311
FS-19	3807	79	130	398	41	370	19	1568
FS-20	3509	76	107	390	42	425	20	1467
FS-21	3676	69	119	410	37	218	18	1350
FS-22	4426	75	121	521	48	851	21	1364
FS-23	4318	82	132	466	48	791	24	1479
FS-24	4193	77	123	606	49	688	24	1599
FS-25	5207	93	138	523	55	936	24	1549
FS-26	3986	64	104	425	39	549	18	1126
FS-27	4190	72	148	480	44	1190	18	1139
FS-28	5768	64	80	468	34	1916	14	1375
FS-29	5051	75	134	581	49	446	20	2159
FS-30	5178	59	90	489	40	394	18	1121
FS-31	5577	79	148	680	40	1207	21	1337
FS-32	5703	59	115	532	38	877	18	1024
FS-33	4853	76	113	387	33	438	20	1133
FS-34	4673	82	125	421	41	1097	20	1051
FS-35	4455	71	124	482	44	627	18	1312
FS-36	4986	73	129	514	44	1161	19	1118
FS-37	4512	56	108	523	29	194	17	1409
FS-38	3450	71	100	370	38	485	17	1224

Sample No.	Mn ppb	Co ppb	Cu ppb	Zn ppb	As ppb	Sr ppb	Cs-133 ppb	Ba ppb
FS-39	3742	64	91	381	35	703	15	872
FS-40	3742	63	95	341	39	395	15	864
FS-41	4268	62	135	454	44	1215	16	1286
FS-42	6527	75	100	562	55	25839	16	3558
FS-43	6162	76	109	586	49	1682	16	1953
FS-44	4789	60	96	508	43	12695	16	2517
FS-45	5078	81	119	612	43	682	17	953
FS-46	3660	73	111	467	38	245	19	1001
FS-47	3780	72	106	385	35	280	19	895
FS-48	4483	65	118	468	40	2270	16	1152
FS-49	3872	69	112	407	41	707	16	1045
FS-50	3553	59	83	390	32	791	14	763
GS-1	7658	96	128	532	62	9114	20	2717
GS-2	8243	114	156	750	65	17534	21	3171
GS-3	7635	110	142	794	58	22264	21	3096
GS-4	5565	83	128	544	46	6109	14	2320
GS-5	7640	97	135	688	62	2067	19	1906
GS-6	8355	107	164	520	55	4803	19	1927
GS-7	5101	77	145	418	42	3507	16	1355
GS-8	5588	85	126	504	47	2521	18	1451
GS-9	5660	85	145	453	45	1590	18	1362
GS-10	3450	56	104	321	28	487	14	810
GS-11	4727	77	170	678	37	1264	19	1397
GS-12	6250	84	138	465	47	1744	17	1493
GS-B-12	5342	77	137	379	42	1960	15	1564
GS-13	4479	85	146	415	48	792	20	1928
GS-14	3977	73	139	420	46	1227	19	1519
GS-15	3129	77	117	421	42	508	19	1652
GS-16	10379	105	122	497	54	2432	19	1782
GS-B-16	4419	73	101	434	41	981	16	1109
GS-17	8365	122	193	611	63	4135	21	2285
GS-18	6526	87	166	494	50	2679	20	1916
GS-19	7843	76	121	415	45	5544	16	1414
GS-20	4907	83	134	416	51	991	20	1824
GB 01	4214	43	56	237	33	3176	10	1069
GB 02	2611	32	39	179	20	14449	7	1206
GB 03	4826	63	106	339	26	552	12	712
GB 04	3706	52	89	309	28	610	12	683

Table A 8 Elements tested by ICP-MS for surface soil and gully samples (Part 3)

Sample No.	Pb ppb	U-238 ppb	Si ppb	Ti ppb	Ge ppb	Br ppb	Zr ppb	Nb ppb
FS-1	88	8	1698	379	0.48	151	158	1.79
FS-2	86	7	2073	392	0.45	112	159	1.44
FS-3	101	8	2753	703	0.57	126	159	1.79
FS-4	85	9	3091	1005	0.51	143	145	1.98
FS-5	109	8	3569	1266	0.59	178	170	2.03
FS-6	85	7	2738	901	0.59	164	152	2.84
FS-7	103	10	3442	1287	0.66	190	183	2.90
FS-8	107	11	5037	1572	0.68	186	176	4.89
FS-9	99	9	4385	1298	0.54	211	162	2.05
FS-10	100	11	5019	1797	0.70	170	172	2.87
FS-11	101	10	3594	794	0.62	272	176	2.52
FS-12	90	11	2050	1014	0.56	146	172	10.4
FS-13	85	9	2133	1341	0.53	181	173	1.81
FS-14	88	10	2079	1231	0.45	196	159	1.69
FS-15	93	9	2052	1321	0.62	187	183	1.50
FS-16	112	14	2270	1509	0.51	144	115	3.36
FS-17	94	11	2284	1434	0.49	142	129	2.69
FS-18	106	12	2622	1726	0.59	117	178	2.52
FS-19	107	11	2204	1646	0.58	128	184	2.20
FS-20	116	11	2360	1738	0.66	150	194	2.66
FS-21	99	10	1173	1723	0.48	94	164	2.99
FS-22	111	13	1080	1015	0.63	104	223	2.72
FS-23	121	14	992	832	0.61	125	217	2.76
FS-24	123	13	1091	896	0.67	166	244	3.28
FS-25	132	13	1729	872	0.71	104	277	3.01
FS-26	98	10	1186	695	0.54	86	190	2.35
FS-27	113	10	1310	878	0.51	157	166	4.21
FS-28	111	11	1089	571	0.49	141	148	3.04
FS-29	113	10	1318	1145	0.52	147	132	4.97
FS-30	104	8	1269	943	0.75	104	152	3.06
FS-31	166	9	1341	859	0.69	201	174	5.20
FS-32	121	8	899	618	0.56	142	92	4.79
FS-33	92	9	1114	904	0.48	104	162	2.28
FS-34	92	9	680	404	0.52	103	218	2.17
FS-35	106	10	1241	723	0.58	98	155	4.51
FS-36	112	13	987	747	0.45	94	120	4.23
FS-37	112	7	866	1075	0.57	137	130	4.97
FS-38	79	8	823	885	0.49	127	155	3.60

Sample No.	Pb ppb	U-238 ppb	Si ppb	Ti ppb	Ge ppb	Br ppb	Zr ppb	Nb ppb
FS-39	87	8	1928	520	0.60	104	166	1.47
FS-40	75	7	2233	603	0.57	73	151	1.36
FS-41	105	8	1460	420	0.44	132	152	1.83
FS-42	137	8	1720	527	0.42	140	129	1.91
FS-43	156	11	2283	462	0.51	138	161	2.24
FS-44	118	9	1383	397	0.42	153	140	1.69
FS-45	111	9	1709	1250	0.59	129	167	1.98
FS-46	97	10	1376	926	0.67	65	183	4.23
FS-47	88	9	1720	836	0.58	52	169	2.93
FS-48	95	10	1491	472	0.40	70	154	1.72
FS-49	99	9	1424	493	0.53	99	187	1.66
FS-50	97	8	1528	353	0.57	76	187	1.50
GS-1	118	14	2965	530	0.95	87	251	1.90
GS-2	150	14	2747	589	1.01	77	251	2.03
GS-3	137	13	3456	693	1.01	75	252	5.41
GS-4	107	10	1375	363	0.60	80	208	1.41
GS-5	133	13	2334	543	0.84	111	207	3.37
GS-6	100	14	1829	384	0.66	98	236	1.75
GS-7	79	9	1310	571	0.50	99	206	1.68
GS-8	96	14	2015	564	0.63	124	272	1.68
GS-9	97	9	1448	624	0.52	119	211	1.91
GS-10	64	7	783	265	0.40	130	126	0.90
GS-11	100	9	3333	459	0.57	107	186	1.15
GS-12	83	10	3153	390	0.75	67	210	0.76
GS-B-12	74	10	1919	500	0.54	78	210	0.90
GS-13	103	10	1835	594	0.69	86	225	1.56
GS-14	107	10	1737	418	0.65	175	194	2.44
GS-15	96	8	1406	625	0.63	112	205	1.73
GS-16	96	14	2684	660	0.76	92	244	2.27
GS-B-16	83	11	2752	466	0.78	96	203	1.36
GS-17	134	11	2572	623	0.96	132	259	1.68
GS-18	101	9	1526	593	0.65	77	212	1.79
GS-19	86	8	1863	545	0.40	97	185	1.41
GS-20	88	10	1864	823	0.56	91	194	1.87
GB 01	46	6	707	188	0.46	47	104	0.56
GB 02	36	4	506	389	0.35	36	62	0.57
GB 03	52	10	638	484	0.55	83	119	0.74
GB 04	51	6	615	358	0.58	30	125	0.53

Table A 9 Elements tested by ICP-MS for surface soil and gully samples (Part 4)

Sample No.	Mo ppb	Sn ppb	Hf ppb	Cs-137 MBq/g	N %	C %	S %	H %
FS-1	2.56	7.36	3.25	2581	0.18	1.82	0.11	0.23
FS-2	1.91	6.94	3.71	1869	0.15	0.92	0.08	0.17
FS-3	2.40	7.43	3.83	3257	0.16	1.03	0.07	0.23
FS-4	2.85	8.02	3.46	238	0.15	1.15	0.06	0.24
FS-5	2.37	6.59	4.04	2422	0.23	1.30	0.06	0.26
FS-6	3.51	6.29	3.36	2589	0.15	1.48	0.06	0.22
FS-7	3.48	7.45	4.26	2058	0.17	1.00	0.05	0.24
FS-8	3.02	7.31	4.02	1067	0.17	1.54	0.05	0.24
FS-9	1.83	5.41	4.08	2452	0.20	1.42	0.05	0.29
FS-10	2.91	7.97	4.40	2662	0.15	1.07	0.04	0.23
FS-11	2.53	5.95	3.90	872	0.18	1.27	0.04	0.28
FS-12	2.41	5.76	4.08	576	0.15	1.07	0.04	0.29
FS-13	2.01	5.58	4.47	2590	0.20	1.74	0.05	0.41
FS-14	1.50	5.35	3.74	1088	0.19	1.29	0.04	0.33
FS-15	1.92	5.26	5.35	878	0.14	1.05	0.04	0.31
FS-16	4.58	5.39	2.54	3089	0.20	2.15	0.08	0.30
FS-17	2.70	5.00	2.88	3036	0.17	1.82	0.07	0.27
FS-18	2.53	5.92	4.59	2011	0.15	0.88	0.07	0.23
FS-19	2.14	5.64	5.23	2302	0.15	1.04	0.06	0.28
FS-20	2.36	5.89	5.11	2543	0.22	1.37	0.08	0.56
FS-21	3.39	7.24	4.20	2850	0.16	1.23	0.12	0.29
FS-22	3.64	9.44	6.66	1620	0.18	1.11	0.07	0.29
FS-23	3.57	6.27	6.13	2382	0.17	1.12	0.06	0.28
FS-24	3.68	7.01	6.69	1756	0.27	2.15	0.08	0.66
FS-25	4.10	7.46	7.18	2491	0.19	1.49	0.06	0.50
FS-26	2.81	7.48	5.08	3295	0.17	1.20	0.06	0.29
FS-27	3.94	7.67	3.32	5437	0.29	2.86	0.15	0.61
FS-28	3.91	4.69	2.58	15686	0.19	3.09	0.09	0.23
FS-29	8.39	7.06	2.25	9732	0.28	2.90	0.09	0.36
FS-30	5.56	6.42	1.77	3954	0.18	1.89	0.08	0.29
FS-31	4.70	8.66	3.93	6184	0.26	2.11	0.08	0.36
FS-32	4.18	4.70	1.69	16880	0.30	2.82	0.08	0.41
FS-33	2.66	7.58	4.92	2695	0.10	0.80	0.04	0.22
FS-34	3.57	4.93	5.71	2348	0.16	3.35	0.06	0.50
FS-35	4.69	5.62	2.80	6501	0.24	2.59	0.06	0.39
FS-36	4.79	5.52	2.05	7654	0.24	2.76	0.07	0.36
FS-37	3.90	8.46	2.85	5104	0.27	2.29	0.07	0.40
FS-38	3.81	6.80	3.41	3006	0.15	2.70	0.05	0.28

Sample No.	Mo ppb	Sn ppb	Hf ppb	Cs-137 MBq/g	N %	C %	S %	H %
FS-39	3.02	5.32	3.09	3057	0.14	1.58	0.05	0.22
FS-40	2.86	4.91	2.83	1642	0.14	1.91	0.05	0.32
FS-41	5.09	4.25	3.05	8788	0.26	2.06	0.06	0.43
FS-42	5.79	4.73	2.18	13008	0.26	2.26	0.11	0.35
FS-43	3.69	6.94	3.01	11922	0.23	2.42	0.07	0.35
FS-44	3.18	3.80	2.78	14275	0.23	2.22	0.07	0.42
FS-45	3.37	5.72	2.81	5017	0.30	2.41	0.06	0.49
FS-46	4.05	8.28	5.11	2854	0.21	1.19	0.06	0.30
FS-47	3.79	7.20	4.54	2250	0.16	1.05	0.06	0.27
FS-48	2.97	4.54	3.46	5526	0.21	1.19	0.06	0.30
FS-49	2.88	4.86	3.63	7673	0.16	1.05	0.06	0.27
FS-50	2.74	4.94	3.70	5868	0.20	2.15	0.05	0.35
GS-1	6.33	12.03	6.33	968	0.12	0.89	0.06	0.25
GS-2	6.42	9.80	4.73	1020	0.17	1.73	0.06	0.26
GS-3	6.76	11.49	5.41	1048	0.18	1.66	0.06	0.29
GS-4	3.43	5.44	4.03	762	0.16	1.63	0.06	0.33
GS-5	4.78	9.27	4.49	1056	0.20	2.06	0.06	0.28
GS-6	3.95	8.99	7.02	906	0.11	2.09	0.05	0.25
GS-7	2.85	6.38	5.70	1078	0.18	1.99	0.05	0.25
GS-8	4.41	9.66	6.09	1373	0.15	1.85	0.04	0.26
GS-9	3.47	6.42	4.69	1483	0.18	2.07	0.08	0.33
GS-10	1.80	3.30	2.80	2059	0.22	1.67	0.05	0.31
GS-11	2.44	3.59	3.30	2862	0.21	2.58	0.06	0.39
GS-12	3.73	6.16	4.85	0	0.13	1.83	0.04	0.28
GS-B-12	3.42	5.58	5.22	558	0.13	2.03	0.04	0.29
GS-13	2.95	6.60	5.90	1198	0.16	1.45	0.04	0.35
GS-14	3.08	5.19	4.71	3491	0.19	1.69	0.05	0.39
GS-15	4.09	5.50	5.50	1364	0.17	0.98	0.04	0.34
GS-16	5.81	9.34	5.81	538	0.22	2.23	0.32	0.29
GS-B-16	3.68	7.75	4.84	495	0.13	1.33	0.10	0.21
GS-17	5.53	8.41	5.53	612	0.17	1.29	0.08	0.39
GS-18	3.90	5.52	4.71	1838	0.19	1.82	0.27	0.36
GS-19	4.84	6.45	4.03	599	0.16	1.92	0.78	0.20
GS-20	4.66	6.16	4.66	410	0.21	1.98	1.20	0.45
GB 01	2.41	2.78	2.68	171	0.14	0.86	0.20	0.30
GB 02	1.60	1.92	0.89	1237	0.18	1.95	0.14	0.27
GB 03	1.75	2.77	2.43	987	0.15	1.91	0.09	0.28
GB 04	1.76	2.21	3.63	124	0.08	0.96	0.07	0.29

Table A 10 Elements tested by ICP-MS for sediment trap samples (Part 1)

Trap No.	Li ppb	B ppb	Na ppb	Mg ppb	Al ppb	P ppb	Ca ppb	V ppb
1	182	32	707	75400	96700	5000	135300	143
1	218	45	818	86000	121000	5210	137500	194
1	220	37	1070	88200	115000	4940	139700	169
1	237	42	983	90300	122000	5890	141900	180
1	215	6189	958	90856	160278	6221	152740	267
1	216	-1395	1477	72982	183639	5178	148466	259
1	231	9571	1301	139980	163310	6299	276171	252
4	204	41	1240	98700	103000	4600	104500	178
4	226	54	941	150000	114000	5760	182600	188
4	362	85	3060	200500	165000	7060	275000	270
4	307	43	2450	127000	168000	6560	148500	231
4	312	14679	3501	211554	206810	8206	323547	355
4	322	7582	1810	110859	243840	7851	103601	334
4	314	2986	2732	199781	170217	6260	254828	275
5	242	35	863	118000	132000	4730	138600	209
5	415	65	5270	192000	179000	5980	198000	260
5	306	87	3710	168000	160000	5520	180400	265
5	318	4286	3845	176136	217803	6316	215311	375
5	294	2298	1573	175325	152847	6681	198801	293
5	503	30518	52598	223497	319537	13927	211429	406
5	669	-1399	5926	306655	344424	7518	186851	477
6	384	156	1210	245500	168000	7700	277200	249
6	280	12210	1503	138593	178959	6134	154490	276
9	264	48	2060	124000	137000	6060	146300	217
9	252	59	1019	128000	150000	6290	157300	225
9	353	69	1980	170000	182000	8850	240900	278
9	303	89	3440	157000	179000	12400	233200	299
9	375	5794	89486	208941	244456	14356	326174	329
9	278	10867	1175	167797	181256	6668	218345	318
9	376	-4285	6349	191909	265444	7901	260064	354
11	331	49	1320	147000	143000	6550	218900	225
11	292	4492	5083	151742	210542	8934	210642	295
11	371	2196	2138	188623	249701	6921	242515	383
11	391	-299	2153	168643	246686	7984	219276	341
Z2	239	47	1390	235000	93200	5330	342100	172
Z2	352	5084	44607	214036	232978	71219	431662	252
Z3	235	110	2320	151000	166000	5880	198000	238
Z3	235	59	1037	151000	113000	5670	189200	201

Trap No.	Li ppb	B ppb	Na ppb	Mg ppb	Al ppb	P ppb	Ca ppb	V ppb
Z3	228	48	1150	168000	111000	6050	249700	237
Z3	230	84	1260	158000	117000	6540	227700	235
Z3	230	-1296	1463	182208	148100	6376	242346	258
Z4	258	40	876	70200	136000	5120	75460	192
Z4	229	52	777	70400	130000	5650	75130	205
Z4	264	59	2890	83700	154000	5680	86790	242
Z4	236	47	785	76300	134000	5380	90090	206
Z4	249	300	7537	103467	185102	7660	123901	256
Z4	269	9386	1815	178832	149176	5976	208687	270
Z4	248	9894	737	61883	205077	5089	109934	276
Z4	209	-7167	1129	67460	152299	4659	70476	224
Z5	212	52	1270	112000	104000	5600	170500	178
Z5	244	120	2870	122000	126000	32000	312400	192
Z5	302	62	1080	136000	141000	6010	202400	225
Z5	288	-1600	6592	155769	205159	8387	242951	288
Z5	251	8982	2353	131138	156287	7841	205589	251

Table A 11 Elements tested by ICP-MS for sediment trap samples (Part 2)

Trap No.	Mn ppb	Co ppb	Cu ppb	Zn ppb	As ppb	Sr ppb	Cs-133 ppb	Ba ppb
1	4010	64	205	799	27	5290	12	2700
1	5560	77	347	1770	33	5980	16	2830
1	5330	75	248	1030	31	7190	15	2740
1	6090	81	307	713	34	6510	16	2810
1	6599	84	213	802	47	5640	22	2456
1	7254	88	242	997	58	4514	21	2640
1	8993	96	134	703	59	1515	20	2034
4	2770	53	211	782	26	881	13	1120
4	3840	69	208	620	30	1380	15	1390
4	6585	87	257	964	44	2600	18	2245
4	4040	81	217	2150	40	1730	19	2270
4	9497	103	495	1967	60	3305	21	2307
4	7213	102	220	1072	58	1546	21	1731
4	5783	81	221	779	45	2578	18	1563
5	3990	73	198	944	31	1040	15	1520
5	6320	95	265	809	41	1890	18	2060
5	4440	79	209	604	37	1670	18	1460
5	8034	96	266	1031	54	2392	24	1994
5	4675	74	201	696	38	1998	17	1129
5	8876	136	944	4687	80	2344	22	2374
5	7034	143	473	2088	78	2588	25	2058
6	5635	85	221	708	37	1185	18	1335
6	4690	85	261	1450	40	1061	19	1306
9	5100	90	537	2070	37	1050	18	1600
9	4480	80	207	674	39	946	19	1510
9	11000	102	317	842	50	1640	21	2450
9	44800	116	325	1520	97	1710	20	3560
9	21643	123	571	2203	77	2657	24	2737
9	6500	98	494	1705	49	1476	20	1486
9	10373	121	518	1365	53	1903	26	2830
11	13800	98	177	673	49	11100	16	3620
11	25976	102	439	1208	68	3873	23	2256
11	8932	123	259	964	68	6168	24	2345
11	9937	113	226	912	58	2771	26	2003
Z2	3690	66	136	458	28	841	15	1960
Z2	4965	78	683	2801	68	1505	21	1296
Z3	4440	85	564	3180	39	1100	17	1250
Z3	4030	64	161	544	30	965	15	1160

Trap No.	Mn ppb	Co ppb	Cu ppb	Zn ppb	As ppb	Sr ppb	Cs-133 ppb	Ba ppb
Z3	5620	74	144	542	36	992	16	1530
Z3	5660	75	189	2580	35	1110	17	1650
Z3	5725	80	183	690	43	1197	18	1316
Z4	4720	81	287	959	35	883	17	1520
Z4	4460	75	216	750	36	889	17	1560
Z4	5930	81	393	654	42	1720	19	1770
Z4	4480	69	170	541	35	1270	16	1430
Z4	6944	86	279	1259	47	2028	19	1379
Z4	4643	72	195	648	40	1967	15	1248
Z4	8225	91	242	1149	60	5926	19	2878
Z4	4370	66	159	620	36	948	16	1095
Z5	4900	73	271	954	33	7210	14	1550
Z5	5140	63	349	692	37	7270	13	1620
Z5	6070	81	243	841	38	12000	16	1930
Z5	7119	96	370	1046	60	13097	20	2240
Z5	6866	80	234	803	43	7495	17	1577

Table A 12 Elements tested by ICP-MS for sediment trap samples (Part 3)

Trap No.	Pb ppb	U-238 ppb	Si ppb	Ti ppb	Ge ppb	Br ppb	Zr ppb	Nb ppb
1	207	6	1240	118	0.48	98	141	1.07
1	247	7	669	140	0.53	90	161	1.32
1	195	7	787	153	0.50	122	167	1.08
1	195	7	1285	171	0.54	140	171	1.58
1	158	9	541	457	0.80	28	184	2.34
1	118	10	558	397	0.75	47	182	1.98
1	106	11	601	561	0.72	23	163	1.29
4	147	7	689	195	0.41	82	141	0.66
4	191	9	819	189	0.43	93	161	0.79
4	171	11	666	186	0.47	218	216	1.95
4	176	9	557	131	0.47	326	192	0.84
4	215	12	388	635	0.63	122	199	2.57
4	126	10	663	353	1.01	79	214	1.71
4	96	10	722	610	0.66	65	171	1.15
5	205	7	822	132	0.47	222	183	0.70
5	142	8	619	142	0.49	327	239	1.05
5	140	8	876	170	0.45	169	205	1.16
5	141	8	331	557	0.74	79	241	2.21
5	91	9	514	544	0.61	41	165	2.32
5	249	13	625	740	0.65	364	275	1.66
5	170	12	1309	551	0.83	170	360	1.63
6	167	10	675	198	0.43	71	192	2.15
6	110	9	560	423	0.72	39	176	1.21
9	348	8	649	222	0.51	136	184	4.93
9	205	8	713	156	0.56	115	190	1.62
9	183	10	846	141	0.52	196	231	2.13
9	319	9	874	172	0.51	208	197	1.20
9	203	10	445	607	0.76	328	221	1.90
9	121	10	634	465	0.65	39	186	1.92
9	190	10	643	576	0.91	140	260	1.24
11	141	9	665	113	0.43	173	209	1.30
11	160	9	572	489	0.80	190	196	1.60
11	141	11	504	459	0.79	85	250	1.99
11	128	10	743	569	0.92	70	236	1.53
Z2	72	10	555	105	0.33	65	167	1.08
Z2	443	23	476	968	0.55	186	144	2.89
Z3	252	8	2420	323	0.44	71	152	1.19
Z3	187	8	1080	152	0.43	80	151	1.16

Trap No.	Pb ppb	U-238 ppb	Si ppb	Ti ppb	Ge ppb	Br ppb	Zr ppb	Nb ppb
Z3	116	10	577	122	0.39	143	167	1.87
Z3	134	8	787	158	0.48	130	165	1.31
Z3	93	9	480	510	0.55	32	157	0.81
Z4	244	7	755	186	0.56	101	167	1.10
Z4	190	7	786	158	0.57	93	162	0.76
Z4	201	8	957	176	0.78	129	193	1.99
Z4	128	7	593	119	0.50	103	156	1.93
Z4	112	9	526	354	0.71	119	169	0.77
Z4	81	10	422	472	0.52	78	158	1.41
Z4	162	10	417	386	0.80	52	195	1.77
Z4	87	8	625	333	0.76	71	146	0.83
Z5	251	7	915	184	0.44	94	141	0.91
Z5	244	7	934	394	0.41	126	99	2.68
Z5	179	8	655	153	0.49	126	191	1.90
Z5	150	10	515	539	0.75	187	210	1.66
Z5	99	9	443	468	0.61	82	147	1.88

Table A 13 Elements tested by ICP-MS for sediment trap samples (Part 4)

Trap No.	Mo ppb	Sn ppb	Hf ppb	Cs-137 MBq/g	N %	C %	S %	H %
1	1.62	3.48	0.32	2771	0.19	1.98	0.09	0.70
1	1.96	1.91	0.32		0.15	1.93	0.05	0.67
1	1.77	2.27	0.31	1076	0.13	1.64	0.06	0.61
1	2.13	2.24	0.34		0.20	2.36	0.09	0.77
1	3.61	2.13	3.95		0.24	2.14	0.13	0.51
1	2.99	1.60	4.22		0.20	2.29	0.14	0.63
1	2.88	6.89	3.56		0.13	2.39	0.07	0.49
4	1.05	2.76	0.37		0.12	1.35	0.04	0.52
4	1.24	3.06	0.42	1028	0.14	1.89	0.05	0.65
4	1.96	2.22	0.49		0.25	3.38	0.07	0.90
4	1.19	3.18	0.48		0.23	2.45	0.07	1.03
4	2.58	2.14	5.26		0.25	3.16	0.08	0.66
4	2.57	1.72	6.19	2695	0.12	2.06	0.07	0.37
4	2.32	2.83	4.91		0.15	2.49	0.07	0.53
5	1.08	5.03	0.44	152	0.09	1.39	0.04	0.44
5	1.47	2.51	0.54		0.27	3.31	0.08	1.16
5	1.49	2.63	0.53		0.16	2.15	0.05	0.68
5	2.10	2.17	6.70		0.23	2.70	0.07	0.66
5	2.33	2.22	5.39		0.16	2.28	0.06	0.44
5	3.45	10.87	8.90		0.30	2.93	0.48	1.03
5	3.30	8.56	10.70		0.24	2.80	0.12	1.18
6	1.61	2.56	2.44	722	0.13	2.23	0.05	0.55
6	2.26	1.47	5.08		0.07	0.90	0.06	0.34
9	1.51	2.38	0.41		0.17	2.14	0.07	0.79
9	1.96	2.46	0.50	1605	0.14	2.12	0.06	0.76
9	2.43	2.65	5.54		0.29	3.54	0.12	1.10
9	2.51	2.29	0.40		0.29	3.38	0.12	1.13
9	4.62	5.91	5.02		0.36	3.55	0.68	0.98
9	2.02	1.67	5.38		0.15	2.48	0.06	0.54
9	3.34	2.29	6.94		0.23	3.34	0.15	1.02
11	3.05	3.62	4.60		0.24	3.22	0.09	0.99
11	3.07	2.61	5.41		0.24	2.62	0.12	0.71
11	3.39	1.48	6.81		0.26	3.15	0.10	0.85
11	3.11	6.06	5.72		0.08	1.14	0.06	0.20
Z2	2.07	2.73	4.65	1810	0.13	2.96	0.08	0.50
Z2	6.70	9.75	3.39		0.33	3.01	1.01	0.74
Z3	2.27	2.29	1.90		0.13	2.05	0.05	0.60
Z3	1.58	2.49	0.34	2126	0.13	2.05	0.04	0.55

Trap No.	Mo ppb	Sn ppb	Hf ppb	Cs-137 MBq/g	N %	C %	S %	H %
Z3	1.68	1.89	2.99		0.20	3.15	0.05	0.56
Z3	1.52	1.93	0.32		0.17	2.55	0.05	0.67
Z3	2.12	38.89	4.70		0.10	2.14	0.08	0.38
Z4	1.78	2.66	0.41	848	0.13	1.19	0.07	0.73
Z4	1.46	2.72	0.37	2008	0.11	0.97	0.05	0.60
Z4	3.46	3.28	0.49	358	0.08	0.82	0.07	0.35
Z4	2.08	3.07	4.58	987	0.12	1.04	0.04	0.39
Z4	2.22	1.87	4.18		0.33	3.01	1.01	0.74
Z4	1.86	1.94	5.16		0.16	1.69	0.07	0.64
Z4	3.44	1.95	5.52		0.34	2.94	0.99	0.72
Z4	1.92	9.65	3.63		0.07	0.90	0.06	0.34
Z5	1.68	2.39	0.29	1114	0.25	2.44	0.16	0.93
Z5	3.57	4.69	0.18		0.24	2.99	0.09	0.65
Z5	2.39	2.65	4.56		0.07	0.90	0.06	0.34
Z5	3.76	1.73	4.61		0.33	3.01	1.01	0.74
Z5	2.64	1.38	3.17		0.15	2.38	0.08	0.46

Table A 14 Particle size distributions for the surface and gully samples

Sample No.	Sand %	Silt %	Clay %
FS-1	36	50	14
FS-2	34	52	14
FS-3	41	44	15
FS-4	41	44	15
FS-5	36	50	14
FS-6	33	50	17
FS-7	45	42	13
FS-8	46	40	14
FS-9	27	52	21
FS-10	46	42	12
FS-11	42	44	14
FS-12	44	42	14
FS-13	26	50	24
FS-14	29	50	21
FS-15	31	46	23
FS-16	30	54	16
FS-17	30	54	16
FS-18	42	44	14
FS-19	32	48	20
FS-20	43	38	19
FS-21	35	50	15
FS-22	46	40	14
FS-23	38	44	18
FS-24	46	36	18
FS-25	49	34	17
FS-26	39	46	15
FS-27	40	44	16
FS-28	38	50	12
FS-29	38	46	16
FS-30	46	40	14
FS-31	34	46	20
FS-32	24	62	14
FS-33	26	52	22
FS-34	33	44	24
FS-35	32	48	20
FS-36	28	54	18
FS-37	34	52	14
FS-38	28	54	18
FS-39	40	44	16
FS-40	36	48	16
FS-41	34	50	16
FS-42	40	46	14
FS-43	60	28	12
FS-44	38	44	18

Sample No.	Sand %	Silt %	Clay %
FS-45	48	36	16
FS-46	39	46	15
FS-47	33	52	15
FS-48	30	54	16
FS-49	34	46	20
FS-50	36	48	16
GS-1	68	20	12
GS-2	70	20	10
GS-3	70	20	10
GS-4	50	30	20
GS-5	64	24	12
GS-6	54	32	14
GS-7	40	44	16
GS-8	52	30	18
GS-9	42	36	22
GS-10	28	48	24
GS-11	30	44	26
GS-12	46	34	20
GS-B-12	44	40	16
GS-13	42	36	22
GS-14	38	42	20
GS-15	36	40	24
GS-16	60	26	14
GS-B-16	48	36	16
GS-17	58	22	20
GS-18	38	42	20
GS-19	50	36	14
GS-20	46	34	20
GB 01	55	28	18
GB 02	67	20	14
GB 03	27	52	22
GB 04	45	38	18

Table A 15 Particle size distributions for the sediment trap samples

Trap No.	Sand %	Silt %	Clay %
1	46	40	14
1	30	48	22
1	14	64	22
1	52	32.4	15.6
1	66	22.4	11.6
1	38	38.4	23.6
4	40	44	16
4	26	54.4	19.6
4	22	56.4	21.6
5	54	28	18
5	32	46.4	21.6
5	18	46.4	35.6
5	22	54.4	23.6
5	18	50.4	31.6
6	30	50	20
9	42	40	18
9	24	46.4	29.6
11	18	48.4	33.6
Z2	44	38	18
Z2	26	50.4	23.6
Z3	40	42	18
Z3	34	46.4	19.6
Z3	20	54.4	25.6
Z4	44	34	22
Z4	48	36	16
Z4	44	38.4	17.6
Z4	20	42.4	37.6
Z4	48	38.4	13.6
Z4	40	44.4	15.6
Z5	46	38.4	15.6
Z5	32	46.4	21.6

Acid Extraction Procedures

i. Grind soil sample, then wet sieving through a 63 μm mesh sieve.

ii. Ovens dry the sample at 105 ℃ overnight.

iii. Weigh 1 g of dry sample to the nearest 0.01 g and transfer to a 100 ml glass tube.

iv. Add 10 ml concentrated HNO_3, mix the slurry, and cover with a watch glass.

v. Heat the sample to 90 ℃ ± 5 ℃ and reflux for 10 to 15 minutes without boiling.

vi. Allow the sample to cool, add 5 ml of concentrated HNO_3, replace the cover, and reflux for 30 minutes.

vii. If brown fumes are generated, indicating oxidation of the sample by HNO_3, repeat this step (addition of 5 ml of concentrated HNO_3) until no brown fumes are given off by the sample indicating the complete reaction with HNO_3.

viii. Using a ribbed watch glass heat at 90 ℃ ± 5 ℃ without boiling for two hours. Ensure the sample does not evaporate below 5 ml.

ix. Cool sample.

x. Add 2 ml of water, cover the vessel with a watch glass, warm to start the peroxide reaction.

xi. Slowly add 3 ml of 30% H_2O_2 in 1 ml increments to the sample. For high organic content, additional H_2O_2 may be needed, but do not add more than a total of 10 ml of H_2O_2. Care must be taken to ensure that losses do not occur due to excessively vigorous effervescence.

xii. Cool sample.

xiii. Filter samples through Whatman No. 41 filter using PE funnel, collect in 100 ml flasks, rinse filter paper thoroughly with 18 MΩ water.

xiv. Fill the 100 ml flask to mark and mix.

xv. Sample is now ready for analysis by ICP-MS.

VITA

BING LIU

Candidate for the Degree of

Doctor of Philosophy

Thesis: USING ISOTOPES TO ANALYZE SOIL EROSION AND DEPOSITION FOR THE BULL CREEK WATERSHED IN OKLAHOMA

Major Field: Environmental Science

Biographical:

Education:

Completed the requirements for the Doctor of Philosophy in Environmental Science at Oklahoma State University, Stillwater, Oklahoma in December, 2013.

Completed the requirements for the Master of Science in Physical Geography at Beijing Normal University, Beijing, China in 2010.

Completed the requirements for the Bachelor of Science in Geography Information System at Beijing Normal University, Beijing, China in 2007.

Experience: Teaching Assistant and Research Assistant.

Professional Memberships: ASABE and Golden Key.